NPS69-82-001

AD A119338

NAVAL POSTGRADUATE SCHOOL
Monterey, California

THESIS

EFFECTS OF CONDENSATE INUNDATION
AND VAPOR VELOCITY ON HEAT
TRANSFER IN A CONDENSER TUBE BUNDLE

by

Paul Jeffrey Noftz

June 1982

Thesis Advisor: Dr. P.J. Marto

DTIC FILE COPY

82

Naval Postgraduate School
Monterey, California

Rear Admiral John J. Ekelund   David A. Schrady
Superintendent   Provost (Acting)

   Reproduction of all or part of this report is authorized.

Released as a
Technical Report by: ·

William M. Tolles
Dean of Research

REPORT DOCUMENTATION PAGE		READ INSTRUCTIONS BEFORE COMPLETING FORM
1. REPORT NUMBER NPS69-82-001	2. GOVT ACCESSION NO. AD-A11933 8	3. RECIPIENT'S CATALOG NUMBER
4. TITLE (and Subtitle) Effects of Condensate Inundation and Vapor Velocity on Heat Transfer in a Condenser Tube Bundle		5. TYPE OF REPORT & PERIOD COVERED Master's Thesis; June 1982
		6. PERFORMING ORG. REPORT NUMBER
7. AUTHOR(s) Paul Jeffrey Noftz		8. CONTRACT OR GRANT NUMBER(s)
9. PERFORMING ORGANIZATION NAME AND ADDRESS Naval Postgraduate School Monterey, California 93940		10. PROGRAM ELEMENT, PROJECT, TASK AREA & WORK UNIT NUMBERS 62543: SF43400391 N00167-82-WR2-0114
11. CONTROLLING OFFICE NAME AND ADDRESS David Taylor Naval Ship Research and Development Center Bethesda, Maryland		12. REPORT DATE June 1982
		13. NUMBER OF PAGES 188
14. MONITORING AGENCY NAME & ADDRESS(if different from Controlling Office)		15. SECURITY CLASS. (of this report) Unclassified
		15a. DECLASSIFICATION/DOWNGRADING SCHEDULE

16. DISTRIBUTION STATEMENT (of this Report)

Approved for public release; distribution unlimited.

17. DISTRIBUTION STATEMENT (of the abstract entered in Block 20, if different from Report)

18. SUPPLEMENTARY NOTES

19. KEY WORDS (Continue on reverse side if necessary and identify by block number)

Horizontal Tube Bundle
Heat Transfer Coefficients
Vapor Velocity
Condensate Inundation

20. ABSTRACT (Continue on reverse side if necessary and identify by block number)

A five-tube column test condenser was modified to facilitate easier tube removal and installation and to allow for the simulation of larger depth tube bundles. Heat transfer coefficients were then determined for sixty-two runs conducted at steam supply pressures of 35, 40, 45, and 50 psig with the system operated at test condenser pressures of approximately 2 and 15

DD FORM 1473 EDITION OF 1 NOV 65 IS OBSOLETE
1 JAN 73
S/N 0102-014-6601

psia. Each run was five minutes long with temperature, pressure, and flow rate data taken at one minute intervals.

The results revealed that the average tube wall temperature and the heat transfer coefficients for a given tube of a tube bundle increased as the mean vapor velocity increased, but decreased as the amount of condensate inundation increased. The experimentally obtained values for the heat transfer coefficients were compatible with the Nusselt predictions for the runs conducted at 15 psia, but greatly exceeded the Nusselt predictions for the runs conducted at 2 psia. However, for the 2 psia runs, the heat transfer coefficients for the top tubes agreed closely with an experimental correlation proposed by Fujii. The simulation of a tube bundle of more than five active tubes per column at the 2 psia test condenser pressure demonstrated heat transfer coefficients closer to the Nusselt theory than when only five active tubes were considered.

Recommendations to improve the test apparatus and to conduct additional tests are provided.

Effects of Condensate Inundation
and Vapor Velocity on Heat
Transfer in a Condenser Tube Bundle

by

Paul Jeffrey Noftz
Lieutenant, United States Navy
B.S., Ohio University, 1972

Submitted in partial fulfillment
of the requirements for the degree of

MASTER OF SCIENCE IN MECHANICAL ENGINEERING

from the

NAVAL POSTGRADUATE SCHOOL
June 1982

Author _____

Approved by: _____
Thesis Advisor

_____
Chairman, Department of Mechanical Engineering

_____
Dean of Science and Engineering

3

ABSTRACT

A five tube column test condenser was modified to facili-
tate easier tube removal and installation and to allow for
the simulation of larger depth tube bundles. Heat transfer
coefficients were then determined for sixty-two runs conducted
at steam supply pressures of 35, 40, 45, and 50 psig with the
system operated at test condenser pressures of approximately
2 and 15 psia. Each run was five minutes long with tempera-
ture, pressure, and flow rate data taken at one minute intervals.

The results revealed that the average tube wall tempera-
ture and the heat transfer coefficients for a given tube of a
tube bundle increased as the mean vapor velocity increased,
but decreased as the amount of condensate inundation increased.
The experimentally obtained values for the heat transfer coef-
ficients were compatible with the Nusselt predictions for the
runs conducted at 15 psia, but greatly exceeded the Nusselt
predictions for the runs conducted at 2 psia. However, for
the 2 psia runs, the heat transfer coefficients for the top
tubes agreed closely with an experimental correlation proposed
by Fujii. The simulation of a tube bundle of more than five
active tubes per column at the 2 psia test condenser pressure
demonstrated heat transfer coefficients closer to the Nusselt
theory than when only five active tubes were considered.

Recommendations to improve the test apparatus and to con-
duct additional tests are provided.

TABLE OF CONTENTS

5

LIST OF TABLES

LIST OF FIGURES

9

NOMENCLATURE

A	Heat transfer area of one tube (m^2).
A_i	Heat transfer area of i th tube (m^2).
A_{mf}	Mean flow area of condenser cross-section (m^2).
C	Specific heat at constant pressure (kJ/kg $\cdot$ $^\circ$C).
C_i	Specific heat at constant pressure, i th tube (kJ/kg $\cdot$ $^\circ$C).
C_p	Specific heat at constant pressure (kJ/kg $\cdot$ $^\circ$C).
D	Outside diameter (m).
d	Outside diameter (m).
d_o	Outside diameter (m).
g	Acceleration of gravity (9.81 m/s^2).
h	Heat transfer coefficient (kw/m^2 $\cdot$ $^\circ$C).
h_i	Experimentally determined value for the heat transfer coefficient of the i th tube (kw/m^2 $\cdot$ $^\circ$C).
h_{fg}	Latent heat of vaporization (kJ/kg).
h_N	Local heat transfer coefficient for the N th tube (kW/m^2 $\cdot$ $^\circ$C).
$\tilde{h}_N$	Average heat transfer coefficient for a column of N tubes (kW/m^2 $\cdot$ $^\circ$C).
h_{Nu}	Heat transfer coefficient calculated from the Nusselt equation (kW/m^2 $\cdot$ $^\circ$C).
h_o	Heat transfer coefficient derived from the Fujii correlation (kW/m^2 $\cdot$ $^\circ$C).

10

k Thermal conductivity ($w/m \cdot {}^{\circ}C$).

k_L Thermal conductivity, liquid ($w/m \cdot {}^{\circ}C$).

$\dot{m}$ Mass flow rate of cooling water (kg/s).

$\dot{m}_i$ Mass flow rate of cooling water for the i th tube (kg/s).

$\dot{m}_{COND}$ Total mass flow rate of the condensate (kg/s).

N The number of tubes in a column, or the tube number of a given tube.

N_c The number of unit cells across the width of a condenser.

Nu_m Mean Nusselt number for a tube.

Nu_m^o Mean Nusselt number for a tube without inundation.

Pr Prandtl number.

P_{ss} Supply steam pressure (psig).

P_T Condenser pitch to diameter ratio.

P_{TC} Test condenser pressure (mm Hg abs.).

q Heat transferred per unit time (kW).

q_i Heat transferred per unit time for the i th tube (kW).

q/A Heat flux (kW/m^2).

Re_L Two phase Reynolds number, $U_\infty d_o/\nu_L$.

S/D Spacing to diameter ratio, same as P_T.

T_{ci} Cooling water inlet temperature (${}^{\circ}C$).

T_{co} Cooling water outlet temperature (${}^{\circ}C$).

T_s Saturation temperature of steam (${}^{\circ}C$).

T_v Vapor (steam) temperature (${}^{\circ}C$).

$\overline{T}_w$	Average tube wall temperature ($^{\circ}$C).
U_∞	Vapor velocity (m/s).
v	Specific volume of the steam (m^3/kg).
$\dot{V}_d$	Volumetric flow rate of water to the desuperheater (ml/min).
V_m	Vapor velocity based on the mean flow area (m/s).
$\dot{V}_{PT}$	Volumetric flow rate of water to the porous tube (m/s).
$\dot{V}_{SC}$	Volumetric flow rate of condensate from the secondary condenser (ml/min).
$\dot{V}_{TC}$	Volumetric flow rate of condensate from the test condenser, condensation rate (ml/min).
w	The amount of condensate formed on the N th tube per unit time as used in Equation (5); the rate of inundation falling onto a tube as used in Equation (10).
W	The amount of condensate draining onto the N th tube, Equation (5).
w°	The rate of condensation on a tube corresponding to Nu°, Equation (10).
ΔT	Temperature difference ($^{\circ}$C).
ξ	Acceleration parameter ($k\Delta T/\mu h_{fg}$).
ν	Kinematic viscosity (m^2/hr).
μ	Dynamic viscosity (kg/m-s).
ζ	Heat capacity parameter ($C_p T/h_{fg}$)
ρ	Density (kg/m^3).
ρ_v	Vapor density (kg/m^3).

ACKNOWLEDGEMENT

I dedicate this thesis to my wife, Nida, and daughters, Pamela and Ericka, through whose sacrifice, patience, and moral support this study was made possible.

I would also like to express my sincerest appreciation to my thesis advisor, Dr. Paul J. Marto, for his assistance and direction throughout the preparation of this thesis and to the Model Shop personnel, headed by Mr. Ken Mothersell, for their technical assistance and support.

I. HISTORICAL BACKGROUND

A continuing interest exists in the Navy to design smaller and lighter marine steam condensers by the use of enhanced heat transfer techniques. This is an outgrowth of recent improvements in turbine machinery and boiler design which have brought about increases in the horsepower to weight ratio of marine propulsion plants, but with the lack of similar improvements made to condenser design. Through the application of enhanced heat transfer techniques to condenser design, further significant increases in the horsepower to weight ratio can be attained and/or steam cycle efficiency can be further increased.

Marine steam condenser design is currently based upon the Heat Exchange Institute (HEI) standards for steam condensers [Ref. 1] and the standards of the Tubular Exchanger Manufacturers Association (TEMA) [Ref. 2]. Search [Ref. 3] studied existing marine steam condensers to determine the feasibility of improving condenser performance by enhanced heat transfer techniques and concluded that these techniques could result in a forty percent reduction in condenser weight and volume, indicating a need to establish new design criteria for marine steam condensers.

Beck [Ref. 4], Pence [Ref. 5], Reilly [Ref. 6], Fenner [Ref. 7], and Ciftci [Ref. 3] conducted experimental research into various kinds of enhancement using a single tube heat

transfer apparatus. The above investigations determined
that for the same diameter tube, the overall heat transfer
coefficients of enhanced tubes exceeded those for smooth
tubes by almost 100%.

Marto, Reilly, and Fenner [Ref. 9] determined that most
of the improvement occurred on the cooling water side of the
tube due to a combination of increased surface area and an
increased turbulence and swirl in the cooling water flow.
This gain in heat transfer was accomplished at the expense
of a substantial increase in the cooling water pressure drop
due to friction factors as much as ten times larger than for
smooth tubes. They also noted that enhanced tubes with deep
grooves had the best heat transfer performance, and that for
a given tube geometry at constant groove depth, heat transfer
performance was dependent upon the groove pitch or helix angle.

To fully evaluate the outside heat transfer performance
of enhanced tubes, it was required to consider the effects
of condensate inundation and vapor velocity. Demirel [Ref. 10]
and Eshleman [Ref. 11] consecutively modified the test appara-
tus originally designed by Beck (for single tube experimenta-
tion) to study the effects of condensate inundation on a
column of five horizontal, smooth tubes in a staggered arrange-
ment. Their work was inconclusive however, since problems
with non-condensable gases, side drainage, and secondary steam
flow within the condenser resulted in ambiguous tube perfor-
mance data for the bottom two tubes.

15

A new test apparatus was designed by Morrison [Ref. 12] in an attempt to eliminate the problems encountered by Demirel and Eshleman, and to provide a system which would operate closer to the conditions of the Nusselt theory. Morrison's test condenser was smaller in length than that of Demirel and Eshleman and employed a new diffuser section at the steam inlet in an attempt to eliminate the secondary steam flow. The condenser tubes were also arranged in-line vice staggered to assist in the reduction of side drainage. The above factors also allowed for more efficient removal of non-condensable gases by the steam flow through the condenser. Thermocouples were also installed within the active tube walls so that direct calculation of the outside heat transfer coefficients was possible. Preliminary data taken after the publication of Morrison's work indicated that the apparatus was suitable for condensate inundation studies, producing tube performances in close accordance with the Nusselt theory.

Though Morrison's test apparatus eliminated or reduced the problems encountered by Demirel and Eshleman, several other problems were noted. Air leaks at the joints and welds limited the vacuum that could be attained and introduced non-condensable gases into the system. The tube wall thermocouples were very fragile and broke easily when tubes were installed or removed. This was compounded by the fact that the O-ring tube sealing method used required considerable force to be applied to the tubes during installation and removal. Dropwise condensation

persisted on the upper two tubes despite the use of various tube cleaning methods, and the difficulty of tube removal and reinstallation limited the frequency of thorough tube cleaning.

The objectives of this thesis were therefore to:

1. Further modify Morrison's test apparatus to eliminate or reduce the tube wall thermocouple breakage and the active tube removal and reinstallation problems.

2. Establish a tube cleaning procedure to eliminate or reduce the dropwise condensation problem.

3. Further modify Morrison's test apparatus through the inclusion of a porous, water supply tube above the first of five active tubes such that the apparatus could be used to simulate tubes in larger tube bundles.

4. Obtain baseline heat transfer performance data for the test condenser utilizing 16 mm O.D. smooth copper tubes.

II. THEORETICAL BACKGROUND

Nusselt's theory of film condensation, based on work completed in 1916, provided the basis for most of the knowledge developed to date in regard to condensation on plates and horizontal tubes. Nusselt's work was based on the following assumptions for single tubes as noted by Nobbs [Ref. 13]:

1. The wall temperature is constant.

2. The flow is laminar in the condensate film.

3. Heat transfer in the condensate is by conduction, and subcooling may be neglected.

4. The fluid properties are constant within the condensate film.

5. The forces due to hydrostatic pressure, surface tension, inertia, and vapor-liquid interfacial shear are negligible when compared to the viscous and gravitational forces.

6. The surrounding steam and vapor/liquid interface are at saturation temperature.

7. The film thickness is small when compared with normal tube diameters and the effects of curvature are small.

When a column of tubes is to be considered, Eissenberg [Ref. 14] noted that the following two added assumptions are required:

18

8. Condensate drains as a laminar sheet from a tube bottom to a tube top such that velocity and temperature gradients are not lost in the fall between tubes.

9. The saturation temperature and the tube wall temperature are constant for all tubes in the bank.

For a single horizontal tube, Nusselt determined that the outside heat transfer coefficient could be obtained from the equation:

$$h_{Nu} = .725 \left[\frac{k^3 \rho (\rho - \rho_v) h_{fg} g}{\mu D (T_s - T_w)} \right]^{1/4} \tag{1}$$

where,

k = thermal conductivity of the condensate

ρ = density of the condensate

ρ_v = density of the vapor

h_{fg} = latent heat of vaporization

g = acceleration of gravity

μ = dynamic viscosity of the condensate

D = outside diameter of the tube

T_s = temperature of the steam

T_w = average tube wall temperature

Jacob [Ref. 15] determined that for a tube column of N tubes, an average outside heat transfer coefficient for the column, $\bar{h}_N$, could be obtained from the equation:

$$\bar{h}_N = .725 \left[\frac{k^3 \, \rho \, (\rho - \rho_v) \, h_{fg} \, g}{\mu \, ND \, (T_s - T_w)} \right]^{1/4} \qquad (2)$$

Using equations (1) and (2), the Nusselt result is normally expressed as the ratio of the average heat transfer coefficient ($\bar{h}_N$) to the heat transfer coefficient of the top tube (h_{Nu}):

$$\frac{\bar{h}_N}{h_{Nu}} = N^{-1/4} \qquad (3)$$

It may also be expressed as the ratio of the local heat transfer coefficient of a given tube in a column to the heat transfer coefficient of the top tube:

$$\frac{h_N}{h_{Nu}} = N^{3/4} - (N - 1)^{3/4} \qquad (4)$$

It has been noted that most experimentally determined results are on the order of twenty percent greater than those obtained from the above equations. This is due to the nature of the assumptions made in the derivation of Nusselt's theory. In actual marine steam condensers, the vapor can have a fairly high velocity over a large portion of its flow path; and under changing turbine speeds, the steam velocity is certainly not negligible. The vapor velocity causes vapor-liquid interfacial shear. With a downward flow of vapor and condensate, a shear force is added to the gravitational force. Consequently

as the condensate film velocity increases, the film thickness decreases and the heat transfer coefficient from the vapor to the wall increases.

Moreover, as noted by Kutateladze [Ref. 16]; Shklover and Buevich [Ref. 17]; Yung, Lorenz, and Ganic [Ref. 18]; and Eissenberg [Ref. 14], condensate does not flow from each tube as a continuous film or sheet. Instead, the condensate flows in the form of separate drops or streams. The condensate dripping from an upper tube will split around the tube below but will not flow axially; it may hit the lower tube off-center or may miss the lower tube altogether, depending upon the tube bundle geometry. The thickness of the film on a lower tube can therefore vary greatly, and where thinnest, greatest heat transfer will occur.

Fuks [Ref. 19] developed an experimental correlation for the normalized local heat transfer coefficient in the form:

$$\frac{h_N}{h_1} = [\frac{W + w}{w}]^{-0.07} = N^{-0.07} \tag{5}$$

Where W is the amount of condensate draining onto the N th tube per unit time and w is the amount of condensate formed on the N th tube per unit time.

Chen [Ref. 20] derived a formula which considered boundary conditions influenced by:

1. the momentum gain of the falling condensate between tubes, and

2. the condensation of vapor on the condensate between tubes.

His result was:

$$\frac{\bar{h}_N}{h_{Nu}} = N^{-1/4} \left[1 + 0.2\zeta(N-1) \left[\frac{1 - 0.68 \zeta + 0.02 \zeta \xi}{1 + 0.95 \xi - 0.15 \zeta \xi} \right] \right]^{1/4} \quad (6)$$

where,

$\xi = K\Delta T/\mu h_{fg}$

$\zeta = C_p \Delta T/h_{fg}$

and,

$\xi = \zeta/Pr$.

Eissenberg [Ref. 14] experimentally investigated the effects of steam velocity, condensate inundation, and non-condensable gases on the heat transfer coefficient. Based on the results of those experiments, he developed a side drainage model for staggered tube bundles by which condensate may drain onto tubes not directly below one another as depicted in Figure 1. For comparison to the above, Figure 2a depicts the Nusselt in-line tube bundle drainage model in which condensate drains to lower tubes in sheets; while Figure 2b illustrates a more realistic in-line tube bundle drainage model in which condensate drains to lower tubes in drops, with considerable splashing.

Eissenberg identified the following conditions as affecting side drainage:

22

1. Orientation - Staggered tube bundles are more suscep-
   tible to side drainage than in-line tube bundles;

2. Spacing - The smaller S/D is, the more frequently side
   drainage should occur;

3. Momentum - The greater the horizontal component of
   momentum of a drop leaving a tube, the greater the
   side drainage;

4. Steam velocity - When steam flows horizontally across
   tubes at sufficient velocity, the drop trajectory will
   reflect the added lateral momentum. When steam flows
   vertically, its direction change with each tube may
   also impart lateral momentum to the drops; and

5. Misaligned tubes - A tube misaligned in a bundle may
   receive greater or lesser amounts of condensate depend-
   ing on its orientation with respect to the side tubes.

Utilizing a pure side drainage model for a staggered tube
bundle, Eissenberg obtained:

$$\frac{\bar{h}_N}{h_{Nu}} = 0.60 + 0.42 \, N^{-1/4} \tag{7}$$

Since experimental results deviate from each other and
from the Nusselt theory, results are often fitted to the
following equation form:

$$\frac{\bar{h}_N}{h_{Nu}} = N^{-s} \tag{8}$$

23

where s is an experimentally determined exponent with a reported range of values of 0.07 to 0.20.

Nobbs [Ref. 13] concluded the following from his investigation of the combined effects of downward vapor velocity and condensate inundation on the rate of condensate formation in horizontal tube bundles:

1. Vapor velocity increases the condensate heat transfer coefficient on both inundated and uninundated tubes in a tube bundle.

2. The effect of inundation is to reduce the heat transfer coefficient. The rate of reduction with increase in inundation rate becomes smaller as the vapor velocity is increased.

3. The condensate drainage path is often not vertically downwards but in a diagonal direction. This can result in tubes receiving differing amounts of inundation.

Fujii [Ref. 21] used the data obtained in the experiments of Nobbs and Mayhew to correlate the effects of inundation and vapor velocity. For the top or uninundated tube in an in-line tube bundle, the following equation was obtained:

$$Nu_m^o = 10.74 \ Re_L^{0.312} \tag{9}$$

where

Nu_m^o = Nusselt number, $h_o d_o / k_L$, for steam without inundation

24

Re_L = two-phase Reynolds number, $U_\infty d_O / \nu_L$

k_L = thermal conductivity of liquid

d_O = outside diameter of tube

ν_L = kinematic viscosity of liquid

U_∞ = vapor velocity

For any tube in an in-line tube bundle, Fujii also obtained the equation:

$$\frac{Nu_m}{Nu_m^O} = \left(\frac{Re_L}{2 \times 10^6} \right)^{0.071\,(w/w^O)^{0.65}} \tag{10}$$

where,

Nu_m = mean Nusselt number for a tube

w = rate of inundation falling onto a tube

w^O = rate of condensation of a tube corresponding to Nu_m^O

When calculating vapor velocity, most studies have used the entrance vapor velocity which is based upon the condenser cross-sectional area. However, as steam flows through a condenser, its velocity is alternately increased and decreased due to the restriction in actual flow area caused by the tubes. Therefore, using the entrance velocity (or for that matter, the maximum velocity obtained at the point of minimum flow area) does not result in a true picture of the effect of vapor velocity on heat transfer. Nobbs [Ref. 13] used a mean velocity of vapor based upon a mean flow width. Figures 3

25

and 4 show the derivations of the mean flow width for the cases of a square pitch and an equilateral triangle tube bundle, respectively. From these Figures one can obtain for the in-line or square pitch tube bundle:

$$A_{mf} = N_c \, dL \, (P_T - \pi/4 P_T) \qquad (11)$$

where,

A_{mf} = mean flow area

N_c = number of unit cells

d = tube outside diameter

P_T = tube pitch to diameter ratio

L = tube length

Then, for the purposes of mean vapor velocity calculations and for use in Equation (9), the following was used in this study:

$$V_m = \frac{\dot{m}_{COND} \, v}{A_{mf}} \qquad (12)$$

where,

V_m = mean vapor velocity

$\dot{m}_{COND}$ = mass flow rate of condensate

v = specific volume of vapor at the steam saturation temperature

Note that although the above is an improvement over the use of the entrance vapor velocity, it does not account for the decrease in vapor velocity through the tube bundle due to the reduction in the amount of steam flow due to the condensation of the steam.

Figure 5 compares the equations of Nusselt (Equation 3), Eissenberg (Equation 7), and Chen (Equation 6) for $\bar{h}_N/h_{Nu}$. Figure 6 compares the equations of Nusselt (Equation 4) and Fuks (Equation 5) for h_N/h_1.

III. EXPERIMENTAL APPARATUS

The test apparatus designed by Morrison [Ref. 13] was
modified to allow for the simulation of an active tube column
having a number of tubes in increments of five tubes deep
(five, ten, fifteen, etc. tubes deep) and to correct the design
deficiencies noted above. Some components of the original test
apparatus were also relocated to allow for more efficient opera-
tion of the system. The following system descriptions update
those presented in Morrison's thesis to incorporate the modifi-
cations that were made. Figures 7a and 7b, and the key thereto,
show the assembled test apparatus as modified and detail the
major components.

A. TEST CONDENSER

The test condenser, shown in Figures 8-12, measured 305 mm
x 305 mm x 79 mm and was made of stainless steel. The dimen-
sions allowed for a maximum of twenty-seven 16 mm O.D. tubes
arranged in an in-line configuration of three columns of nine
tubes each. However, the in-line tube configuration initially
used was one of a column of five active tubes flanked on
either side by a column of five dummy tubes. Directly above
the upper active tube, a porous, distilled water supply tube
was positioned, flanked on either side by dummy tubes.

The square in-line arrangement of tubes with a spacing-to-diameter ratio of 1.5 was utilized for the conducted experiments. However, the test section design allowed for the rearrangment of dummy tubes to give a staggered arrangement as well. This was made possible by machining slots in the end plates of the test condenser and providing tube sheets for the dummy tubes which fit into the slots such that they could be changed to suit the type of arrangement desired. Each end of the dummy tubes was inserted into its respective tube sheet, and the tube sheets were then slid into the end plate slots and secured into place by screws.

An opening (Fig. 12) running vertically along the center-line of each condenser end plate provided for active and porous tube penetration of the test section. The tubes were then fixed in position, with a spacing-to-diameter ratio of 1.5, by means of nylon tube sheets that were attached to the exterior of the condenser end plates. A new set of tube sheets would be required for each desired spacing-to-diameter ratio.

To facilitate ease of active tube removal and installation, and to prevent damage to the thermocouples soldered into the active tube walls, the tube sheets and tube sealing method were redesigned. For each test condenser side, a nylon tube sheet one inch thick was fabricated with six holes (S/D=1.5) such that about 0.5 mm tube clearance existed which allowed for the tubes to be easily slid in or out of the tube sheets. Grooves were machined into the exterior side of each tube sheet

29

around each hole to accommodate O-rings. The aluminum tube
sheets from the original test condenser, but with a sixth hole
added and all holes machined to about a 0.5 mm tube clearance,
were then used as sealing plates. When installed, rubber
gaskets were placed between the test condenser end plates and
the nylon tube sheets; O-rings were placed in the tube sheet
grooves; and the aluminum seal plates were positioned on the
tube sheets. These assemblies were then secured to the test
condenser end plates by means of screws. With the screws
loosened, the active tubes could be readily removed or in-
stalled; but when the screws were tightened down with the
tubes in place, the O-rings were sufficiently compressed
around the tubes to provide a tight seal.

The diffuser, exhaust plenum, transition piece, vortex
annihilator, and the exhaust and condensate piping (Figs.
8-10) as well as the viewing window were unchanged from
Morrison's design.

3. TEST CONDENSER TUBES

The active tubes were made of 16 mm O.D. half hard, smooth
copper tubes with a 1.65 mm wall thickness. In Morrison's
original apparatus, the active tubes extended through the tube
sheets such that the portion of the tubes extending outside
of the test condenser acted as highly conductive fins. New
active tubes were made approximately 305 mm long, the width
of the test condenser, with 16 mm O.D. stainless steel tube

extensions fixed to each end of the active tubes for the pur-
pose of tube sealing and connection to the cooling water supply
and discharge lines.

Four thermocouples were soldered into grooves 90 degrees
apart within the wall of each active tube such that the sensing
portion of each thermocouple was about at the midpoint of the
wall thickness. The grooves extended from the center of each
copper section axially about 15 cm into the stainless steel
extension. Upon completion of the soldering, the soldered
surfaces of the tubes were ground and tubes polished so that
the tube surfaces were as uniformly smooth as possible. The
high thermal conductivity of the copper tubes and silver solder
ensured that the thermocouples gave reasonably accurate measure-
ment of the tube wall temperature. The free ends of the thermo-
couples were secured to the tubes with tape to minimize the
risk of damage.

The dummy tubes flanking the active tubes were made of 16
mm O.D. stainless steel. These tubes served to direct the
steam flow so as to simulate actual conditions in a condenser.
Cooling water was not supplied to these tubes and they did not
penetrate the test condenser end plates.

C. POROUS TUBE WATER SUPPLY SYSTEM

As shown in Figure 13, this system consisted of a porous,
water supply tube (positioned above the uppermost active tube),
a water heater which served as a supply tank, a rotameter to

regulate the amount of water supplied to the porous tube, a pump driven by a 1/2 HP electric motor, and associated piping and valves.

The stainless steel porous tube was 305 mm long, the length of the test condenser, with non-porous stainless steel tube extensions silver soldered on to each end for the purpose of tube sealing and connection to the supply tubing. Water entered one end of this tube; the other end was blanked off.

The supply tank was a 25 gallon hot water heater which was modified by the replacement of its thermostatic control with a more accurate temperature controller. The temperature controller was capable of maintaining the water temperature to within approximately $1^{\circ}C$ of its set point. To aid in keeping the active tubes free of contamination that could lead to drop-wise condensation, distilled water was used exclusively in this system. The water was pumped to the rotameter by the 1/2 HP electric motor driven pump, and by regulating the rotameter and the tank's recirculation valve, the flow rate to the porous tube could be controlled with reasonable accuracy.

The system was used to supply water to the top active tube of the test condenser at the existing condenser steam saturation temperature. By this method, the five active tubes installed in the test condenser could be inundated with condensate from above to simulate a tube column of more than the five active tubes.

C. CONDENSATE SYSTEM

The condensate system, as shown in Figure 14, was composed
of the test condenser and hotwell, the secondary condenser and
hotwell, the condensate pump, and associated piping and valves.
The only modifications to this sytem were those to the test
condenser noted above.

The test condenser and secondary condenser hotwell sight
glasses were calibrated so that the amount of condensate pro-
duced could be measured. The condensate formed in the test
condenser was collected in the test condenser hotwell by closing
valve C-1. Opening the valve allowed the condensate to be
gravity fed to the secondary condenser hotwell. Additionally,
condensate in the secondary hotwell was obtained from the
secondary condenser, which condensed all steam not condensed
in the test condenser, and from the desuperheater drain. All
condensate collected in the secondary condenser hotwell could
be removed by means of an electrically driven condensate pump
(1/2 HP) and dumped into the building's drainage system.

By measuring the condensate produced per unit time in the
test condenser, the porous tube rotameter could be set to
increment the condensate to the top tube to simulate additional
tubes. By measuring the total amount of condensate produced
per unit time, in both the test and secondary condensers and
substracting the amount of water supplied to the porous tube,
the vapor velocity could be calculated as previously noted.

33

E. STEAM SYSTEM

The steam system, shown in Figure 15, was unchanged from
Morrison's design. The steam used for the test apparatus was
locally generated house steam. A 19 mm O.D. stainless steel
line supplied steam through a steam supply valve, MS-3, to a
cost iron steam separator. Downstream of the separator, a
19 mm O.D. stainless steel line supplied steam to two Nupro
bellows valves which were used in conjunction with the supply
valve to regulate the steam supply pressure. From these valves,
the steam was fed through another 19 mm O.D. stainless steel
line to the desuperheater, and from the desuperheater through
a 64 mm I.D. stainless steel pipe to the test condenser diffuser.
The steam supply pressure was monitored by a gage just down-
stream of the steam supply valve. A compound gage downstream
of the Nupro valves could be used to monitor the pressure drop
across the valves if desired.

Since house steam was used, the operator had no control
over the state point, quality, non-condensable gas content,
or contamination of the supply steam. Moreover, it was not
practically or economically feasible to monitor these condi-
tions at the time experiments were conducted.

F. COOLING WATER SYSTEM

The cooling water system was a shown in Figure 13. Normal
house water was utilized for the test apparatus, with the
water stored in a 1.2 meter cubical plexiglass tank. The

water was pumped from the supply tank by a 5 HP electrically
driven pump through a 51 mm O.D. plastic pipe to a header.
Five rotameters were connected to the header, with each used
to control the flow through a separate active tube. The water
leaving the rotameters passed through 16 mm O.D. stainless
steel tubing to the active tubes. These tube runs were at
least 1.8 m long to ensure fully developed flow going into the
test condenser. The water leaving the active tubes was returned
to the supply tank where a 7 1/2 HP electrically driven pump dis-
charged the water through a filter to a cooling tower to main-
tain a constant cooling water supply temperature and to keep
the water as clean as possible. The cooling tower was located
outside the building and consisted of four truck radiators
across which air was blown by a fan. The heat exchanger and
fan were enclosed in a wooden structure with louvered openings
for ventilation.

The tubing runs between the rotameters and active tubes
were divided into several sections. A 45 cm section was con-
nected, by 5 cm lengths of tygon tubing and hose clamps, to
each active tube and to a 12 cm section which housed the cool-
ing water inlet thermocouples. The 12 cm sections were then
connected, by 5 cm lengths of tygon tubing and hose clamps,
to the cooling water supply line. Thus on the inlet side, the
cooling water lines could be readily disassembled to facili-
tate active tube removal and installation or repairs to the
thermocouples. On the outlet side of the test condenser, 12 cm

35

sections containing the outlet cooling water thermocouples were connected, again by tygon tubing and hose clamps, to the active tubes and the discharge piping.

G. VACUUM SYSTEM

As shown in Figure 14, an air driven air ejector was utilized to remove the non-condensable gases and to maintain the test condenser vacuum as per Morrison's design. The air ejector pulled a suction on the secondary condenser hotwell and discharged through a muffler to reduce the noise hazard. Air was supplied to the air ejector at minimum of about 100 psig from an Ingersol-Rand air compressor. The system was capable of maintaining a minimum test condenser vacuum of about 100 mm Hg absolute.

H. DESUPERHEATER SYSTEM

The desuperheater system, shown in Figure 15, was used to control the steam inlet temperature to the test condenser so that a maximum of 10°C superheat was maintained. This was necessary to avoid a correction to the heat transfer coefficients for h_{fg}. In practice, the desuperheater was not required for the atmospheric pressure runs, but was used for the vacuum runs for which the degree of superheat was controlled to about 2°C of superheat.

The system consisted of a desuperheater tank, a water supply tank, a 1/3 HP electrically driven pump, a rotameter and associated piping and valves. The desuperheater was

constructed of a stainless steel tank, 318 mm in diameter and 508 mm in height. The tank top was welded onto the discharge pipe and was then bolted onto the tank. A rubber gasket provided for sealing between the tank and the tank top. Four fan type spray nozzles were inserted equidistant around the circumference and approximately 10 cm from the top of the desuperheater to supply the cooling water in a fine spray. A drain line was also installed in the base of the desuperheater tank.

Cooling water, distilled to aid in active tube cleanliness, was stored in a 10 gallon aluminum tank. The water was pumped from the tank through 9 mm O.D. copper tubing to a rotameter and valve and then to the spray nozzles.

I. INSTRUMENTATION

1. Flow Rates

a. The cooling water flow rate was measured separately for each active tube through the use of rotameters. Starting from the top active tube to the bottom active tube, the supplying rotameters had calibrated 100% maximum flow rates of 18.5 ± 0.2, 18.5 ± 0.2, 13.5 ± 0.2, 19.2 ± 0.2, and 17.6 ± 0.2 GPM.

b. The desuperheater cooling water flow rate was measured by a rotameter having a calibrated 100% maximum flow rate of 1242 ± 12 ml/min.

c. The porous tube water supply flow rate was measured by a rotameter having a calibrated 100% maximum flow rate of 999 ± 10 ml/min.

d. All rotameters were calibrated using the procedure listed in Appendix A of Reference 5.

2. Temperatures

Stainless steel sheathed copper-constantan thermocouples were utilized as the temperature monitoring devices. Figure 16 shows the locations of the thermocouples. Two thermocouples measured the cooling water inlet temperature, and three measured the cooling water outlet temperature for each active tube in an attempt to obtain an accurate bulk temperature at each sensing location. Four 0.51 mm O.D. thermocouples were silver soldered into axial grooves within the wall of the active tubes as noted above. Additionally, thermocouples were used to monitor the test condenser steam inlet temperature and the temperature of the condensate in the test condenser hotwell. All thermocouples were calibrated following the procedure of Appendix A of Reference 5.

A Gulton Industries, West 20, 0-500°F temperature controller was used to control the temperature of the porous tube supply water. The controller had a manufacturers stated accuracy of ± 0.5% of the span (about ± 1.25°F).

3. Pressure

a. The steam supply pressure was monitored by a Bourdon tube gage just downstream of the steam supply valve.

38

b.   The test condenser pressure was monitored by a mercury manometer and by a pressure transducer. The pressure transducer was calibrated against a mercury manometer.

c.   Pressure gages were also used to monitor the test condenser pressure, the secondary condenser hotwell pressure, and the pressure downstream of the Nupro valves. These gages were used strictly for system operation purposes.

4.   Data Collection and Display

An Autodata Nine Scanner was used to record and display the thermocouple and pressure transducer readouts. The temperatures were recorded in degrees Celsius, while the pressure was recorded as a voltage which was converted to a reading in mm Hg absolute by a calibration chart. The pressure transducer was assigned to channel 1 of the Autodata Nine Scanner, while the thermocouples were assigned channels as indicated in Table I.

IV. PROCEDURES

A. OPERATING PROCEDURES

1. Tube Preparation

Prior to installation, and periodically thereafter, each active tube was prepared in accordance with the cleaning procedure outlined in Appendix A of Reference 8. In addition, as a part of the light-off procedure of the test apparatus, the tubes were cleaned by running steam at atmospheric pressure through the test condenser for about twenty minutes without any cooling water flow through the tubes. During this steam cleaning operation, the tubes were periodically rinsed with distilled water utilizing the porous tube water supply system.

The above mentioned procedures were generally found to be sufficient to eliminate any visible signs of drop-wise condensation on the active tubes. When drop-wise condensation did occur during the progress of a day's set of runs, it was discovered that simply rinsing the tubes using the porous tube water supply system was sufficient to restore film-wise condensation.

2. System Operation and Steady State Conditions

Complete operating instructions are listed in Appendix A and Appendix B.

A steady state condition was considered achieved when the cooling water inlet temperature did not vary more than ± 0.6°C/HR and the steam inlet temperature did not vary more than ± 0.3°C/min. In general, a steady state condition was reached about two hours after initial system light-off and about fifteen to thirty minutes after changes to the cooling water or porous tube supply water flow rates.

Once a steady state condition was obtained, the runs were made. The length of each run, or each increment of five tubes, was five minutes. The following data were taken at one minute intervals for each run:

   a. the test condenser and secondary condenser

       hotwell levels,

   b. the manometer reading,

   c. the steam supply pressure,

   d. the setting of each rotameter,

   e. the thermocouple readings, and

   f. the pressure transducer reading

B. DATA REDUCTION PROCEDURES

To simplify the data reduction, actual tube wall temperatures were obtained. Utilizing the wall temperatures directly eliminated the necessity of using the Wilson Plot technique for calculating the steam side heat transfer coefficient. The following approach, that of using standard heat transfer equations and an energy balance, was used to evaluate the raw data:

41

1. <u>Total Heat Transferred per Tube</u>

$$q_i = \dot{m}_i c_i (T_{co} - T_{ci})_i \qquad (10)$$

where,

q_i = total heat transferred for tube i per unit time [kW]

m_i = cooling water mass flow rate for tube i [kg/s]

$(T_{co}-T_{ci})_i$ = the difference between the outlet and inlet cooling water temperature for tube i [$^\circ$C]

c_i = the specific heat of the cooling water [kJ/kg $\cdot$ $^\circ$C]

2. <u>Steam Side Heat Transfer Coefficient</u>

$$h_i = q_i/A_i (T_s - \overline{T}_w) \qquad (11)$$

where,

h_i = the steam side heat transfer coefficient for tube i [kW/m^2 $\cdot$ $^\circ$C]

A_i = the heat transfer area, m^2

T_s = the steam saturation temperature [$^\circ$C]

$\overline{T}_w$ = the average tube wall temperature [$^\circ$C]

Sample calculations are presented in Appendix D.

The steam side heat transfer coefficient was the parameter used to determine the performance of a tube in the tube bundle. Three assumptions were made in applying Equation (11) to the data obtained from the experiment:

42

1. The resistance due to non-condensable gases was negligible. The system was checked for tightness and was found to be satisfactory. Non-condensable gases brought in by the steam were exhausted by the air ejector as the good steam flow conditions in the test condenser continually swept non-condensable gases away from the active tubes.

2. The resistance of the copper active tubes was considered negligible. The calculated $1^{\circ}C$ ΔT across the tube wall was accounted for by assigning a significant uncertainty to the average tube wall temperature which was determined from the thermocouples.

3. Subcooling of the condensate film on the tube walls was neglected.

C. DATA REDUCTION PROGRAM

A computer program was utilized to analyze the data. The program was in Basic language and was run on an HP-35 computer system. A peripheral plotter was used to plot the results. The program is presented in Appendix E.

V.   RESULTS AND DISCUSSION

A.   BACKGROUND INFORMATION

Sixty-two runs were made. Runs 1-40 and Run 62 were con-
ducted with the test condenser at atmospheric pressure. Steam
supply pressures of 50 psig (Runs 1-10 and Run 62), 45 psig
(Runs 11-20), 40 psig (Runs 21-30), and 35 psig (Runs 31-40)
were utilized. To ensure that non-condensable gases were
flushed out of the test condenser, the above runs were con-
ducted with the steam exhaust pipe from the test condenser to
the secondary condenser disconnected and replaced by a 1.5 cm
O.D. pipe which dumped the exhaust steam into the bilges (as
shown in Figure 7a). Runs 41-61 were conducted under vacuum
at steam supply pressures of 35 psig (Runs 41-45), 40 psig
(Runs 46-50), 45 psig (Runs 51-55), and 50 psig (Runs 56-61).
All runs were made with a cooling water mass flow rate of
10.98 kg/min for each active tube. The desuperheater was
required for only the vacuum runs, for which a cooling water
volumetric flow rate of 100 ml/min was used. Runs 1-60 were
made with no water being supplied through the porous tube.
Using the porous tube water supply system to simulate addi-
tional tubes, Runs 61 and 62 were conducted for tube bundles
of 30 and 10 tubes deep, respectively.

The data collected for each run are shown in Tables II
through IV. It should be noted that the data shown are the

averages of the five data sets taken for each run, corrected
using thermocouple, pressure transducer, rotameter, and hot-
well volume calibration curves. A full set of data was
collected for the vacuum runs, but due to the dumping of
exhaust steam into the bilges during the atmospheric pressure
runs, the volumetric flow rate of condensate from the second-
ary condenser could not be measured. This also prohibited
vapor velocity calculation.

The calculated results are tabulated in Table V. The
results are presented to the appropriate number of significant
digits as determined from the uncertainty analysis presented
in Appendix D.

B. OBSERVATIONS

Film-wise condensation without any visible evidence of
drop-wise condensation was observed for all tubes during all
runs. This was accomplished by the cleaning procedures de-
tailed earlier. It must be noted that only the front half of
each tube could be viewed through the test condenser window,
therefore drop-wise condensation could have occurred unnoticed
on the back halves of the tubes. Based on the observation of
the active tubes and the tube wall temperature data, the
effect of drop-wise condensation was considered to be negligible.

Observation of the motion of the condensate drops during
both atmospheric pressure and vacuum conditions revealed a
general logitudinal drop migration on all tubes. The migration

45

was left to right under atmospheric pressure conditions and right to left under vacuum conditions. During several operations requiring the disassembly of the test condenser flanges, it was noted that the piping to and from the condenser did not align properly such that piping had to be forced into position for flange alignment and assembly. Apparently, when the steam exhaust pipe was disconnected for atmospheric pressure operation, the orientation of the test condenser changed, resulting in a change in the direction of drop migration. By adjustment of the leveling nuts on the test condenser support bracket, the amount of drop migration was reduced to a level at which its affect was considered negligible. It was also noted that at certain tube localities, drops moved randomly either left or right possibly due to localized tube irregularities since this observation was not widespread. All evidences of drop migration were then believed to have resulted from condenser leveling and tube irregularity problems, and not the result of secondary vapor flow.

The spacing of the tubes, 24 mm from tube center to tube center or 8 mm between tubes, led to several interesting condensate drop observations. Under of influence of low condensate production or inundation rates, the drops from an upper tube would break away and fall less than two millimeters before striking the tube below. As a consequence, no splashing occurred and the drops appeared to spread in all directions radially from the point of drop impact, incorporating into

46

the condensate film rather than rolling around the tube perimeter. At higher condensate rates, such as under atmospheric pressure or under inundation from the porous tube for vacuum runs, the condensate drops from the upper tube elongated all the distance to the next lower tube. The drops instantaneously joined the upper and lower tube and had the appearance of being sucked into the condensate film on the lower tube. It was also noted that as the condensation or inundation rate increased, drops formed at more locations along a given tube but that the ratios of drops per tube between the tubes remained nearly constant.

It is interesting to note that Shklover and Buevich [Ref. 17] conducted studies of drop behavior for condenser tubes spaced 8 mm apart. Though their operating conditions were not the same as used in this study, they observed similar behaviors as described above, except that they observed the drops to roll over the tube surface and did not observe the case in which the drop separated from the upper tube before reaching the lower tube.

C. AVERAGE TUBE WALL TEMPERATURES

As noted previously, the use of Equations (10) and (11) to calculate the steam side heat transfer coefficient was made possible by the installation of thermocouples 90° apart within the tube walls. However, the questions arose as to how accurately the average tube wall temperature could be

measured and how the average tube wall temperature was to be defined for the direct wall temperature measurement.

Figure 17 is a polar plot of a typical tube wall temperature distribution. It can be seen that the distribution is asymmetric with the majority of the tube surface area at a temperature higher than the average of the top and bottom wall temperatures. This is a consequence of the nonuniform nature of the condensate film thickness around the tube, with the film thickening from top to bottom. The film tends to insulate the wall, yielding lowest wall temperatures where the film is thickest.

The temperature distribution becomes even more complex when events which locally thicken or thin the condensate film are considered. A drop forming at the base of a tube or falling onto the top of the tube will cause temporary reduction in the wall temperature at the point of occurrence. A small area of drop-wise condensation or a localized turbulent eddy can locally increase the wall temperature. When side drainage occurs, a tube can have its condensate film either thinned or thickened resulting in a higher or lower wall temperature, respectively. Additionally, high vapor velocities can either strip away part of the film layer or cause increased drop splashing or rippling of the film all of which increase the tube wall temperature.

The above description demonstrates that the best approximation of the average wall temperature would be attained when the temperature was measured at as many points as possible over

48

the entire tube wall and for an extended period of time. Then, an average of all the data would be needed. The tube size, method of thermocouple installation, and the cost of the thermocouples limited the number of points of temperature measurement to four. Since the tube wall temperature would also vary through the wall thickness, it was decided to install the four thermocouples 90 degrees apart (top, bottom, and two sides) in grooves, as noted previously, such that the thermocouple sensing point would be at the midpoint of the wall thickness. Calculations made using the data obtained from the test runs revealed that the ΔT across the tube wall was, on the average, about $1^{\circ}C$. Therefore, fairly small deviations in thermocouple location could also have a significant effect on the calculated average tube wall temperature.

Considering all the above, and to avoid giving undue weight to the two side wall temperatures, it was decided that the best average tube wall temperature would be obtained by averaging the side wall temperatures, then averaging this result with the top and bottom wall temperatures. It was also decided that the average tube wall temperature must be considered to be subject to fairly significant uncertainty. Additionally, due to damage to thermocouples and the inability to replace them at the time tests were conducted, only the center active tube had a full compliment of thermocouples. Tubes 1, 4, and 5 had three thermocouples each (top, bottom, and side), while tube 2 had only two (top and bottom). For these partially

49

instrumented tubes, the average tube wall temperature was cal-
culated by averaging the readings from the available thermo-
couples. It should be noted that this situation was most
disadvantageous for the case of tube 2 since the wall tempera-
ture obtained for this tube was certainly lower than would be
measured with the side thermocouples available. In this
regard, it can be noted from the tube wall temperatures tab-
ulated in Table II, that the second tube consistently had an
average wall temperature much below that expected. Thus, to
be conservative, an uncertainty of $\pm 1.0^{\circ}C$ was assigned to all
wall temperatures.

We now turn to two other important considerations in regard
to the average wall temperatures. These are the effect of
vapor velocity on the average tube wall temperature and the
consideration of how the location of a tube in a tube bundle
affects its average wall temperature.

The average tube wall temperature should increase as the
vapor velocity increases. This is the result of increased
vapor shear which can thin the condensate film by causing
small portions of the film to be removed from the tube and
entrained in the vapor and by increasing the velocity of the
condensate flowing on the tube. For the vacuum condition
runs, where the mean vapor velocity was calculated, the re-
sults shown in Table VI confirm the increase in the average
tube wall temperature with increased mean vapor velocity even
for the relatively small vapor velocity increases indicated.

This could be seen for all five tubes of the tube bundle, but was most apparent for the first two tubes. Note also that the increase in the average tube wall temperature resulted in a dropping off of $T_s - \overline{T}_w$ which was manifested in a higher heat transfer coefficient with increased mean vapor velocity.

Figures 18 and 19 depict the decrease in the average tube wall temperature through a tube bundle. For the vacuum condition run (Run 61) and the atmospheric pressure run (Run 62), the general trend was one of a sharp initial drop in the average tube wall temperature over the upper tubes followed by a much more gradual reduction through the remainder of the tube bundle. This was best illustrated for Run 61 where about 70% of the total wall temperature drop occurred in the first ten tubes. These drops in the average tube wall temperature through a tube bundle can be attributed to a decreasing vapor velocity as the mass of the steam is reduced by condensation through the tube bundle and to an increasing amount of condensate inundation. Both of these factors would serve to lower the average tube wall temperatures by allowing for an increase in the condensate film thickness. It must be considered, however, that the above results were obtained through the use of the porous tube water supply system, the operation of which still requires refinement.

A study of Table II as well as Figures 18 and 19 demonstrated that the average tube wall temperatures for the second and fifth tubes of the test condenser were lower than would

be expected. This discrepancy for the second tube was due at least in part to the lack of functioning thermocouples on both sides of the tube. Additional test runs with complete instrumentation on this tube will be required before further explanation can be provided. In regard to the fifth tube, it must be noted that the vapor velocity across this tube will be reduced by the effect of an increase in the steam flow area below the tube due to the absence of additional tubes. This could significantly reduce the tube wall temperature. It is therefore considered advisable to install a row of dummy tubes below the fifth tube for test runs in which additional tubes are to be simulated. However, these dummy tube should be removed for runs in which additional tubes are not to be simulated.

D. SINGLE TUBE RESULTS

One method of gauging the validity of experimental results is to make comparisons with theoretical predictions and with experimental correlations. If one compares the results for only the top tube of the five active tube column used for the test runs with such predictions and correlations, then one cannot only determine the validity of the top (single) tube results, but also obtain a better insight into the validity of the multiple tube results.

Tables VII and VIII compare the experimentally obtained heat transfer coefficient (h_1) to the Nusselt prediction

(h_{Nu}) and to the Fujii correlation (h_o). Remember that h_1 was calculated from Equation (11), h_{Nu} from Equation (1), and h_o by using Equations (3) and (12).

Table VII displays the results for the atmospheric runs, with h_o not calculated since vapor velocities could not be determined. It should be noted that although the vapor velocities were unavailable, the vapor velocities should be decreasing from a highest value for Runs 1-10 to a lowest value for Runs 31-40 in response to decreasing steam supply pressure and therefore decreasing system pressure drops. Observation of the exhaust steam dumped into the bilges confirmed the above and also confirmed the fact that fairly quiescent steam conditions prevailed.

The results showed that the experimental and theoretical values for the heat transfer coefficients were compatible, with the experimental values on the order of 10% higher than the Nusselt theory prediction. This was within the as much as 20% discrepancy obtained in many studies, and could be accounted for by the difference between the conditions assumed by the Nusselt theory and the actual conditions of condensation on a horizontal tube. Moreover, it must be considered that the single tube under study was not a single tube at all since the tube was positioned between the porous tube and the second active tube. Knudsen and Katz [Ref. 22] have shown that for air flowing downward over a staggered tube bundle, the first tube can cause turbulence which raises the local Nusselt

53

number (and therefore the local heat transfer coefficient) for the tubes beneath it with the effect being greatest for the second and third tubes. Thus, the porous tube could cause an increase in the heat transfer coefficient for the top active tube. Additionally, when, as observed, condensate drops do not separate from an upper tube but rather form a link between an upper and lower tube, it may be that more condensate is removed from the upper tube than otherwise would take place. The result may be that the tube below the studied "single tube" assisted the "single tube" and raised its heat transfer coefficient, though this is an area which requires further study.

The results also indicated the lack of a clear, distinctive relationship between h_1, h_{Nu}, and the mean vapor velocity trend for the atmospheric runs. Apparently, the degree of change in the mean vapor velocity over the runs was not sufficient, under the noted condition of high inundation, to cause a marked effect on the heat transfer coefficients.

Table VIII presents the results for the vacuum runs. The experimental heat transfer coefficient values (h_1) are seen to be considerably higher than predicted by Nusselt (h_{Nu}), with the extreme case being Run 58 where h_1 was 75% higher than the corresponding h_{Nu}. Upon comparing h_1 to h_o, the later of which considers the effect of vapor velocity, the results were seen to closely agree, especially for the runs at higher vapor velocities. Thus, it was apparent that the

54

vapor velocity effects were significant for the vacuum runs. Note also that as the vapor velocity was increased, h_{Nu} increased only moderately, while h_1 and h_o increased dramatically which indicated that vapor shear was more effective in increasing the heat transfer coefficient as the vapor velocity increased.

A comparison of the heat transfer coefficients for the atmospheric pressure and vacuum runs revealed that both h_1 and h_{Nu} values were consistently greater for the vacuum runs. It was also noted that the difference in the h_1 values between the two sets of runs was much greater than the difference in the h_{Nu} values.

There are two major factors which accounted for the above comparisons. First, as has been noted, the effect of the vapor velocity was greater for the vacuum runs. Increased vapor velocity increases the vapor shear, causing a thinning of the condensate film on the tube, which results in higher average tube wall temperatures. Noting that both the equations, the equations for h_1 and h_{Nu}, have a $(T_s - \overline{T}_w)$ term in their denominators, raising the tube wall temperature raises the heat transfer coefficient, though to a much higher degree for the h_1 calculation. Secondly, the rate of condensation, and therefore the thickness of the tube wall condensate film, was much greater for the runs at atmospheric pressure. This can be seen by comparing the condensation rates, $\dot{V}_{TC}$, in

Table III. For the atmospheric pressure runs, condensate production for the complete tube bundle averaged 580 ml/min compared to only 260 ml/min for the vacuum runs. The greater condensate film thickness for the atmospheric runs resulted in lowered tube wall temperatures and therefore lowered heat transfer coefficients, relative to the vacuum runs. This could be seen by comparing the relative differences between the saturation temperatures and average tube wall temperatures for the atmospheric pressure runs (on the order of a 25% difference) and for the vacuum runs (on the order of a 15% difference) in Table II. Noting again that the calculation of h_1 is more sensitive to a change in $(T_s - \overline{T}_w)$, the h_1 values increased much more between atmospheric pressure and vacuum runs than did the h_{Nu} values.

In summary, the heat transfer coefficients for the top active tube were in close agreement to the Nusselt theory for the atmospheric runs, but were far above the Nusselt theory and in close agreement with the Fujii correlation for the vacuum runs. This can be explained by the dominance of the effect of a thick condensate film for the atmospheric runs and by the dominance of vapor velocity effects for the vacuum runs.

E. MULTIPLE TUBE RESULTS

Table V and Figures 20-35 display the results for the multiple tube runs. Due to the large number of runs, the

normalized average and local heat transfer coefficients,
$\bar{h}_N/h_1$ and h_N/h_1, respectively, were averaged for runs at the
same steam supply and test condenser pressures giving averaged
normalized coefficients, $(\overline{\bar{h}_N/h_1})$ and $(\overline{h_N/h_1})$. These were then
plotted versus the tube number for presentation in the Figures.
The averaging of results was considered justified in view of
the close agreement of the results at the same pressures and
in view of the reduction in the uncertainty of the results
afforded by the averaging process. The uncertainty analysis
is given in Appendix C.

The data points plotted in the Figures were fit, by the
least squares method, to the Nusselt type equations:

$$\frac{\bar{h}_N}{h_1} = N^{-S} \qquad \text{and,}$$

$$\frac{h_N}{h_1} = N^P - (N - 1)^P.$$

For each set of runs, the following values for S and P were
obtained:

RUN #	S	P
1-10	0.21	0.78
11-20	0.19	0.80
21-30	0.22	0.78
31-40	0.21	0.79
41-45	0.12	0.85
46-50	0.14	0.85
51-55	0.13	0.86
56-60	0.17	0.82

57

Note that for the Nusselt equations,

$$S = 0.25 \quad \text{and} \quad P = 0.75.$$

A general trend seen in the Table and Figures, for both atmospheric pressure and vacuum runs, was that the heat transfer coefficient, the normalized heat transfer coefficients, and the heat flux all decreased through the tube bundle for each run or set of runs. This demonstrated the effect of condensate inundation through the tube bundle. The largest decrease in both h and h_N/h_1 relative to the previous tube occurred for the second tube with the next largest decrease for the fifth tube, while decreases for the third and fourth tubes were notably less. The $\bar{h}_N/h_1$ values showed the largest decrease relative to the previous tube for the second tube followed by a gradual decrease through the remaining tubes. Note that the $\bar{h}_N/h_1$ plot smoothed out some of the irregularity seen in the correponding h_N/h_1 plot for the same run. Also for both atmospheric pressure and vacuum runs, the heat transfer coefficient for a given tube increased as the vapor velocity increased, with the effect being more pronounced for the vacuum runs.

Interestingly, the normalized local and average heat transfer coefficients for a given tube decreased with increased vapor velocity for the vacuum runs. No similar trend existed for the atmospheric pressure runs. This was most clear when the $\overline{(h_N/h_1)}$ and $\overline{(h_N/h_1)}$ values were compared for a given tube

58

in Table V. These results are contrary to the expected trend in that they indicate that as the vapor velocity increases, the experimentally determined normalized heat transfer coefficients more closely agree with Nusselt's theory. This can be seen from the Figures and from the values for the S and P exponents tabulated above.

Actually, the relationship between vapor velocity and the normalized heat transfer coefficients given in the previous paragraph is extremely misleading. One is led to believe that an increase in vapor velocity degrades the overall performance of the condenser, when in fact the heat flux (q/A) and the heat transfer coefficient (h) for both a given tube and the tube bundle as a whole increase as the vapor velocity increases. The inconsistancy in the results is resolved when one considers the fact that, as shown in Table V, the heat transfer coefficient for the first tube (h_1) increased notably more with an increase in vapor velocity than did the heat transfer coefficients for the lower four tubes of the bundle. (This could be due to turbulent steam flow over the first tube caused by the porous tube above it and/or due to a decrease in the vapor velocity through the test condenser as the steam is condensed.) Then when $\bar{h}_N$ and especially h_N are normalized by dividing by h_1, the resulting $\bar{h}_N/h_1$ and h_N/h_1 values naturally decreased as the vapor velocity increased. It is therefore apparent that though the normalized heat transfer coefficients are

invaluable in studying the effects of condensate inundation through a tube bundle, they can cause confusion and faulty interpretation of results when used to consider the effects of vapor velocity.

One last comparison between the atmospheric pressure and vacuum runs needs to be made. It was determined that smaller relative decreases in h, $\bar{h}_N/h_1$, and h_N/h_1 occurred for each tube through the tube bundle for vacuum condition runs than for the atmospheric pressure runs. This result was attributed to the greater inundation of tubes for the atmospheric runs and the greater vapor velocities for the vacuum runs. In other words, the effects of vapor velocity to increase the above mentioned coefficients dominated over the effects of condensate inundation to lower them for the vacuum runs, while just the reverse was true for the atmospheric pressure runs.

The final area of multiple tube study was to investigate the use of the porous tube water supply system to simulate a tube bundle with more than five active tubes in a column. A major concern was that the average tube wall temperatures should fall from the upper to lower tubes as would be expected for an actual tube bundle with N number of tubes in a column. Table II and Figure 18 revealed that this condition was satisfied for the first ten tubes of Run 61, but that thereafter, the top tube of each five tube increment was too high. Table II and Figure 19 demonstrated that for Run 62 the sixth tube

had a higher tube wall temperature than the fifth tube. The effect of the average tube wall temperature discrepancies was reflected in the heat transfer coefficients, as shown in Table V and Figures 36-39, which did not fall as expected, but rather followed the trend of the average tube wall temperatures. The wall temperature discrepancies were not excessive; therefore, it was believed that a correction could be accomplished by setting the porous tube inundation water temperature to the condensate temperature as measured coming off the bottom tube of the previous five tube increment. This would allow for the effect of condensate subcooling which was apparently more significant than originally anticipated.

Taking the above into account, a study of Figures 36-39 can give a good indication of the effect of condensate inundation for larger depth tube bundles. Run 61, a vacuum run, demonstrated that a least square curve fit to a larger number of tubes was much closer to the Nusselt prediction than for the case of a five tubes per column bundle. It also appeared that the vapor velocity effects were dominant over the first four or five tubes, while the effects of condensate inundation prevailed for the remainder of the tube bundle. Run 62, an atmospheric pressure run, did not show an appreciable change in heat transfer coefficient relationships with the addition of tubes as compared to the five tubes per column runs.

The least squares curve fits for Runs 61 and 62 yielded exponents as follows:

61

RUN #	S	P
61	0.23	0.75
62	0.21	0.78

From the Figures, it was noted that the curve fits were poor over the upper portion of the tube bundles, but were good for the lower portion.

VI. CONCLUSIONS

As a result of the above mentioned tests, the following conclusions were reached:

1. The average tube wall temperatures increased as the vapor velocity increased, but decreased as the amount of condensate inundation increased. The heat transfer coefficients followed this same trend.

2. The experimentally obtained values for the heat transfer coefficient and the normalized average and local heat transfer coefficients were compatible with the Nusselt predictions for the runs conducted at atmospheric pressure. The same coefficients for the runs conducted under vacuum conditions greatly exceeded the Nusselt predictions due largely to the effects of increased vapor velocity. For the vacuum runs, the heat transfer coefficient for the top tube of the tube bundle agreed closely with the experimental correlation proposed by Fujii.

3. The simulation of a tube bundle of more than five active tubes per column under vacuum conditions demonstrated heat transfer coefficients closer to the Nusselt theory than when only five active tubes per tube bundle column were considered.

4. The results of all runs yielded the following exponents
   for the following Nusselt type equations:

$$\frac{\bar{h}_N}{h_1} = N^{-S}$$

$$\frac{h_N}{h_1} = N^P - (N - 1)^P$$

RUN #	CONDITION	S	P
1-10	atmospheric	0.21	0.78
11-20	"	0.19	0.80
21-30	"	0.22	0.78
31-40	"	0.21	0.79
41-45	vacuum	0.12	0.85
46-50	"	0.14	0.85
51-55	"	0.13	0.86
56-60	"	0.17	0.82
61	"	0.23	0.75
62	atmospheric	0.21	0.78

5. For a tube-to-tube spacing of 8 mm, condensate drops
   barely detached from the upper tube before striking
   the next lower tube at low condensation rates. At
   higher condensation rates, drops elongated to the
   next lower tube, instantaneously linking the tubes.
   For both the above cases, the condensate drops were
   rapidly integrated into the condensate film of the
   lower tube rather than rolling over the tube perimeter.

6. With increasing rates of condensation, the number of
   drops per unit length of a given tube increased. When
   the number of drops per unit length on the top tube
   was compared to the number of drops per unit length

on each of the lower tubes, it was found that the ratios remained constant despite changes in the rate of condensation.

VII.   RECOMMENDATIONS

A.   TEST APPARATUS MODIFICATIONS

To improve the uncertainty and validity of the test results, the following test apparatus modifications are considered advisable:

1. The most significant problem which remains with the test condenser is the breakage of tube wall thermocouples. Due to the cost of the thermocouples and the problems involved in replacing damaged ones, it would be best to use larger diameter, larger wall thickness tubes. This would allow for the in-house fabrication of thermocouples from cheaper fiberglass insulated thermocouple wire, and for the installation of thermocouples to the tube grooves using epoxy cement and copper strips rather than having to crimp and silver solder then in place as was the current practice.

2. The test condenser should be properly leveled and piping targeted to the test condenser to reduce or eliminate the condenser tube leveling problem.

3. The test condenser flanges should be made wider to allow for more sealing area which would eliminate the air leakage problem along the flanges.

4. For the Nusselt curves, the N=5 position, for both normalized heat transfer coefficients, occurs near the

knee of the curve. It is considered that more reliable
data would be obtained if more tubes were added to
the tube bundle. Three additional tube rows of 16 mm
O.D. tubes could be installed in the existing rig.
It would be feasible, with some piping modification,
to further increase the number of tube rows by adding
a flanged section directly below the existing conden-
ser section. The existing steam supply may limit the
number of tube rows that can be installed and still
allow for a sufficiently large volume and velocity of
exhaust steam. It is also considered advisable to
install a row of dummy tubes beneath the last active
tube for use when additional tubes are to be simulated.

5. The existing cooling water rotameters should be replaced
with lower maximum flow rate rotameters. This would
allow for the attainment of lower flow rates, a lower
cooling water ΔT, and improved uncertainty of the
results. All runs in this study were made at about
15% maximum flow rate (corresponding to a cooling
water velocity of about 1.5 m/s) which was about the
lowest setting one could use with good accuracy.

6. For simulation of larger tube bundles, the inundation
water should be at the temperature of the condensate
falling from the bottom tube of the test condenser.
Therefore, instrumentation should be installed to

to measure this temperature. Additionally, the temperature control system for the porous tube water supply tank should be modified to allow for more rapid heating and cooling to avoid long delays between run increments.

7. Installation of a window on the back of the test condenser would allow for viewing of the back side of the tubes so that the absence of drop-wise condensation could be continually verified.

B. ADDITIONAL TESTS

The following additional tests should be conducted.

1. To assure proper removal of non-condensable gases during atmospheric runs, the condenser exhaust steam was dumped to the bilges thus preventing vapor velocity calculations. A set of runs should be made with the exhaust steam piped to the secondary condenser, the vent on the secondary condenser open, and the air ejector secured. The requirement for the securing of the air ejector is necessitated since it can pull a vacuum on the test condenser by itself, however, if a larger vent were installed on the secondary condenser hotwell, it may be possible to operate with the air ejector in operation. The results of the above tests should then be compared to the data presented herein. If build-up of non-condensable gases can be avoided, then all steam

could be condensed and the vapor velocity calculated. Alternatively, a venturi type velocity measuring instrument could be installed in the steam piping between the desuperheater and the test condenser.

2. Runs should be made varying the cooling water flow rates so that a comparison could be made between the method used in this study and the Wilson Plot technique.

3. Verification of the results of this study should be conducted by making sample runs with a full set of tube wall thermocouples installed in each active tube.

4. Movies should be made of the condensation process process so that accurate conclusions could be drawn as to condensate drop phenomena and their relationship to condenser performance.

5. Conduct additional tests to ascertain the effect of the change in vapor velocity through the tube bundle on the heat transfer coefficients.

6. Conduct tests with enhanced tubes after a good smooth tube performance base-line has been verified.

Table I.

Channel Numbers for Stainless Steel Sheathed Copper-Constantan Thermocouples

Location	Channel	Location	Channel	Location	Channel
T_w #1	40	T_w #5	57	T_{co} #1	73
T_w #1	41	T_w #5	58	T_{co} #1	74
T_w #1	42	T_w #5	59	T_{co} #1	75
T_w #1	43	T_s	60	T_{co} #2	76
T_w #2	44	T_s	61	T_{co} #2	77
T_w #2	45	T_s	62	T_{co} #2	78
T_w #2	46	T_{ci} #1	63	T_{co} #3	79
T_w #2	47	T_{ci} #1	64	T_{co} #3	80
T_w #3	48	T_{ci} #2	65	T_{co} #3	81
T_w #3	49	T_{ci} #2	66	T_{co} #4	82
T_w #3	50	T_{ci} #3	67	T_{co} #4	83
T_w #3	51	T_{ci} #3	68	T_{co} #4	84
T_w #4	52	T_{ci} #4	69	T_{co} #5	85
T_w #4	53	T_{ci} #4	70	T_{co} #5	86
T_w #4	54	T_{ci} #5	71	T_{co} #5	87
T_w #4	55	T_{ci} #5	72	T_{DSNTR}	88
T_w #5	56			T_{TSHW}	89

Table II.

Temperature Data

RUN #	TUBE #	T_{ci} (°C)	T_{co} (°C)	$\bar{T}_w$ (°C)	T_v (°C)	T_s (°C)
1	1	27.1	33.5	78.2	101.7	101.0
	2	27.2	33.0	70.7	"	"
	3	27.1	32.0	73.4	"	"
	4	27.1	32.3	70.9	"	"
	5	27.1	3.12	67.2	"	"
2	1	27.2	33.0	78.8	101.7	101.0
	2	27.2	32.2	70.7	"	"
	3	27.2	32.2	73.6	"	"
	4	27.3	32.4	70.2	"	"
	5	27.2	31.3	67.7	"	"
3	1	27.4	33.1	79.6	101.7	100.7
	2	27.5	33.3	71.1	"	"
	3	27.4	32.4	73.5	"	"
	4	27.4	32.6	70.8	"	"
	5	27.5	31.5	68.2	"	"
4	1	27.5	33.1	79.0	101.7	101.0
	2	27.5	33.4	71.0	"	"
	3	27.5	32.4	73.2	"	"
	4	27.6	32.8	70.4	"	"
	5	27.5	31.6	68.4	"	"
5	1	27.5	33.0	78.2	101.7	101.0
	2	27.6	33.4	70.8	"	"
	3	27.6	32.5	73.7	"	"
	4	27.6	32.7	71.2	"	"
	5	27.6	31.6	67.8	"	"

71

RUN #	TUBE #	T_{ci} (°C)	T_{co} (°C)	$\bar{T}_w$ (°C)	T_v (°C)	T_s (°C)
6	1	27.6	33.2	78.9	101.7	101.0
	2	27.7	32.7	71.2	"	"
	3	27.7	32.6	74.2	"	"
	4	27.7	32.9	71.3	"	"
	5	27.7	31.7	68.1	"	"
7	1	27.6	33.3	78.8	101.7	101.1
	2	27.6	32.9	70.8	"	"
	3	27.6	32.6	73.5	"	"
	4	27.7	32.9	71.5	"	"
	5	27.7	31.7	68.1	"	"
8	1	27.4	32.9	78.1	101.7	101.0
	2	27.4	32.4	71.5	"	"
	3	27.4	32.3	73.5	"	"
	4	27.4	32.6	71.0	"	"
	5	27.4	31.4	68.6	"	"
9	1	26.7	32.2	78.5	101.6	100.9
	2	26.7	31.8	71.1	"	"
	3	26.7	31.6	73.4	"	"
	4	26.7	31.9	70.2	"	"
	5	26.7	30.8	68.2	"	"
10	1	26.4	31.9	78.4	101.7	101.0
	2	26.4	31.6	70.7	"	"
	3	26.4	31.3	73.2	"	"
	4	26.5	31.8	71.0	"	"
	5	26.5	30.5	68.2	"	"

72

RUN #	TUBE #	T_{ci} (°C)	T_{CO} (°C)	$\bar{T}_w$ (°C)	T_v (°C)	T_s (°C)
11	1	23.6	29.2	77.6	101.2	100.6
	2	23.6	29.0	70.3	"	"
	3	23.5	28.5	71.0	"	"
	4	23.4	28.8	68.9	"	"
	5	23.6	27.8	68.3	"	"
12	1	23.5	29.2	77.1	101.2	100.6
	2	23.5	29.1	70.0	"	"
	3	23.5	28.3	71.3	"	"
	4	23.6	28.8	68.9	"	"
	5	23.5	27.7	70.6	"	"
13	1	23.4	29.1	77.6	101.2	100.6
	2	23.5	29.0	70.9	"	"
	3	23.4	28.4	71.5	"	"
	4	23.6	28.7	68.6	"	"
	5	23.4	27.7	67.5	"	"
14	1	23.4	29.1	77.4	101.3	100.6
	2	23.4	28.9	70.9	"	"
	3	23.4	28.4	71.5	"	"
	4	23.4	28.8	69.0	"	"
	5	23.4	27.6	70.4	"	"
15	1	23.4	29.1	77.7	101.2	100.6
	2	23.4	28.9	70.8	"	"
	3	23.4	28.3	71.9	"	"
	4	23.4	28.7	68.8	"	"
	5	23.4	27.7	67.7	"	"

RUN #	TUBE #	T_{ci} (°C)	T_{co} (°C)	$\bar{T}_w$ (°C)	T_v (°C)	T_s (°C)
16	1	23.4	29.0	77.6	101.1	100.6
	2	23.4	28.9	70.1	"	"
	3	23.4	28.3	71.3	"	"
	4	23.4	28.6	69.1	"	"
	5	23.4	27.5	69.3	"	"
17	1	23.2	29.0	77.0	101.2	100.6
	2	23.3	28.9	70.5	"	"
	3	23.3	28.3	72.1	"	"
	4	23.4	28.6	69.1	"	"
	5	23.3	27.5	67.3	"	"
18	1	23.2	29.0	77.0	101.2	100.6
	2	23.3	28.9	70.4	"	"
	3	23.3	28.3	71.3	"	"
	4	23.4	28.6	69.5	"	"
	5	23.3	27.6	67.5	"	"
19	1	23.3	29.0	77.3	101.1	100.6
	2	23.3	28.9	70.1	"	"
	3	23.3	28.3	71.6	"	"
	4	23.4	28.6	68.7	"	"
	5	23.3	27.5	67.1	"	"
20	1	23.2	28.9	77.2	101.2	100.6
	2	23.3	28.8	70.0	"	"
	3	23.3	28.3	72.0	"	"
	4	23.4	28.6	69.2	"	"
	5	23.3	27.5	70.1	"	"

74

RUN #	TUBE #	T_{ci} (°C)	T_{co} (°C)	$\bar{T}_w$ (°C)	T_v (°C)	T_s (°C)
21	1	24.7	30.3	77.1	100.7	100.3
	2	24.8	30.1	69.3	"	"
	3	24.7	29.6	70.8	"	"
	4	24.8	29.9	68.7	"	"
	5	24.8	28.9	67.2	"	"
22	1	24.6	30.3	78.4	100.7	100.3
	2	24.7	30.1	69.4	"	"
	3	24.7	29.5	71.6	"	"
	4	24.7	29.8	69.2	"	"
	5	24.7	28.8	67.0	"	"
23	1	24.6	30.3	77.2	100.7	100.3
	2	24.6	30.1	69.8	"	"
	3	24.7	29.6	71.0	"	"
	4	24.7	29.8	69.2	"	"
	5	24.7	28.8	67.1	"	"
24	1	24.8	30.4	77.6	100.7	100.3
	2	24.7	30.2	69.6	"	"
	3	24.8	29.2	71.3	"	"
	4	24.8	29.9	68.9	"	"
	5	24.8	28.9	67.5	"	"
25	1	24.8	30.5	77.8	100.7	100.3
	2	24.8	30.2	70.1	"	"
	3	24.9	29.7	71.6	"	"
	4	25.0	30.0	68.8	"	"
	5	24.9	29.0	67.2	"	"

75

RUN #	TUBE #	T_{ci} (°C)	T_{co} (°C)	$\bar{T}_w$ (°C)	T_v (°C)	T_s (°C)
26	1	25.0	30.6	77.6	100.7	100.3
	2	24.8	30.3	69.8	"	"
	3	25.0	29.8	71.3	"	"
	4	25.0	30.1	68.7	"	"
	5	25.0	29.1	67.0	"	"
27	1	25.0	30.6	78.1	100.8	100.3
	2	25.1	30.4	70.9	"	"
	3	25.1	29.8	70.9	"	"
	4	25.1	30.2	69.4	"	"
	5	25.0	29.2	67.1	"	"
28	1	25.1	30.7	77.9	100.8	100.3
	2	25.1	30.4	70.2	"	"
	3	25.1	29.9	71.2	"	"
	4	25.1	30.3	68.9	"	"
	5	25.1	29.2	67.4	"	"
29	1	25.1	30.8	77.8	100.7	100.3
	2	25.2	30.4	70.1	"	"
	3	25.2	30.0	71.4	"	"
	4	25.2	30.3	69.1	"	"
	5	25.1	29.3	67.0	"	"
30	1	25.1	30.7	77.8	100.8	100.3
	2	25.2	30.5	71.0	"	"
	3	25.1	30.0	71.9	"	"
	4	25.2	30.3	69.7	"	"
	5	25.1	29.2	67.1	"	"

RUN #	TUBE #	T_{ci} (°C)	T_{co} (°C)	$\overline{T}_w$ (°C)	T_v (°C)	T_s (°C)
31	1	24.7	30.1	76.8	100.5	100.2
	2	24.7	29.9	69.1	"	"
	3	24.7	29.4	70.0	"	"
	4	24.7	29.8	68.7	"	"
	5	24.7	28.9	69.1	"	"
32	1	24.6	30.1	77.2	100.5	100.2
	2	24.6	29.8	69.1	"	"
	3	24.6	29.3	70.1	"	"
	4	24.6	29.6	691.	"	"
	5	24.5	28.9	70.8	"	"
33	1	24.4	30.0	77.2	100.5	100.2
	2	24.4	29.7	68.6	"	"
	3	24.4	29.2	70.2	"	"
	4	24.4	29.5	69.2	"	"
	5	24.4	28.6	70.5	"	"
34	1	24.2	29.8	77.3	100.6	100.2
	2	24.4	29.8	68.9	"	"
	3	24.3	29.1	70.4	"	"
	4	24.3	29.3	68.1	"	"
	5	24.3	28.5	70.0	"	"
35	1	24.2	29.7	77.1	100.6	100.2
	2	24.3	29.7	69.1	"	"
	3	24.2	28.9	70.5	"	"
	4	24.2	29.2	69.0	"	"
	5	24.1	28.4	70.0	"	"

77

RUN #	TUBE #	T_{ci} (°C)	T_{co} (°C)	$\bar{T}_w$ (°C)	T_v (°C)	T_s (°C)
36	1	24.1	29.6	77.1	100.6	100.2
	2	24.1	29.4	69.5	"	"
	3	24.1	28.8	70.2	"	"
	4	24.1	29.1	68.4	"	"
	5	24.1	28.3	69.8	"	"
37	1	24.0	29.5	76.7	100.6	100.2
	2	24.2	29.5	69.4	"	"
	3	24.0	28.8	70.2	"	"
	4	24.0	29.0	68.3	"	"
	5	23.9	28.3	69.6	"	"
38	1	23.8	29.4	77.5	100.6	100.2
	2	23.9	29.4	69.1	"	"
	3	23.9	28.6	70.5	"	"
	4	23.9	29.0	68.4	"	"
	5	23.9	28.2	69.4	"	"
39	1	23.8	29.3	77.6	100.5	100.2
	2	23.8	29.2	69.7	"	"
	3	23.8	28.5	70.4	"	"
	4	23.8	28.8	69.1	"	"
	5	23.8	28.1	69.4	"	"
40	1	23.6	29.2	77.4	100.5	100.2
	2	23.6	29.2	68.6	"	"
	3	23.6	28.4	70.3	"	"
	4	23.6	28.6	68.5	"	"
	5	23.6	28.0	69.2	"	"

73

RUN #	TUBE #	T_{ci} (^oC)	T_{co} (^oC)	$\overline{T}_w$ (^oC)	T_v (^oC)	T_s (^oC)
41	1	19.6	22.1	44.3	53.3	52.0
	2	19.5	22.3	42.1	"	"
	3	19.6	21.8	45.1	"	"
	4	19.6	22.0	43.0	"	"
	5	19.6	21.6	41.8	"	"
42	1	19.6	22.3	46.6	56.8	55.3
	2	19.5	22.5	44.1	"	"
	3	19.5	22.0	45.4	"	"
	4	19.6	22.2	44.6	"	"
	5	19.5	21.7	43.4	"	"
43	1	19.6	22.1	45.3	53.8	53.3
	2	19.5	22.2	42.2	"	"
	3	19.5	21.9	43.6	"	"
	4	19.6	22.0	43.3	"	"
	5	19.5	21.6	42.2	"	"
44	1	19.6	22.0	43.9	52.5	51.5
	2	19.5	22.1	41.3	"	"
	3	19.5	21.8	42.3	"	"
	4	19.6	21.9	42.2	"	"
	5	19.5	21.6	41.3	"	"
45	1	19.5	22.0	43.9	52.6	51.2
	2	19.5	22.1	41.6	"	"
	3	19.4	21.7	42.8	"	"
	4	19.5	21.9	42.6	"	"
	5	19.4	21.6	41.4	"	"

79

RUN #	TUBE #	T_{ci} (°C)	T_{co} (°C)	$\bar{T}_w$ (°C)	T_v (°C)	T_s (°C)
46	1	19.7	22.2	44.9	53.4	52.2
	2	19.7	22.4	42.2	"	"
	3	19.6	21.9	43.7	"	"
	4	19.6	22.0	43.2	"	"
	5	19.6	21.6	42.4	"	"
47	1	19.6	22.1	45.0	53.2	51.0
	2	19.5	22.4	42.5	"	"
	3	19.6	21.9	43.6	"	"
	4	19.6	22.0	43.0	"	"
	5	19.6	21.7	42.0	"	"
48	1	19.6	22.2	45.3	53.8	52.1
	2	19.5	22.5	42.7	"	"
	3	19.6	21.9	44.0	"	"
	4	19.6	22.0	43.7	"	"
	5	19.6	21.7	42.7	"	"
49	1	19.6	22.1	45.3	54.1	52.8
	2	19.5	22.5	42.5	"	"
	3	19.6	21.9	44.0	"	"
	4	19.5	22.0	43.6	"	"
	5	19.5	21.6	42.5	"	"
50	1	19.4	22.0	45.5	54.1	52.5
	2	19.3	22.4	43.2	"	"
	3	19.4	21.8	43.9	"	"
	4	19.4	21.8	43.8	"	"
	5	19.3	21.5	42.6	"	"

RUN #	TUBE #	T_{ci} (°C)	T_{co} (°C)	$\bar{T}_w$ (°C)	T_v (°C)	T_s (°C)
51	1	19.0	21.7	46.1	54.6	53.1
	2	19.0	22.0	43.6	"	"
	3	19.0	21.5	44.9	"	"
	4	19.0	21.6	44.1	"	"
	5	18.9	21.2	43.3	"	"
52	1	18.9	21.6	46.0	54.2	53.1
	2	18.8	21.9	43.2	"	"
	3	18.9	21.4	44.6	"	"
	4	18.9	21.5	43.5	"	"
	5	18.9	21.1	42.9	"	"
53	1	18.9	21.6	47.0	55.8	53.1
	2	18.8	22.0	43.8	"	"
	3	18.8	21.5	45.5	"	"
	4	18.8	21.6	44.8	"	"
	5	18.8	21.2	44.1	"	"
54	1	18.9	21.6	47.8	56.7	55.6
	2	18.7	22.1	44.7	"	"
	3	18.8	21.5	46.0	"	"
	4	18.8	21.6	45.5	"	"
	5	18.8	21.2	44.6	"	"
55	1	18.8	21.5	45.7	54.1	53.1
	2	18.7	21.9	43.0	"	"
	3	18.8	21.2	44.4	"	"
	4	18.8	21.4	44.1	"	"
	5	18.8	21.0	43.0	"	"

31

RUN #	TUBE #	T_{ci} (°C)	T_{co} (°C)	$\bar{T}_w$ (°C)	T_v (°C)	T_s (°C)
56	1	18.7	21.5	47.5	55.9	54.3
	2	18.6	22.0	44.2	"	"
	3	18.7	21.4	46.0	"	"
	4	18.7	21.5	45.6	"	"
	5	18.7	21.0	44.5		"
57	1	18.7	21.4	46.9	54.5	53.4
	2	18.6	21.8	43.6	"	"
	3	18.7	21.2	45.1	"	"
	4	18.7	21.3	44.6	"	"
	5	18.6	21.0	43.5		"
58	1	18.6	21.4	47.1	54.6	53.2
	2	18.5	21.8	43.4	"	"
	3	18.6	21.2	45.4	"	"
	4	18.6	21.2	44.8	"	"
	5	18.6	20.9	43.1		"
59	1	18.6	21.4	47.3	55.1	53.8
	2	18.5	21.8	43.7	"	"
	3	18.6	21.1	45.4	"	"
	4	18.6	21.2	44.5	"	"
	5	18.5	20.8	43.5		"
60	1	18.5	21.3	47.4	55.1	53.8
	2	18.4	21.7	43.8	"	"
	3	18.5	21.1	45.6	"	"
	4	18.5	21.2	44.3	"	"
	5	18.4	20.9	43.7		"

RUN #	TUBE #	T_{ci} (°C)	T_{co} (°C)	T_w (°C)	T_v (°C)	T_s (°C)
61	1	18.4	21.3	46.6	54.7	53.5
	2	18.4	21.6	43.9	"	"
	3	18.4	21.0	45.0	"	"
	4	18.4	21.0	44.7	"	"
	5	18.5	20.7	43.7		"
	6	13.2	20.8	42.6	55.7	54.2
	7	18.2	21.3	39.7	"	"
	8	18.2	20.7	41.3	"	"
	9	18.3	20.8	41.0	"	"
	10	18.1	20.4	39.8		"
	11	18.1	20.6	42.3	57.5	56.0
	12	18.0	21.1	39.4	"	"
	13	18.1	20.5	40.9	"	"
	14	18.1	20.6	39.9	"	"
	15	18.1	20.2	39.9		"
	16	17.8	20.1	39.8	56.2	54.6
	17	17.8	20.6	37.8	"	"
	18	17.8	20.1	39.5	"	"
	19	17.8	20.2	39.2	"	"
	20	17.7	19.8	38.2		"
	21	17.2	19.4	39.0	56.3	55.0
	22	17.1	19.6	37.1	"	"
	23	17.2	19.5	38.7	"	"
	24	17.2	19.6	38.9	"	"
	25	17.1	19.2	37.7		"

RUN #	TUBE #	T_{ci} (°C)	T_{co} (°C)	$\bar{T}_w$ (°C)	T_v (°C)	T_s (°C)
61 (contd)	26	17.1	19.2	39.0	56.8	55.0
	27	16.9	19.5	37.2	"	"
	28	17.0	19.3	38.9	"	"
	29	17.0	19.4	38.3	"	"
	30	17.0	19.0	37.9	"	"
62	1	21.6	27.6	78.0	101.4	100.9
	2	21.5	27.5	70.8	"	"
	3	21.6	26.8	71.5	"	"
	4	21.6	26.8	68.4	"	"
	5	21.6	25.8	66.2	"	"
	6	21.6	26.6	71.3	101.7	101.1
	7	21.6	26.6	63.8	"	"
	8	21.6	26.1	65.3	"	"
	9	21.6	26.3	64.0	"	"
	10	21.6	25.5	61.8	"	"

84

Table III.

Pressure and Volumetric Flow Rate Data
(Runs 1-60)

RUN #	P_{TC} (mm Hg)	P_{SS} (psig)	$\dot{V}_d$ (ml/min)	$\dot{V}_{TC}$ (ml/min)	$\dot{V}_{SC}$ (ml/min)
1	788	50	--	590	--
2	788	50	--	600	--
3	790	50	--	600	--
4	788	50	--	610	--
5	788	50	--	540	--
6	789	50	--	610	--
7	791	50	--	540	--
8	790	50	--	650	--
9	787	50	--	590	--
10	789	50	--	600	--
11	776	45	--	610	--
12	776	45	--	620	--
13	776	45	--	590	--
14	776	45	--	600	--
15	776	45	--	620	--
16	776	45	--	600	--
17	776	45	--	620	--
18	776	45	--	620	--
19	776	45	--	580	--
20	776	45	--	600	--

85

RUN #	P_{TC} (mm Hg)	P_{SS} (psig)	$\dot{V}_d$ (ml/min)	$\dot{V}_{TC}$ (ml/min)	$\dot{V}_{SC}$ (ml/min)
21	770	40	--	610	--
22	770	40	--	590	--
23	770	40	--	600	--
24	770	40	--	600	--
25	770	40	--	600	--
26	770	40	--	590	--
27	770	40	--	600	--
28	770	40	--	600	--
29	770	40	--	590	--
30	770	40	--	600	--
31	768	35	--	560	--
32	768	35	--	490	--
33	768	35	--	380	--
34	768	35	--	580	--
35	768	35	--	520	--
36	768	35	--	540	--
37	768	35	--	580	--
38	768	35	--	530	--
39	768	35	--	390	--
40	768	35	--	560	--
41	102	35	100	210	180
42	122	35	100	320	180
43	110	35	100	240	180
44	100	35	100	230	180
45	100	35	100	180	180

RUN #	P_{TC} (mm Hg)	P_{SS} (psig)	$\dot{V}_d$ (ml/min)	$\dot{V}_{TC}$ (ml/min)	$\dot{V}_{SC}$ (ml/min)
46	103	40	100	260	330
47	98	40	100	260	330
48	103	40	100	270	330
49	104	40	100	210	330
50	105	40	100	300	330
51	109	45	100	290	390
52	109	45	100	290	390
53	109	45	100	320	390
54	124	45	100	260	390
55	109	45	100	240	390
56	116	50	100	280	470
57	111	50	100	300	470
58	109	50	100	290	470
59	112	50	100	270	470
60	112	50	100	260	470

Table IV.

Pressure and Volumetric Flow Rate Data
(Runs 61 & 62)

RUN #	TUBE #	P_{TC} (mm Hg)	P_{SS} (psig)	$\dot{V}_d$ (ml/min)	$\dot{V}_{TC}$ (ml/min)	$\dot{V}_{SC}$ (ml/min)	$\dot{V}_{PT}$ (ml/min)
61	1-5	111	50	100	290	400	0
	6-10	115	50	100	160	580	290
	11-15	126	50	100	190	380	450
	16-20	117	50	100	50	680	640
	21-25	120	50	100	20	800	690
	26-30	120	50	100	10	910	710
62	1-5	787	50	--	630	--	0
	6-10	793	50	--	540	--	630

Table V.

Results

RUN #	TUBE #	h $\left(\dfrac{KW}{m^2 \cdot {}^\circ C}\right)$	$\dfrac{\overline{h_N}}{h_1}$	$\left(\dfrac{\overline{h_N}}{h_1}\right)$	$\dfrac{h_N}{h_1}$	$\left(\dfrac{h_N}{h_1}\right)$	$\dfrac{q/A}{\left(\dfrac{KW}{m^2}\right)}$
1	1	14.1	1.0	--	1.0	--	320
	2	9.4	0.84	--	0.67	--	290
	3	8.9	0.77	--	0.63	--	250
	4	8.2	0.72	--	0.58	--	250
	5	6.1	0.66	--	0.43	--	210
2	1	13.1	1.0	--	1.0	--	290
	2	8.1	0.81	--	0.62	--	250
	3	9.2	0.77	--	0.70	--	250
	4	8.1	0.78	--	0.61	--	250
	5	6.0	0.68	--	0.46	--	200
3	1	13.6	1.0	--	1.0	--	290
	2	9.7	0.86	--	0.71	--	290
	3	9.2	0.80	--	0.68	--	250
	4	8.3	0.75	--	0.61	--	250
	5	6.2	0.69	--	0.46	--	200
4	1	12.8	1.0	--	1.0	--	280
	2	9.7	0.88	--	0.76	--	290
	3	8.8	0.81	--	0.69	--	250
	4	8.1	0.77	--	0.63	--	250
	5	6.3	0.72	--	0.49	--	210

RUN #	TUBE #	$\dfrac{h}{\left(\dfrac{KW}{m^2 \cdot {}^\circ C}\right)}$	$\dfrac{\bar{h}_N}{h_1}$	$\left(\dfrac{\bar{h}_N}{h_1}\right)$	$\dfrac{h_N}{h_1}$	$\left(\dfrac{h_N}{h_1}\right)$	$\dfrac{q/A}{\left(\dfrac{KW}{m^2}\right)}$
5	1	12.1	1.0	--	1.0	--	280
	2	9.5	0.89	--	0.78	--	290
	3	9.0	0.84	--	0.74	--	250
	4	8.2	0.80	--	0.67	--	240
	5	6.1	0.74	--	0.50	--	200
6	1	12.7	1.0	--	1.0	--	280
	2	9.8	0.88	--	0.77	--	290
	3	9.2	0.83	--	0.72	--	250
	4	8.3	0.79	--	0.66	--	250
	5	6.1	0.72	--	0.48	--	200
7	1	12.8	1.0	--	1.0	--	290
	2	8.6	0.84	--	0.67	--	260
	3	9.1	0.79	--	0.71	--	250
	4	8.4	0.76	--	0.65	--	250
	5	6.1	0.70	--	0.47	--	200
8	1	12.1	1.0	--	1.0	--	280
	2	8.4	0.85	--	0.69	--	250
	3	8.9	0.81	--	0.74	--	250
	4	8.3	0.78	--	0.68	--	250
	5	6.2	0.73	--	0.51	--	200
9	1	12.3	1.0	--	1.0	--	280
	2	8.4	0.84	--	0.68	--	250
	3	9.0	0.80	--	0.73	--	250
	4	8.1	0.77	--	0.65	--	250
	5	6.3	0.71	--	0.51	--	210

90

RUN #	TUBE #	$h\left(\dfrac{KW}{m^2 \cdot {}^\circ C}\right)$	$\dfrac{\bar{h}_N}{h_1}$	$\left(\dfrac{\bar{h}_N}{h_1}\right)$	$\dfrac{h_N}{h_1}$	$\left(\dfrac{h_N}{h_1}\right)$	$\dfrac{q/A}{\left(\dfrac{KW}{m^2}\right)}$
10	1	12.2	1.0	---	1.0	---	280
	2	8.5	0.85	---	0.69	---	260
	3	8.8	0.81	---	0.72	---	250
	4	8.4	0.78	---	0.69	---	250
	5	6.1	0.72	---	0.50	---	200
1-10	1	---	---	1.0	---	1.0	---
	2	---	---	0.85	---	0.71	---
	3	---	---	0.80	---	0.71	---
	4	---	---	0.76	---	0.64	---
	5	---	---	0.71	---	0.48	---
11	1	12.2	1.0	---	1.0	---	280
	2	8.8	0.86	---	0.72	---	270
	3	8.5	0.80	---	0.69	---	250
	4	8.1	0.77	---	0.66	---	260
	5	6.8	0.72	---	0.56	---	210
12	1	12.2	1.0	---	1.0	---	290
	2	9.0	0.87	---	0.74	---	280
	3	8.2	0.81	---	0.68	---	240
	4	7.8	0.76	---	0.64	---	250
	5	7.0	0.73	---	0.58	---	210
13	1	12.2	1.0	---	1.0	---	280
	2	9.1	0.87	---	0.75	---	270
	3	8.5	0.81	---	0.69	---	250
	4	7.6	0.76	---	0.62	---	240
	5	6.5	0.72	---	0.53	---	220

RUN #	TUBE #	$\dfrac{h}{\left(\dfrac{KW}{m^2 \cdot °C}\right)}$	$\dfrac{\overline{h}_N}{h_1}$	$\left(\dfrac{\overline{h}_N}{h_1}\right)$	$\dfrac{h_N}{h_1}$	$\left(\dfrac{h_N}{h_1}\right)$	$\dfrac{q/A}{\left(\dfrac{KW}{m^2}\right)}$
14	1	12.3	1.0	--	1.0	--	290
	2	9.1	0.87	--	0.74	--	270
	3	8.6	0.81	--	0.70	--	250
	4	8.1	0.77	--	0.66	--	260
	5	7.0	0.73	--	0.57	--	210
15	1	12.5	1.0	--	1.0	--	290
	2	9.1	0.86	--	0.73	--	270
	3	8.6	0.80	--	0.69	--	250
	4	7.9	0.76	--	0.64	--	250
	5	6.6	0.71	--	0.52	--	220
16	1	12.2	1.0	--	1.0	--	280
	2	8.9	0.86	--	0.73	--	270
	3	8.4	0.81	--	0.69	--	250
	4	7.9	0.76	--	0.64	--	250
	5	6.4	0.72	--	0.52	--	200
17	1	12.3	1.0	--	1.0	--	290
	2	9.2	0.87	--	0.74	--	280
	3	8.8	0.82	--	0.71	--	250
	4	7.9	0.77	--	0.64	--	250
	5	6.3	0.72	--	0.51	--	210
18	1	12.1	1.0	--	1.0	--	290
	2	9.2	0.88	--	0.75	--	280
	3	8.6	0.82	--	0.71	--	250
	4	8.0	0.78	--	0.66	--	250
	5	6.5	0.73	--	0.54	--	220

RUN #	TUBE #	$h \left(\dfrac{KW}{m^2 \cdot {}^\circ C}\right)$	$\dfrac{\overline{h}_N}{h_1}$	$\left(\dfrac{\overline{h}_N}{h_1}\right)$	$\dfrac{h_N}{h_1}$	$\left(\dfrac{h_N}{h_1}\right)$	$\dfrac{q/A}{\left(\dfrac{KW}{m^2}\right)}$
19	1	12.3	1.0	--	1.0	--	290
	2	9.1	0.87	--	0.74	--	280
	3	8.7	0.81	--	0.70	--	250
	4	7.9	0177	--	0.63	--	250
	5	6.	0.72	--	0.51	--	210
20	1	12.0	1.0	--	1.0	--	280
	2	9.0	0.88	--	0.75	--	280
	3	8.8	0.83	--	0.73	--	250
	4	7.9	0.78	--	0.66	--	250
	5	6.9	0.74	--	0.58	--	210
11-20	1	--	--	1.0	--	1.0	--
	2	--	--	0.87	--	0.74	--
	3	--	--	0.81	--	0.70	--
	4	--	--	0.77	--	0.64	--
	5	--	--	0.72	--	0.54	--
21	1	12.1	1.0	--	1.0	--	280
	2	8.4	0.85	--	0.70	--	260
	3	8.3	0.79	--	0.69	--	250
	4	7.7	0.75	--	0.63	--	240
	5	6.2	0.71	--	0.51	--	210
22	1	12.8	1.0	--	1.0	--	280
	2	8.6	0.84	--	0.67	--	270
	3	8.4	0.78	--	0.65	--	240
	4	8.0	0.74	--	0.62	--	250
	5	6.2	0.68	--	0.48	--	210

93

RUN #	TUBE #	$\dfrac{h}{\left(\dfrac{KW}{m^2 \cdot {}^{\circ}C}\right)}$	$\dfrac{\overline{h_N}}{h_1}$	$\left(\dfrac{\overline{h_N}}{h_1}\right)$	$\dfrac{h_N}{h_1}$	$\left(\dfrac{h_N}{h_1}\right)$	$\dfrac{q/A}{\left(\dfrac{KW}{m^2}\right)}$
23	1	12.2	1.0	--	1.0	--	280
	2	8.9	0.87	--	0.73	--	270
	3	8.4	0.81	--	0.69	--	250
	4	7.8	0.77	--	0.64	--	240
	5	6.2	0.71	--	0.51	--	210
24	1	12.4	1.0	--	1.0	--	280
	2	8.8	0.86	--	0.71	--	270
	3	7.6	0.78	--	0.62	--	220
	4	7.7	0.74	--	0.62	--	240
	5	6.3	0.69	--	0.51	--	210
25	1	12.7	1.0	--	1.0	--	290
	2	8.8	0.85	--	0.69	--	270
	3	8.4	0.78	--	0.66	--	240
	4	7.6	0.74	--	0.59	--	240
	5	6.2	0.69	--	0.49	--	210
26	1	12.4	1.0	--	1.0	--	280
	2	8.9	0.86	--	0.72	--	270
	3	8.3	0.80	--	0.67	--	240
	4	7.7	0.75	--	0.62	--	240
	5	6.2	0.70	--	0.50	--	210
27	1	12.7	1.0	--	1.0	--	280
	2	8.9	0.85	--	0.70	--	260
	3	8.0	0.78	--	0.63	--	240
	4	7.9	0.74	--	0.62	--	240
	5	6.4	0.69	--	0.50	--	210
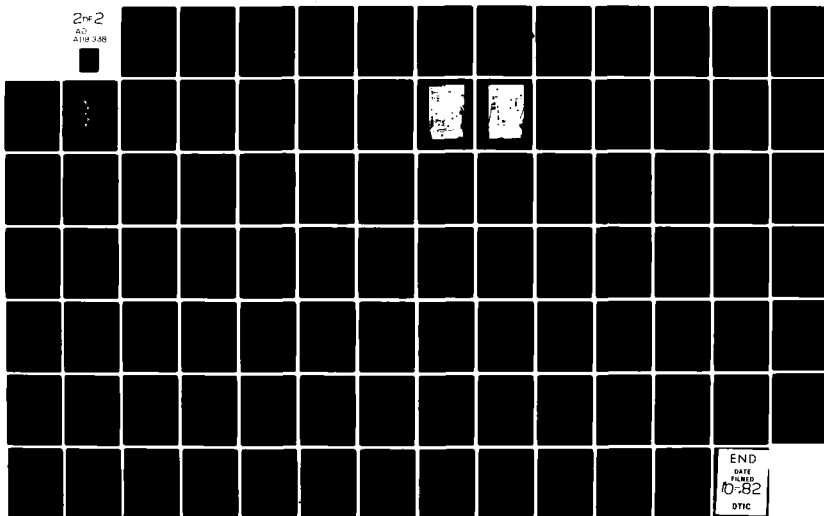
RUN #	TUBE #	$\dfrac{h}{\left(\frac{KW}{m^2 \cdot {}^\circ C}\right)}$	$\dfrac{\bar{h}_N}{h_1}$	$\left(\dfrac{\bar{h}_N}{h_1}\right)$	$\dfrac{h_N}{h_1}$	$\left(\dfrac{h_N}{h_1}\right)$	$\dfrac{q/A}{\left(\frac{KW}{m^2}\right)}$
28	1	12.6	1.0	---	1.0	---	280
	2	8.7	0.85	---	0.69	---	260
	3	8.3	0.78	---	0.66	---	240
	4	7.9	0.74	---	0.63	---	250
	5	6.3	0.70	---	0.50	---	210
29	1	12.5	1.0	---	1.0	---	280
	2	8.5	0.84	---	0.68	---	260
	3	8.3	0.78	---	0.67	---	240
	4	7.8	0.74	---	0.62	---	240
	5	6.3	0.70	---	0.51	---	210
30	1	12.5	1.0	---	1.0	---	280
	2	8.9	0.86	---	0.71	---	260
	3	8.7	0.80	---	0.69	---	250
	4	7.9	0.76	---	0.64	---	240
	5	6.4	0.71	---	0.51	---	210
21-30	1	---	---	1.0	---	1.0	---
	2	---	---	0.85	---	0.70	---
	3	---	---	0.79	---	0.66	---
	4	---	---	0.75	---	0.62	---
	5	---	---	0.70	---	0.50	---
31	1	11.6	1.0	---	1.0	---	270
	2	8.2	0.86	---	0.71	---	260
	3	7.8	0.80	---	0.67	---	240
	4	7.7	0.76	---	0.66	---	240
	5	6.8	0.73	---	0.58	---	210

RUN #	TUBE #	$\dfrac{h}{\left(\dfrac{KW}{m^2 \cdot {}^{\circ}C}\right)}$	$\dfrac{\bar{h}_N}{h_1}$	$\left(\dfrac{\bar{h}_N}{h_1}\right)$	$\dfrac{h_N}{h_1}$	$\left(\dfrac{h_N}{h_1}\right)$	$\dfrac{q/A}{\left(\dfrac{KW}{m^2}\right)}$
32	1	12.0	1.0	---	1.0	---	280
	2	8.2	0.84	---	0.69	---	260
	3	7.8	0.78	---	0.65	---	240
	4	7.7	0.74	---	0.64	---	240
	5	7.5	0.72	---	0.63	---	220
33	1	12.2	1.0	---	1.0	---	280
	2	8.3	0.84	---	0.68	---	260
	3	8.0	0.78	---	0.66	---	240
	4	7.8	0.74	---	0.64	---	240
	5	7.1	0.71	---	0.58	---	210
34	1	12.3	1.0	---	1.0	---	280
	2	8.5	0.85	---	0.69	---	270
	3	8.1	0.78	---	0.66	---	240
	4	7.4	0.74	---	0.60	---	240
	5	7.0	0.70	---	0.57	---	210
35	1	12.0	1.0	---	1.0	---	280
	2	8.6	0.86	---	0.72	---	270
	3	7.9	0.79	---	0.66	---	240
	4	7.6	0.75	---	0.64	---	240
	5	7.2	0.72	---	0.60	---	220
36	1	12.0	1.0	---	1.0	---	280
	2	8.5	0.86	---	0.71	---	260
	3	7.9	0.79	---	0.66	---	240
	4	7.5	0.75	---	0.63	---	240
	5	6.9	0.72	---	0.58	---	210

RUN #	TUBE #	$\dfrac{h}{\left(\dfrac{KW}{m^2 \cdot {}^{o}C}\right)}$	$\dfrac{\bar{h}_N}{h_1}$	$\left(\overline{\dfrac{\bar{h}_N}{h_1}}\right)$	$\dfrac{h_N}{h_1}$	$\left(\overline{\dfrac{h_N}{h_1}}\right)$	$\dfrac{q/A}{\left(\dfrac{KW}{m^2}\right)}$
37	1	11.8	1.0	00	1.0	--	280
	2	8.5	0.86	--	0.72	--	260
	3	8.0	0.80	--	0.68	--	240
	4	7.5	0.76	--	0.64	--	240
	5	7.2	0.73	--	0.61	--	220
38	1	12.4	1.0	00	1.0	--	280
	2	8.7	0.85	--	0.70	--	270
	3	7.9	0.78	--	0.64	--	240
	4	7.6	0.74	--	0.62	--	240
	5	7.0	0.71	--	0.57	--	220
39	1	12.2	1.0	--	1.0	--	280
	2	8.7	0.86	--	0.71	--	270
	3	7.9	0.79	--	0.65	--	240
	4	7.7	0.75	--	0.63	--	240
	5	7.0	0.71	--	0.57	--	220
40	1	12.3	1.0	--	1.0	--	280
	2	8.7	0.85	--	0.71	--	280
	3	8.1	0.79	--	0.65	--	240
	4	7.5	0.74	--	0.61	--	240
	5	7.1	0.71	--	0.58	--	220
31-40	1	--	--	1.0	--	1.0	--
	2	--	--	0.85	--	0.70	--
	3	--	--	0.79	--	0.66	--
	4	--	--	0.75	--	0.63	--
	5	--	--	0.72	--	0.59	--

RUN #	TUBE #	$\frac{h}{\left(\frac{KW}{m^2 \cdot {}^{\circ}C}\right)}$	$\frac{\bar{h}_N}{h_1}$	$\left(\frac{\bar{h}_N}{h_1}\right)$	$\frac{h_N}{h_1}$	$\left(\frac{h_N}{h_1}\right)$	$\frac{q/A}{\left(\frac{KW}{m^2}\right)}$
41	1	16.3	1.0	—	1.0	—	130
	2	14.0	0.93	—	0.86	—	140
	3	16.0	0.95	—	0.98	—	110
	4	13.4	0.91	—	0.82	—	120
	5	9.8	0.85	—	0.60	—	100
42	1	15.6	1.0	—	1.0	—	140
	2	13.2	0.92	—	0.85	—	150
	3	12.7	0.89	—	0.81	—	130
	4	12.2	0.86	—	0.78	—	130
	5	9.3	0.81	—	0.60	—	110
43	1	15.7	1.0	—	1.0	—	130
	2	12.0	0.88	—	0.76	—	130
	3	12.4	0.85	—	0.79	—	120
	4	12.1	0.83	—	0.77	—	120
	5	9.5	0.79	—	0.61	—	110
44	1	15.9	1.0	—	1.0	—	120
	2	12.6	0.90	—	0.79	—	130
	3	12.6	0.86	—	0.79	—	120
	4	12.4	0.84	—	0.78	—	120
	5	10.3	0.80	—	0.65	—	110
45	1	17.2	1.0	—	1.0	—	130
	2	13.4	0.89	—	0.78	—	130
	3	13.8	0.86	—	0.80	—	120
	4	14.0	0.85	—	0.81	—	120
	5	11.3	0.81	—	0.66	—	110

RUN #	TUBE #	$\dfrac{h}{\left(\dfrac{KW}{m^2 \cdot {}^\circ C}\right)}$	$\dfrac{\overline{h}_N}{h_1}$	$\left(\dfrac{\overline{h}_N}{h_1}\right)$	$\dfrac{h_N}{h_1}$	$\left(\dfrac{h_N}{h_1}\right)$	$\dfrac{q/A}{\left(\dfrac{KW}{m^2}\right)}$
41-45	1	--	--	1.0	--	1.0	--
	2	--	--	0.90	--	0.81	--
	3	--	--	0.88	--	0.84	--
	4	--	--	0.86	--	0.79	--
	5	--	--	0.81	--	0.62	--
45	1	17.2	1.0	--	1.0	--	130
	2	13.3	0.89	--	0.77	--	130
	3	13.6	0.85	--	0.79	--	120
	4	13.4	0.84	--	0.78	--	120
	5	10.2	0.79	--	0.60	--	100
47	1	20.9	1.0	--	1.0	--	130
	2	16.8	0.90	--	0.80	--	140
	3	15.6	0.85	--	0.75	--	120
	4	15.1	0.82	--	0.72	--	120
	5	11.7	0.77	--	0.56	--	110
48	1	19.2	1.0	--	1.0	--	130
	2	15.8	0.91	--	0.82	--	150
	3	14.3	0.85	--	0.74	--	120
	4	14.4	0.83	--	0.75	--	120
	5	11.2	0.78	--	0.58	--	110
49	1	17.9	1.0	--	1.0	--	130
	2	15.1	0.92	--	0.84	--	150
	3	13.9	0.87	--	0.78	--	120
	4	14.4	0.86	--	0.80	--	130
	5	10.8	0.80	--	0.60	--	110

RUN #	TUBE #	$\dfrac{h}{\left(\frac{KW}{m^2\cdot{}^oC}\right)}$	$\dfrac{\overline{h}_N}{h_1}$	$\left(\dfrac{\overline{h}_N}{h_1}\right)$	$\dfrac{h_N}{h_1}$	$\left(\dfrac{h_N}{h_1}\right)$	$\dfrac{q/A}{\left(\frac{KW}{m^2}\right)}$
50	1	18.7	1.0	--	1.0	--	130
	2	16.5	0.94	--	0.88	--	150
	3	14.0	0.88	--	0.75	--	120
	4	13.9	0.84	--	0.74	--	120
	5	11.2	0.79	--	0.60	--	110
46-50	1	--	--	1.0	--	1.0	--
	2	--	--	0.91	--	0.84	--
	3	--	--	0.86	--	0.76	--
	4	--	--	0.84	--	0.76	--
	5	--	--	0.79	--	0.59	--
51	1	19.4	1.0	--	1.0	--	140
	2	15.6	0.90	--	0.80	--	150
	3	15.3	0.86	--	0.79	--	130
	4	14.5	0.84	--	0.75	--	130
	5	11.8	0.79	--	0.61	--	120
52	1	19.1	1.0	--	1.0	--	140
	2	15.5	0.90	--	0.81	--	150
	3	14.8	0.86	--	0.77	--	130
	4	13.6	0.82	--	0.71	--	130
	5	10.8	0.77	--	0.57	--	110
53	1	22.2	1.0	--	1.0	--	140
	2	17.0	0.88	--	0.76	--	160
	3	17.8	0.86	--	0.80	--	140
	4	17.0	0.83	--	0.76	--	140
	5	13.4	0.79	--	0.60	--	120

RUN #	TUBE #	$\dfrac{h}{\left(\dfrac{KW}{m^2 \cdot {}^\circ C}\right)}$	$\dfrac{\bar{h}_N}{h_1}$	$\left(\dfrac{\bar{h}_N}{h_1}\right)$	$\dfrac{h_N}{h_1}$	$\left(\dfrac{h_N}{h_1}\right)$	$\dfrac{q/A}{\left(\dfrac{KW}{m^2}\right)}$
54	1	17.4	1.0	--	1.0	--	140
	2	15.4	0.94	--	0.89	--	170
	3	14.1	0.90	--	0.81	--	140
	4	13.9	0.87	--	0.80	--	140
	5	12.0	0.83	--	0.63	--	120
55	1	18.3	1.0	--	1.0	--	140
	2	15.6	0.93	--	0.85	--	160
	3	13.9	0.87	--	0.76	--	120
	4	14.5	0.85	--	0.79	--	130
	5	10.9	0.80	--	0.60	--	110
51-55	1	--	--	1.0	--	1.0	--
	2	--	--	0.91	--	0.82	--
	3	--	--	0.87	--	0.79	--
	4	--	--	0.84	--	0.76	--
	5	--	--	0.79	--	0.60	--
56	1	20.7	1.0	--	1.0	--	140
	2	16.6	0.90	--	0.80	--	170
	3	16.3	0.86	--	0.79	--	140
	4	16.2	0.84	--	0.78	--	140
	5	11.8	0.79	--	0.57	--	120
57	1	20.9	1.0	--	1.0	--	140
	2	16.1	0.89	--	0.77	--	160
	3	15.1	0.83	--	0.72	--	130
	4	14.8	0.80	--	0.71	--	130
	5	12.2	0.76	--	0.58	--	120

RUN #	TUBE #	$\dfrac{h}{\left(\dfrac{KW}{m^2 \cdot °C}\right)}$	$\dfrac{\overline{h}_1}{h_1}$	$\left(\dfrac{\overline{h}_N}{h_1}\right)$	$\dfrac{h_N}{h_1}$	$\left(\dfrac{h_N}{h_1}\right)$	$\dfrac{q/A}{\left(\dfrac{KW}{m^2}\right)}$
58	1	23.1	1.0	–	1.0	–	140
	2	16.6	0.86	–	0.72	–	160
	3	16.8	0.82	–	0.73	–	130
	4	15.6	0.78	–	0.67	–	130
	5	11.4	0.72	–	0.50	–	120
59	1	21.6	1.0	–	1.0	–	140
	2	16.1	0.87	–	0.74	–	160
	3	15.0	0.81	–	0.69	–	130
	4	14.0	0.77	–	0.65	–	130
	5	11.2	0.72	–	0.52	–	120
60	1	22.0	1.0	–	1.0	–	140
	2	16.3	0.87	–	0.74	–	160
	3	15.9	0.82	–	0.72	–	130
	4	14.3	0.78	–	0.65	–	140
	5	12.4	0.74	–	0.57	–	130
56-60	1	–	–	1.0	–	1.0	–
	2	–	–	0.88	–	0.76	–
	3	–	–	0.83	–	0.73	–
	4	–	–	0.80	–	0.69	–
	5	–	–	0.75	–	0.55	–
61	1	21.1	1.0	–	1.0	–	150
	2	16.5	0.89	–	0.78	–	160
	3	15.4	0.84	–	0.73	–	130
	4	14.8	0.80	–	0.70	–	130
	5	11.3	0.75	–	0.53	–	110

RUN #	TUBE #	$h\left(\dfrac{KW}{m^2 \cdot {}^\circ C}\right)$	$\dfrac{\overline{h}_N}{h_1}$	$\left(\dfrac{\overline{h}_N}{h_1}\right)$	$\dfrac{h_N}{h_1}$	$\left(\dfrac{h_N}{h_1}\right)$	$\dfrac{q/A}{\left(\dfrac{KW}{m^2}\right)}$
61 (contd)	6	11.3	0.71	---	0.53	---	130
	7	10.6	0.68	---	0.50	---	160
	8	9.7	0.65	---	0.46	---	130
	9	9.5	0.63	---	0.45	---	130
	10	8.0	0.61	---	0.38	---	120
	11	9.2	0.59	---	0.43	---	130
	12	8.9	0.58	---	0.42	---	150
	13	8.0	0.56	---	0.38	---	120
	14	7.8	0.55	---	0.37	---	130
	15	6.6	0.53	---	0.31	---	110
	16	7.8	0.52	---	0.37	---	120
	17	8.2	0.51	---	0.39	---	140
	18	7.7	0.51	---	0.36	---	120
	19	7.8	0.50	---	0.37	---	120
	20	6.4	0.49	---	0.30	---	110
	21	6.9	0.48	---	0.33	---	110
	22	6.9	0.47	---	0.33	---	120
	23	7.1	0.47	---	0.34	---	120
	24	7.5	0.46	---	0.35	---	120
	25	6.1	0.46	---	0.29	---	110
	26	6.6	0.45	---	0.31	---	110
	27	7.2	0.45	---	0.34	---	130
	28	7.2	0.44	---	0.34	---	120
	29	7.2	0.44	---	0.34	---	120
	30	6.2	0.43	---	0.29	---	110

RUN #	TUBE #	$\dfrac{h}{\left(\dfrac{KW}{m^2 \cdot {}^\circ C}\right)}$	$\dfrac{\bar{h}_N}{h_1}$	$\left(\dfrac{\bar{h}_N}{h_1}\right)$	$\dfrac{h_N}{h_1}$	$\left(\dfrac{h_N}{h_1}\right)$	$\dfrac{q/A}{\left(\dfrac{KW}{m^2}\right)}$
62	1	13.2	1.0	--	1.0	--	300
	2	9.8	0.87	--	0.75	--	300
	3	8.9	0.81	--	0.68	--	260
	4	8.0	0.76	--	0.61	--	260
	5	6.1	0.70	--	0.46	--	210
	6	8.4	0.69	--	0.64	--	250
	7	6.6	0.66	--	0.50	--	250
	8	6.3	0.64	--	0.48	--	230
	9	6.4	0.62	--	0.48	--	240
	10	5.0	0.60	--	0.38	--	200

Table VI.

Average Tube Wall Temperatures

$$\left(\begin{array}{c}\text{all temperatures in }^{\circ}C\\ V_m \text{ in m/s}\end{array}\right)$$

RUN #	$\bar{T}_{w1}$	$\bar{T}_{w2}$	$\bar{T}_{w3}$	$\bar{T}_{w4}$	$\bar{T}_{w5}$	T_s	$T_s - \bar{T}_{w1}$	V_m
41	44.3	42.1	45.1	43.0	41.8	52.0	7.7	5.9
42	46.6	44.1	45.4	44.6	43.4	55.3	8.7	6.2
43	45.3	42.2	43.6	43.3	43.3	53.3	8.0	5.9
44	43.9	41.3	42.3	42.2	41.3	51.5	7.6	6.3
45	43.9	41.6	42.8	42.6	41.4	51.2	7.3	5.9
46	44.9	42.2	43.7	43.2	42.4	52.2	7.3	8.2
47	45.0	42.5	43.6	43.0	42.0	51.0	6.0	8.7
48	45.3	42.7	44.0	43.7	42.7	52.1	6.8	8.4
49	45.3	42.5	44.0	43.6	42.5	52.3	7.0	7.6
50	45.5	43.2	43.9	43.8	42.6	52.5	7.0	8.6
51	46.1	43.6	44.9	44.1	43.3	53.1	7.0	8.9
52	46.0	43.2	44.6	53.5	42.9	53.1	7.1	8.9
53	47.0	43.8	45.5	44.8	44.1	53.1	6.1	9.2
54	47.8	44.7	46.0	45.5	44.6	55.6	7.8	7.5
55	45.7	43.0	44.4	44.1	43.0	53.1	7.4	8.4
56	47.5	44.2	46.0	45.6	44.5	54.3	6.8	9.1
57	46.9	43.6	45.1	44.6	43.5	53.4	6.5	9.7
58	47.1	43.4	45.4	44.8		53.2	6.1	9.7
59	47.3	43.7	45.3	44.5		53.8	6.5	9.2
60	47.4	43.8	45.6	44.3	43.7	53.8	6.4	9.1

Table VII.

Comparison of Heat Transfer Coefficients
for a Single Uninundated Tube

(Atmospheric Pressure Runs)
(All coefficients in $kW/m^2 \cdot {}^\circ C$)

RUN #	h_1	h_{Nu}	RUN #	h_1	h_{Nu}
1	14.1	11.1	21	12.1	11.0
2	13.1	11.2	22	12.3	11.2
3	13.6	11.4	23	12.2	11.1
4	12.3	11.2	24	12.4	11.1
5	12.1	11.1	25	12.7	11.1
6	12.7	11.2	26	12.4	11.1
7	12.8	11.2	27	12.7	11.2
8	12.1	11.1	28	12.6	11.2
9	12.3	11.2	29	12.5	11.1
10	12.2	11.2	30	12.5	11.1
11	12.2	11.1	31	11.6	11.0
12	12.2	11.0	32	12.0	11.1
13	12.2	11.1	33	12.2	11.1
14	12.3	11.0	34	12.3	11.1
15	12.5	11.1	35	12.0	11.1
16	12.2	11.1	36	12.0	11.1
17	12.3	11.0	37	11.3	11.0
18	12.1	11.0	38	12.4	11.0
19	12.3	11.0	39	12.2	11.1
20	12.0	11.0	40	12.3	11.1

Table VIII.

Comparison of Heat Transfer Coefficients and Mean Vapor Velocity for a Single Uninundated Tube Under Vacuum Conditions

$$\left(\begin{array}{c}\text{all coefficients in } kW/m^2 \cdot {}^{\circ}C \\ V_m \text{ in } m/s\end{array}\right)$$

RUN #	V_m	h_l	h_{Nu}	h_o
41	5.9	16.3	12.9	18.1
42	6.2	15.6	12.2	18.8
43	5.9	15.7	12.3	18.3
44	6.3	15.9	12.4	18.4
45	5.9	17.2	12.5	18.0
46	8.2	17.2	12.6	20.1
47	8.7	20.9	13.2	20.4
48	8.4	19.2	12.8	20.3
49	7.6	17.9	12.7	19.7
50	8.6	18.7	12.7	20.5
51	3.9	19.4	12.8	20.8
52	8.9	19.1	12.7	20.8
53	9.2	22.2	13.2	21.1
54	7.5	17.4	12.5	20.0
55	8.4	18.3	12.6	20.4
56	9.1	20.7	12.9	21.1
57	9.7	20.9	13.1	21.5
58	9.7	23.1	13.2	21.5
59	9.2	21.6	13.1	21.1
60	9.1	22.0	13.1	21.1
61	8.1	21.1	12.8	20.3
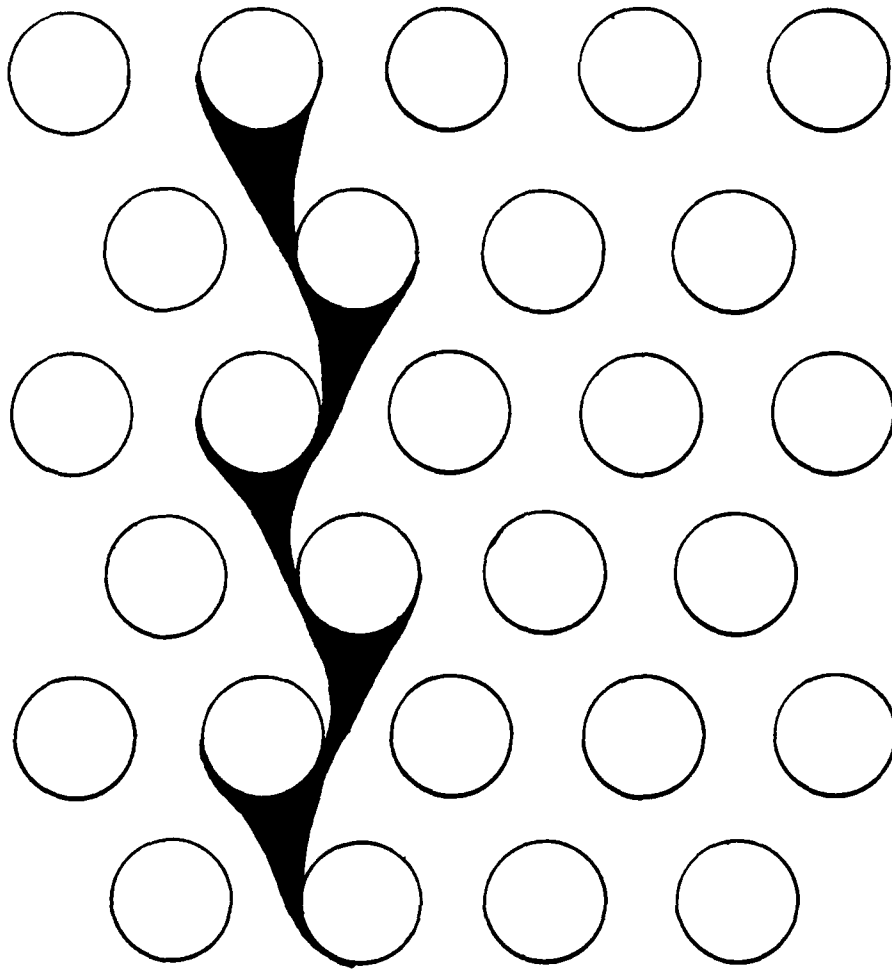
Figure 1: Droplet Path Through a Tube Bundle with Side Drainage

Figure 2a:

Idealized Condensation
on Banks of Tubes
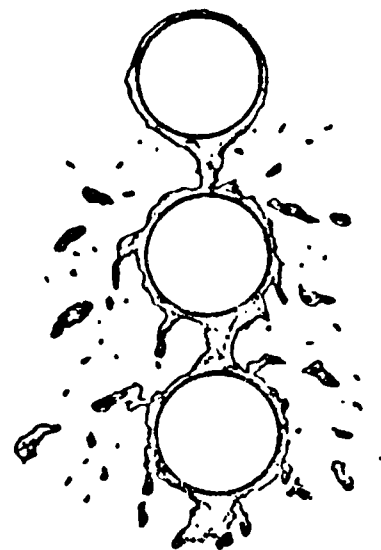
Figure 2b:

More Realistic Picture
of Condensation on
Banks of Tubes
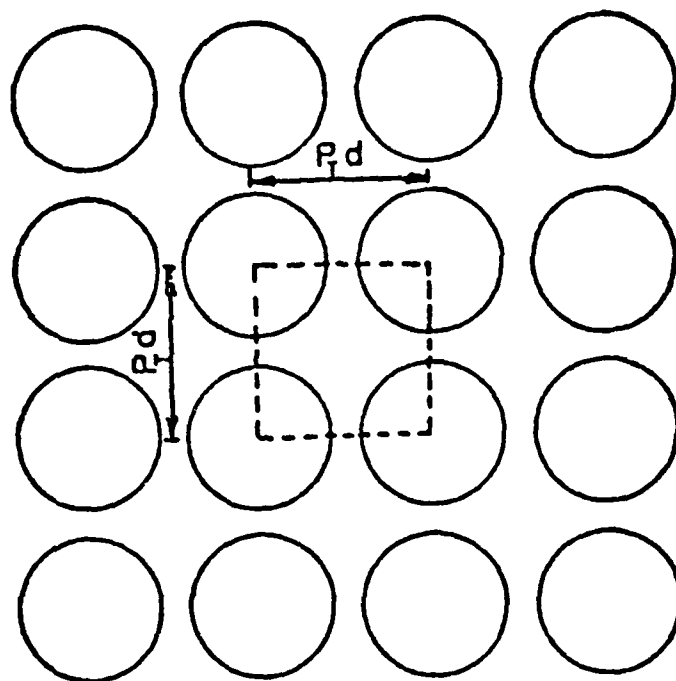
AREA OF UNIT CELL $= (P_T d)^2$

FREE AREA OF CELL $= d^2 (P_T{}^2 - \pi/4)$

MEAN FLOW WIDTH $= d (P_T - \pi/4P_T)$

$(= $ FREE AREA/HEIGHT OF CELL$)$

Figure 3: Mean Flow Width for a Square In-Line Tube Bundle
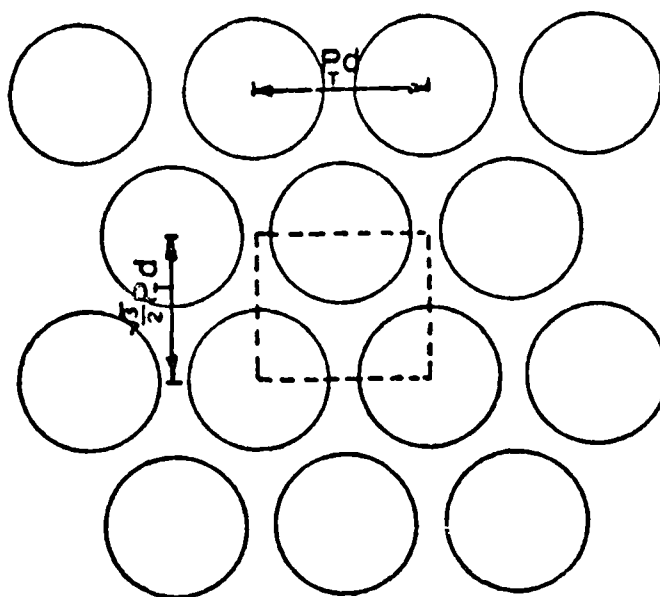
AREA OF UNIT CELL $= \sqrt{3} \; (P_T d)^2 / 2$

FREE AREA OF CELL $= d^2 \; (\sqrt{3} \; P_T{}^2 / 2 - \pi/4)$

MEAN FLOW WIDTH $= d \; (P_T - {}^\pi/2 \; \sqrt{3} \; P_T)$

($=$ FREE AREA/HEIGHT OF CELL)

Figure 4:   Mean Flow Width for a Staggered Tube Bundle
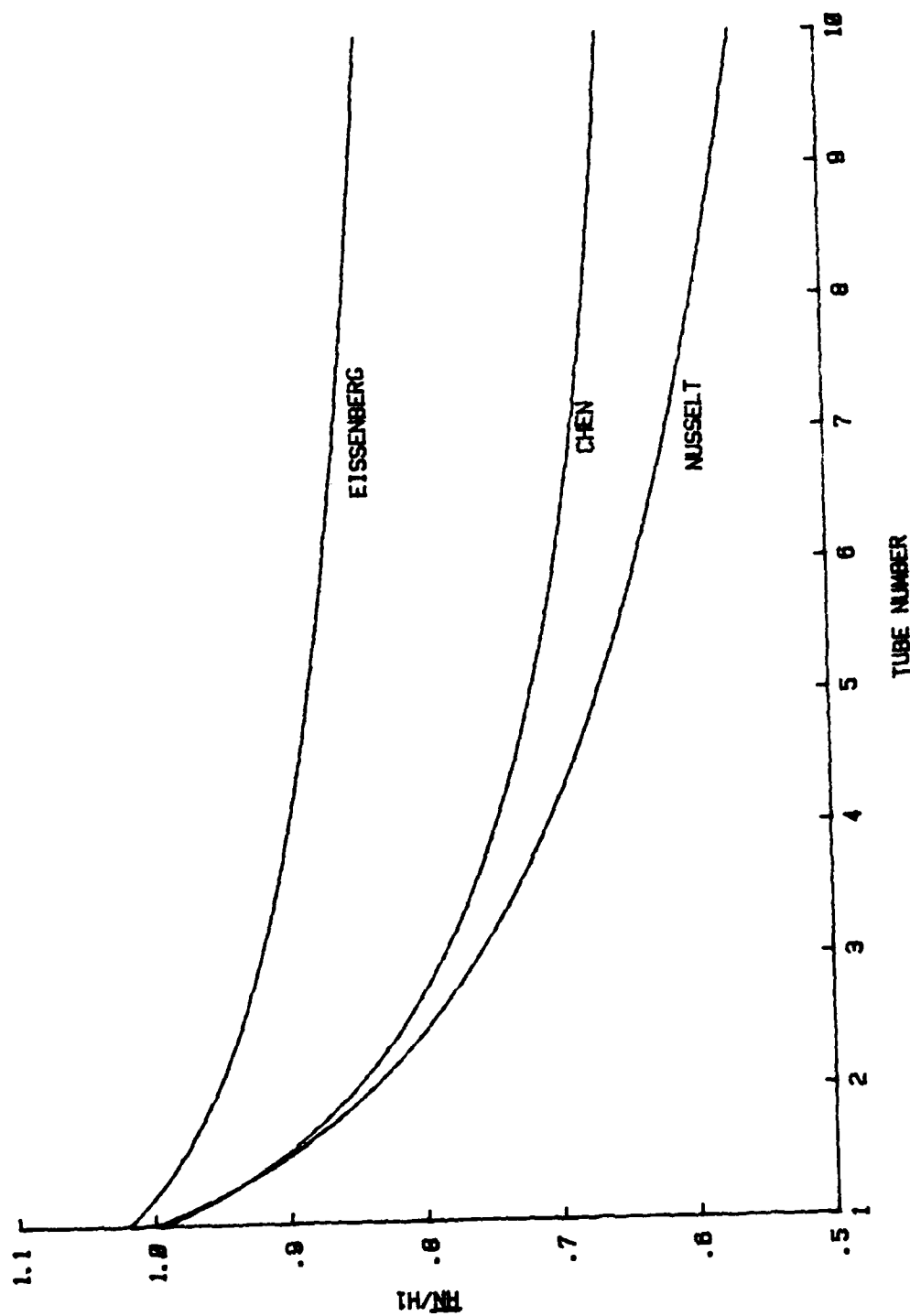
Figure 5: COMPARISON OF PREDICTIONS OF TUBE BUNDLE PERFORMANCE

112
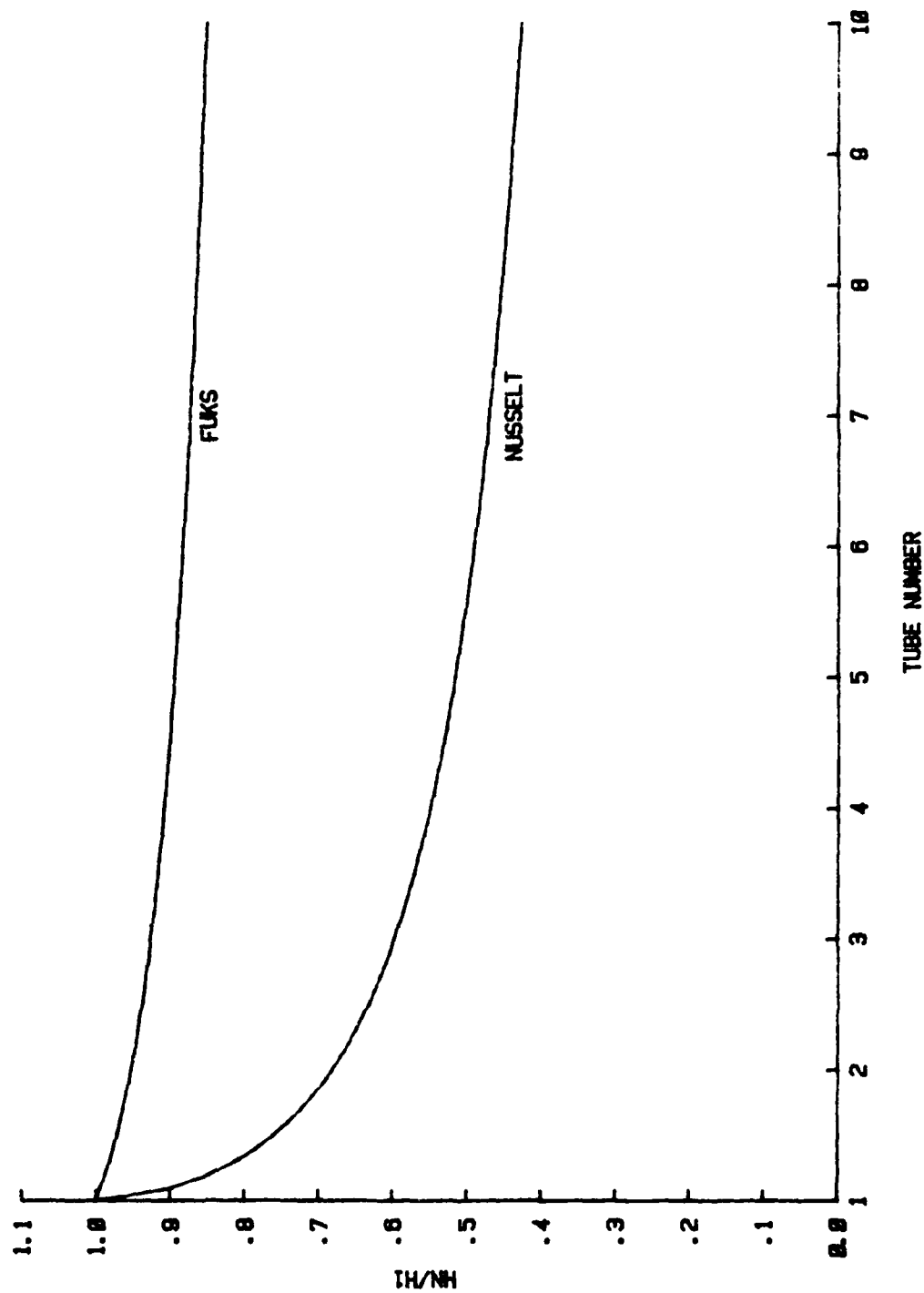
Figure 6: COMPARISON OF PREDICTIONS FOR THE LOCAL HEAT TRANSFER COEFFICIENT
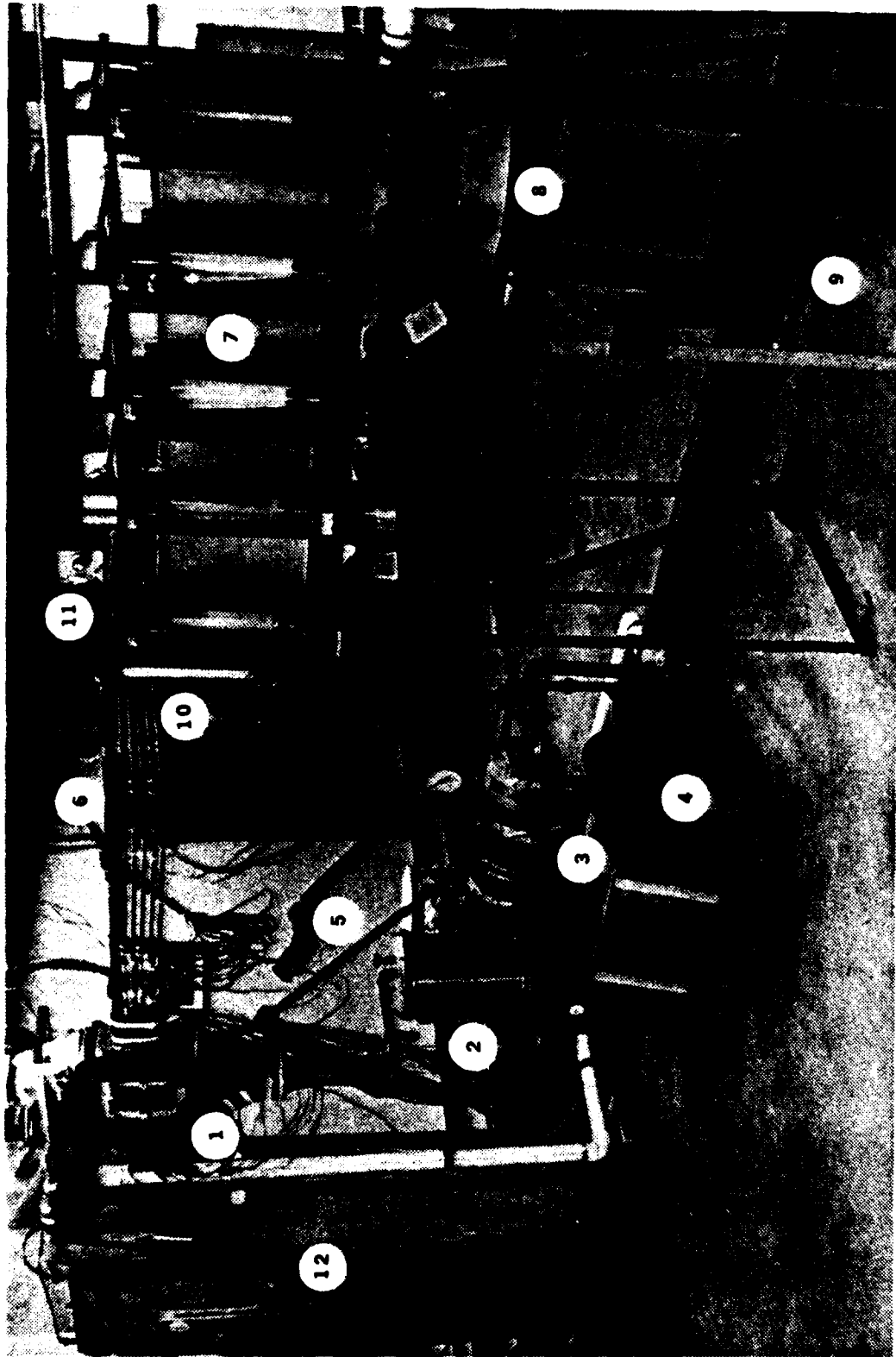
Figure 7a: Front View of Test Apparatus

114
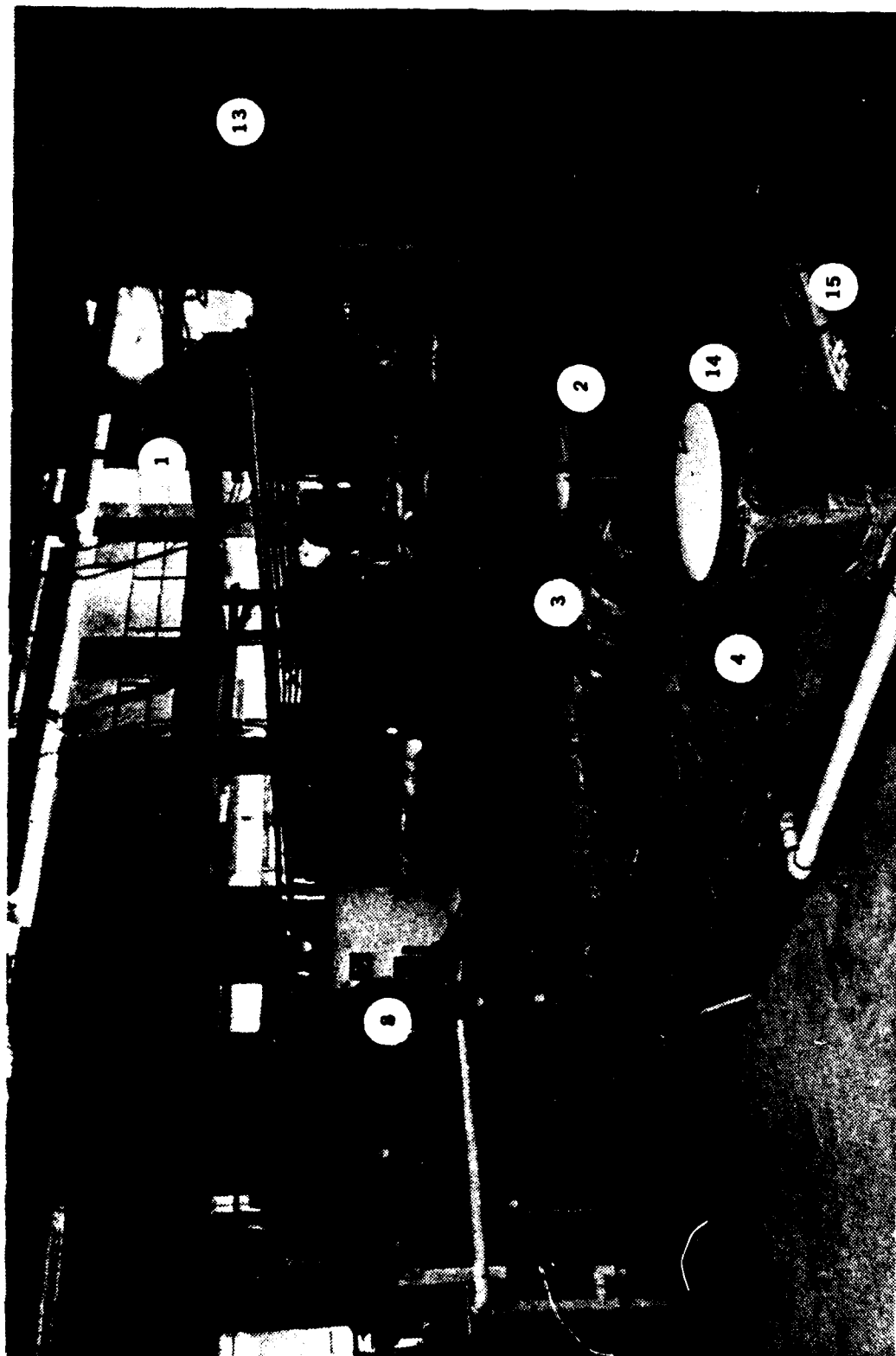
Figure 7b: Rear View of Test Apparatus

115

KEY TO FIGURES 7a AND 7b

1. Test Condenser

2. Test Condenser Hotwell

3. Secondary Condenser

4. Secondary Condenser Hotwell

5. Test Condenser Steam Exhaust Piping
    (Small pipe connected for atmospheric pressure run.
    Larger pipe is used for vacuum runs.)

6. Porous Tube Supply Piping (top pipe) and Cooling Water
    Supply Piping (lower five; note the cooling water inlet
    thermocouple connections.)

7. Cooling Water Rotameters

3. Porous Tube Supply Water Tank

9. Porous Tube Supply Water Pump

10. Porous Tube Rotameter

11. Porous Tube Supply Water Temperature Controller

12. Test Condenser Manometer

13. Desuperheater Tank with Water Spray Nozzles

14. Desuperheater Water Supply Tank

15. Desuperheater Water Supply Pump
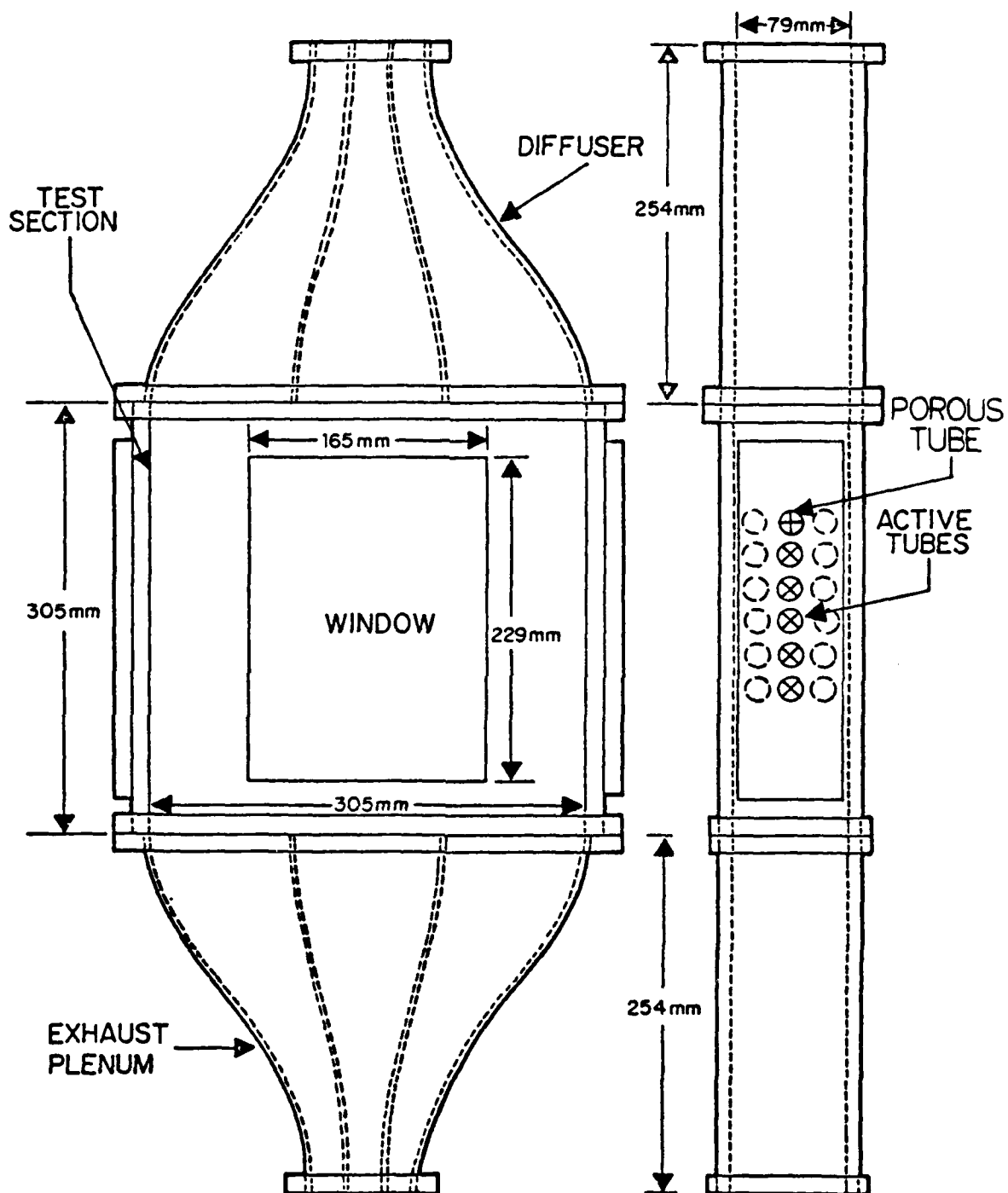
NOTE: ALL COMPONENTS DRAWN TO SCALE

Figure 8:   Sketch of Test Condenser

117
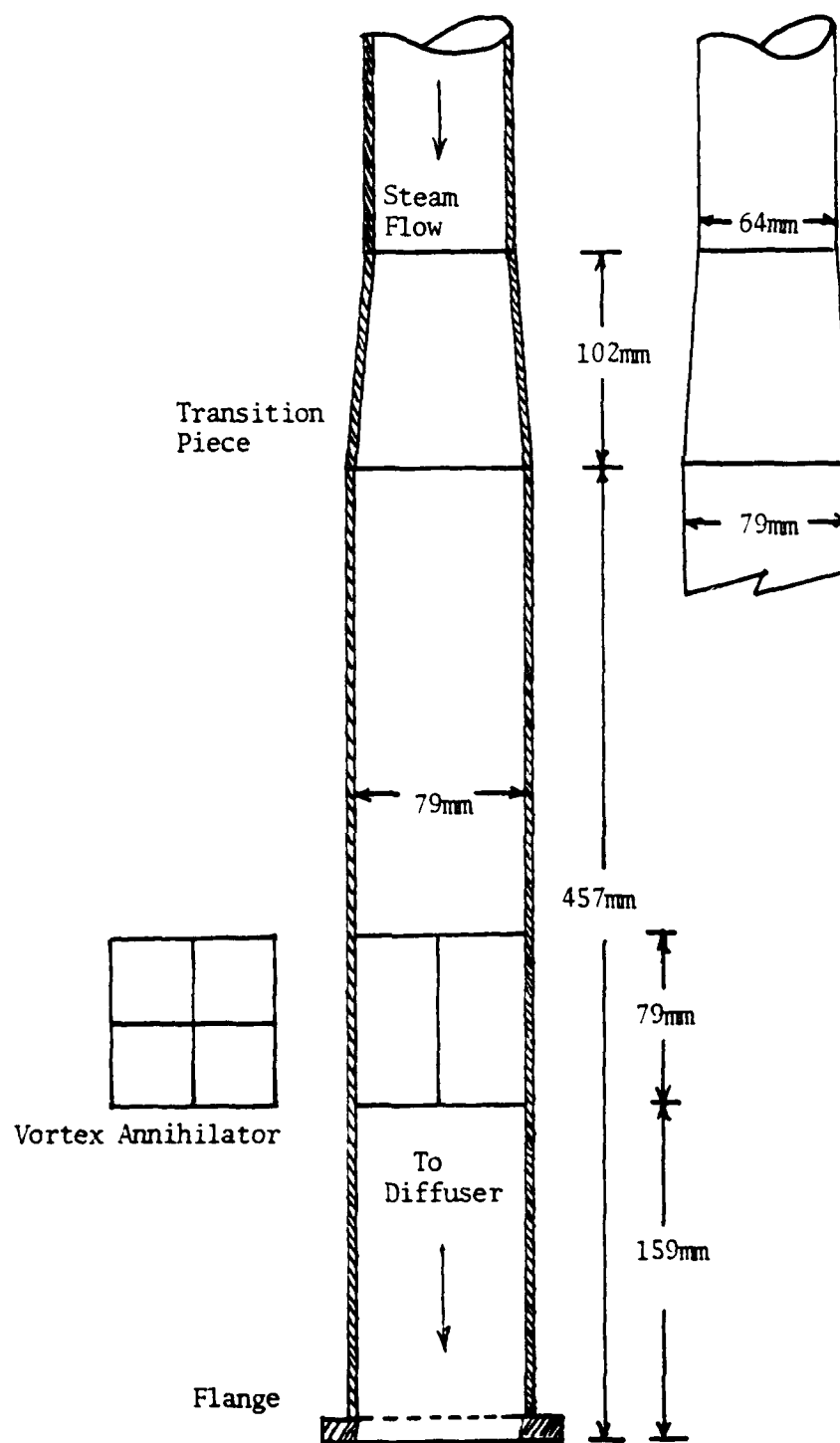
Figure 9: Details of Transition Piece and Vortex Annihilator

118

EXHAUST (STEAM AND CONDENSATE)

102 mm

152 mm

64mm

STEAM TO SECONDARY
CONDENSER HOTWELL

64 mm

25 mm

TO TEST CONDENSER HOTWELL
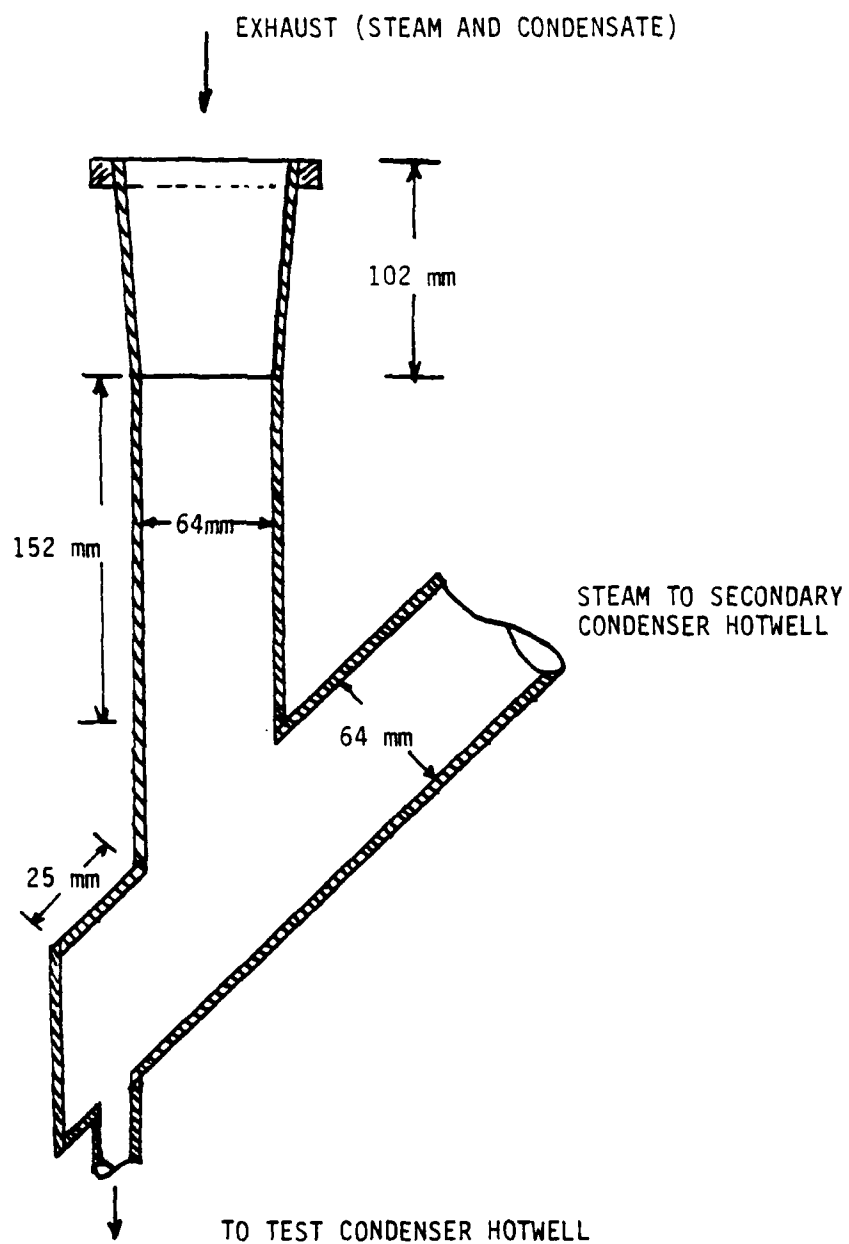
Figure 10: Details of Exhaust and Condensate Piping from the
Exhaust Plenum

119
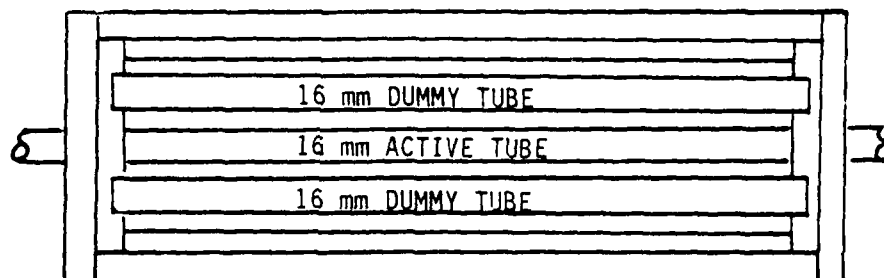
Figure 11: Top View of Test Section
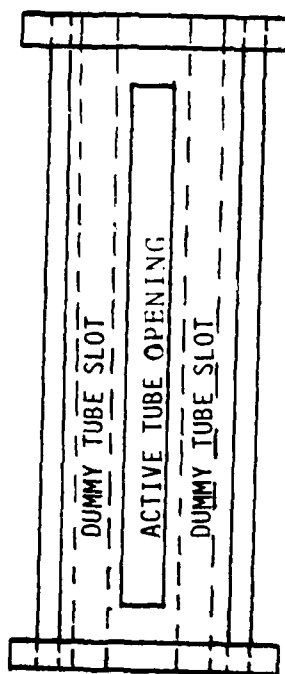
Figure 12: Side View of Test Section

120
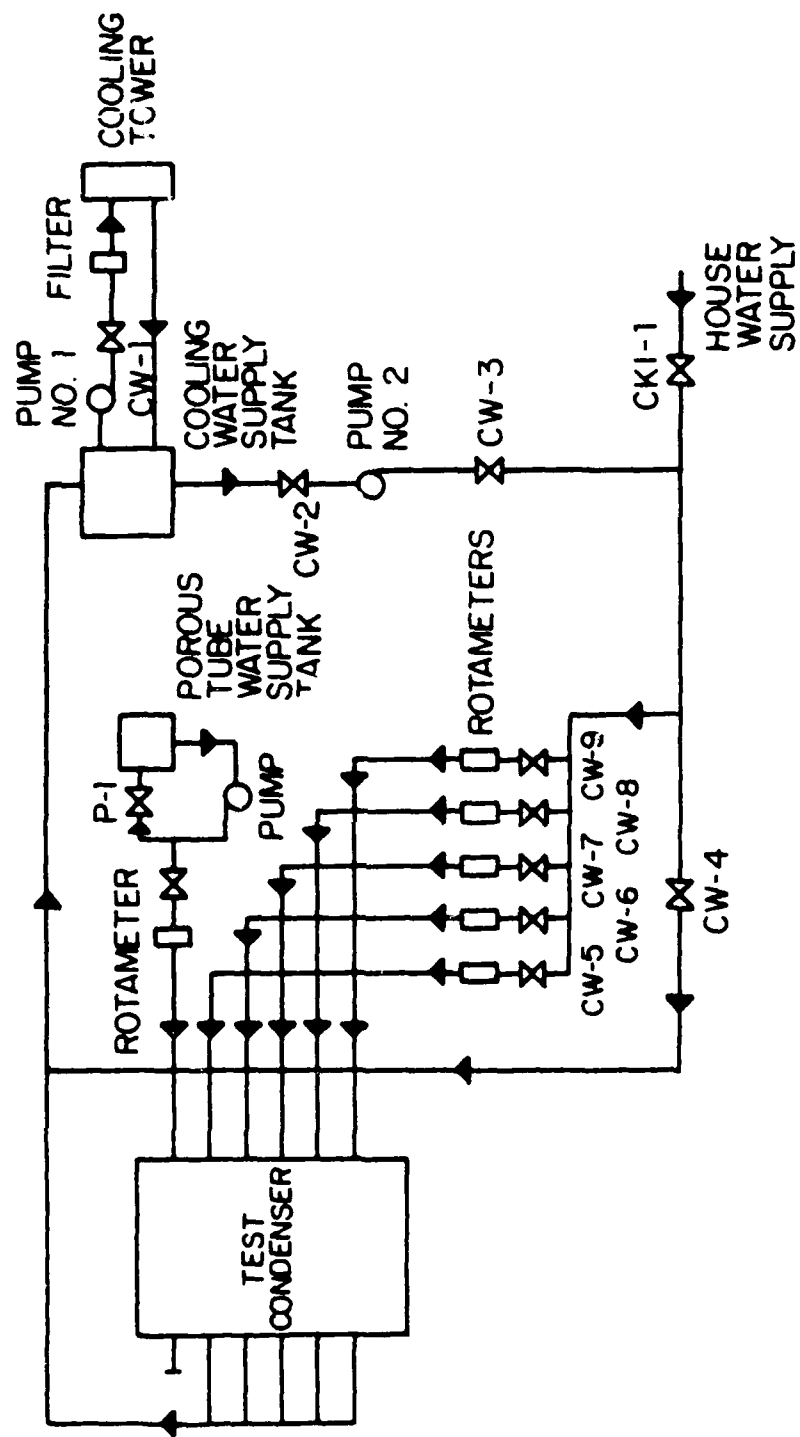
Figure 13: Schematic Diagram of Cooling Water and Porous Tube Water Systems.

121
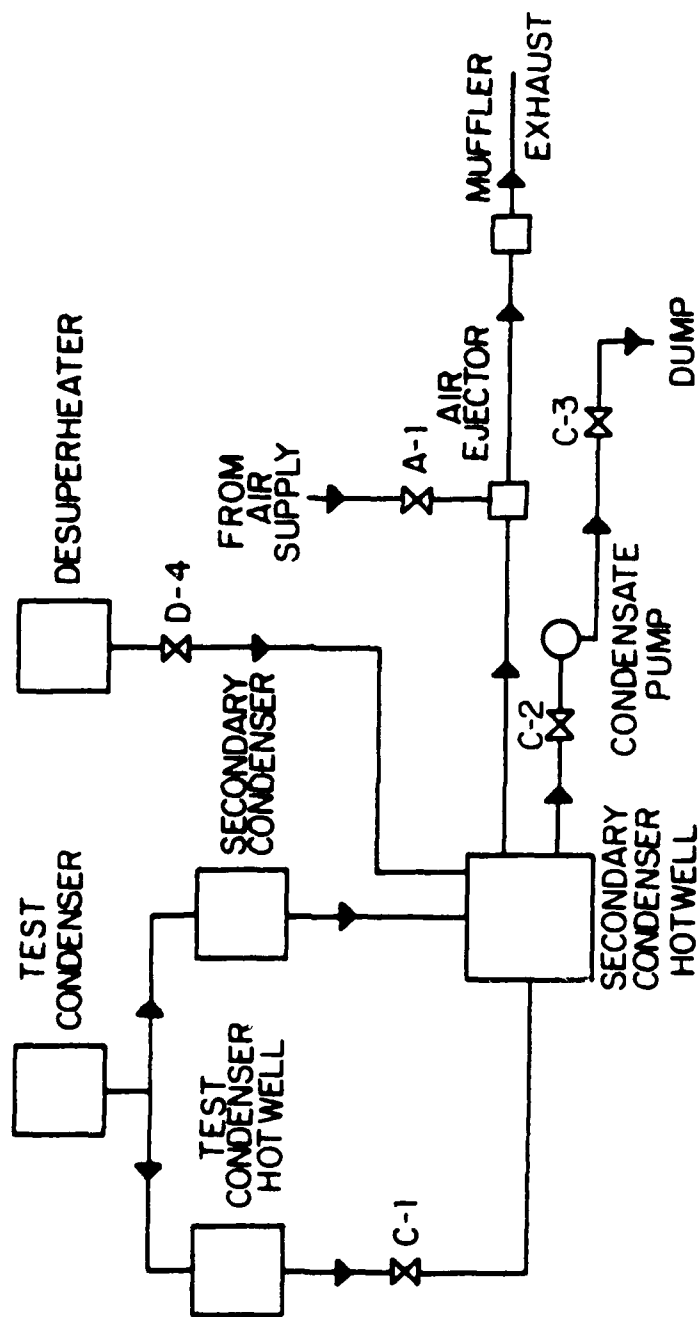
Figure 14: Schematic Diagram of Condensate and Vacuum Systems.

122
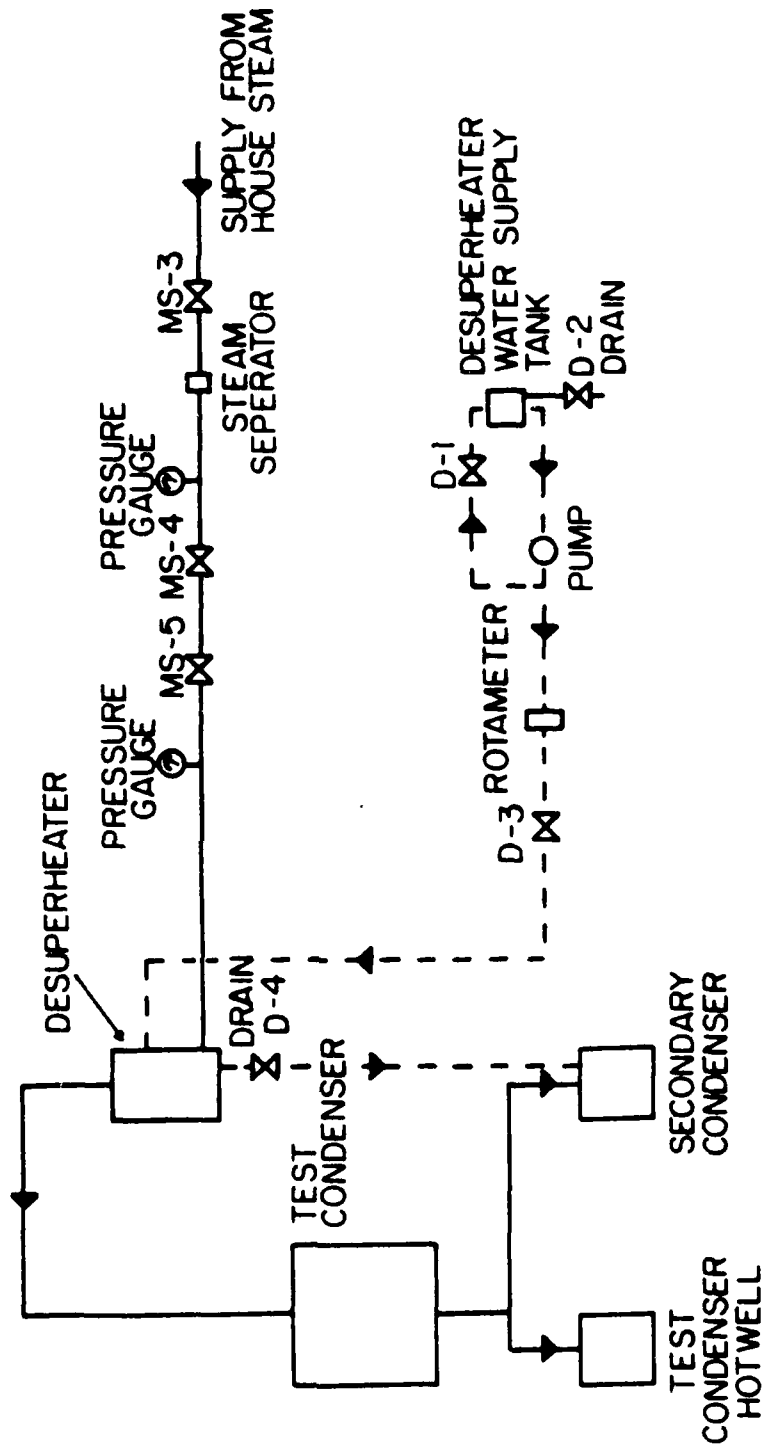
Figure 15: Schematic Diagram of Steam System.

123
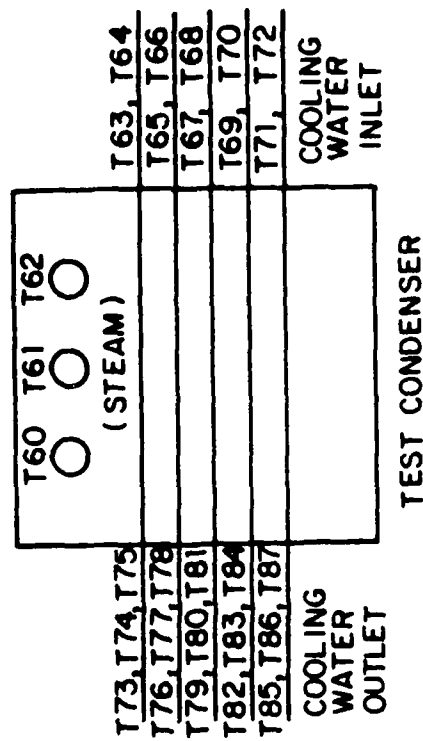
Figure 16: Location as Thermocouples.
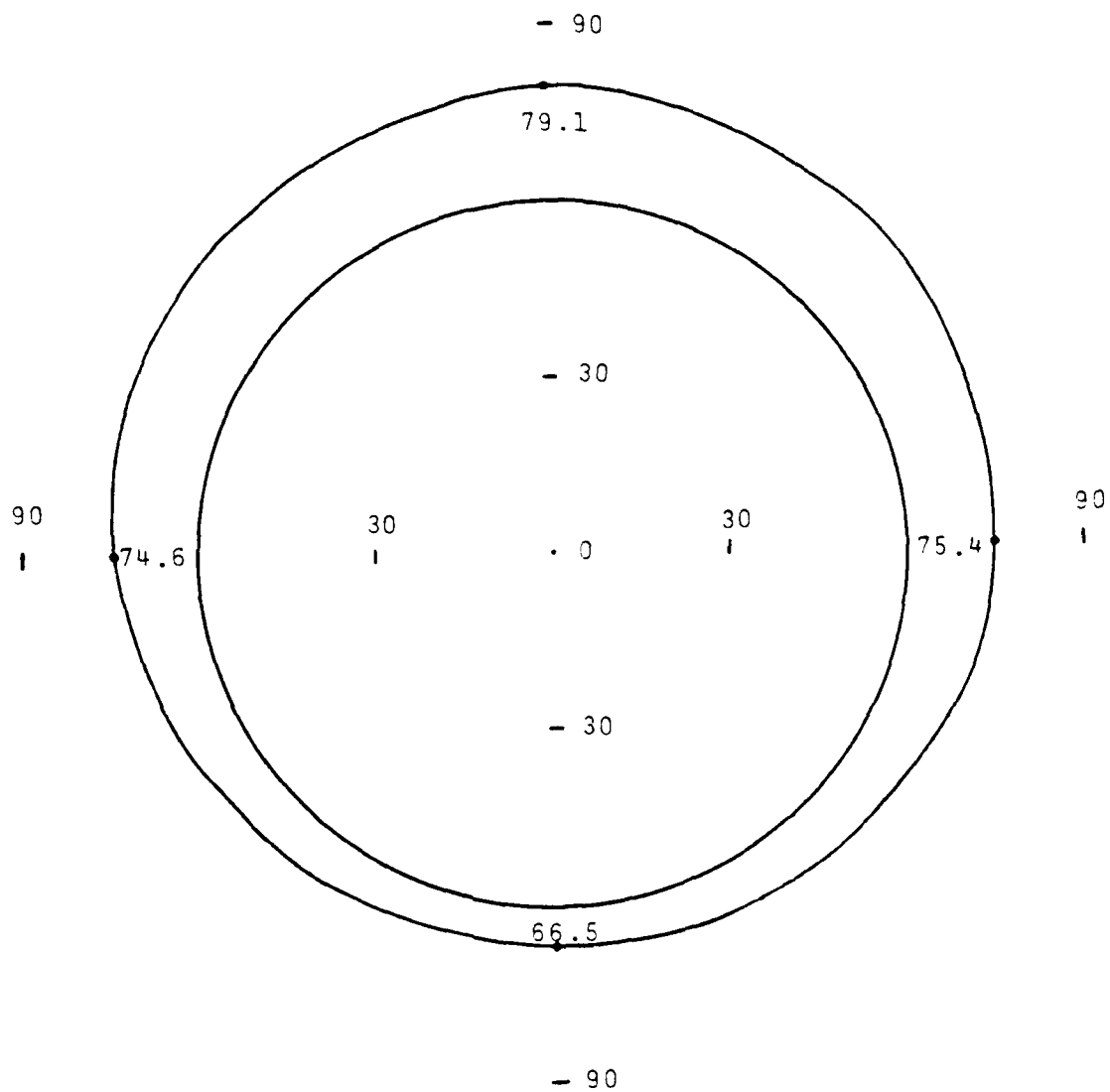
Figure 17: Polar Plot of a Typical Tube Wall Temperature
Distribution (Run 7, Tube 3 - Temperatures in
$^{\circ}$C)
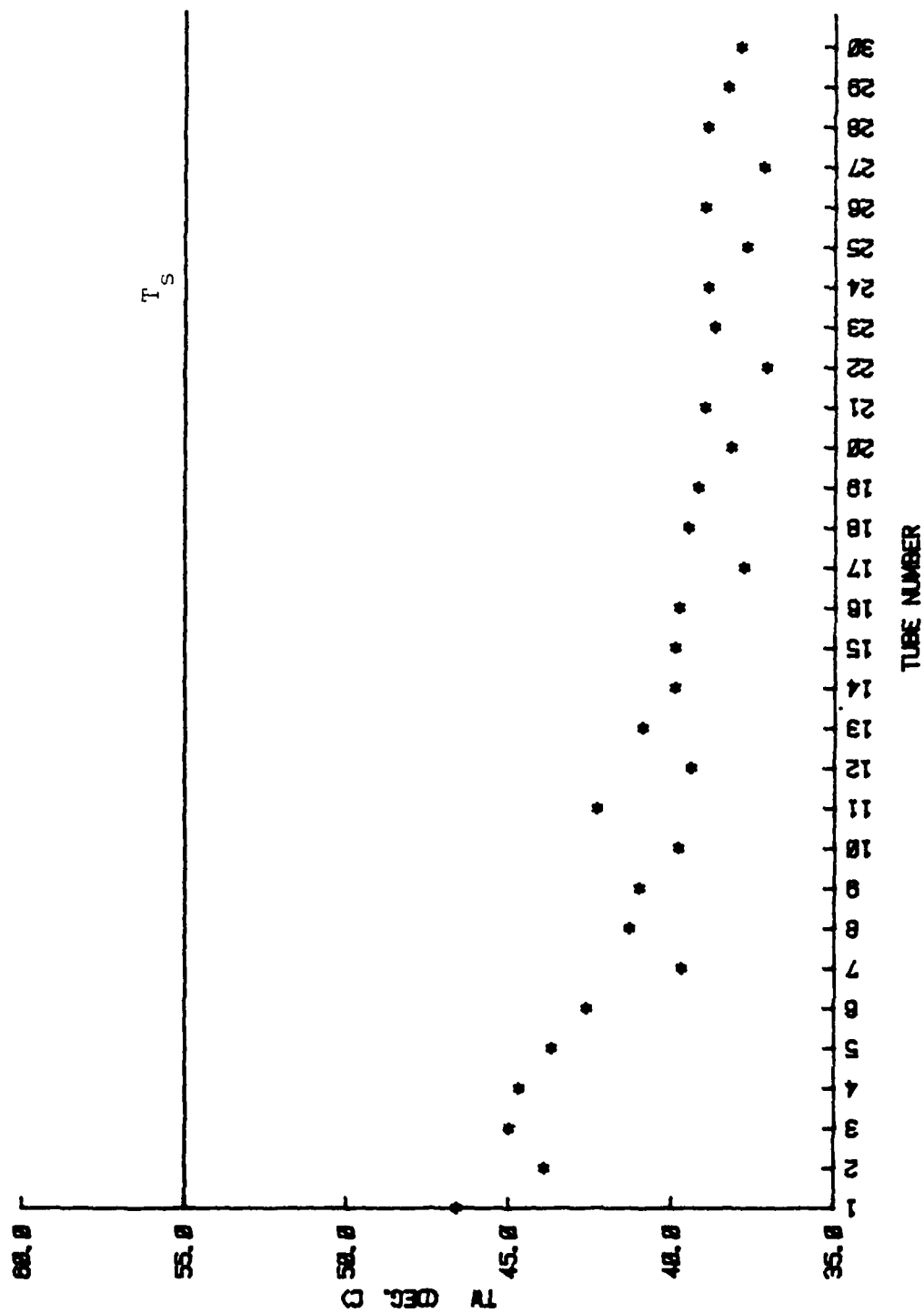
Figure 18: AVG. TV VS TUBE NUMBER   RUN 61

126
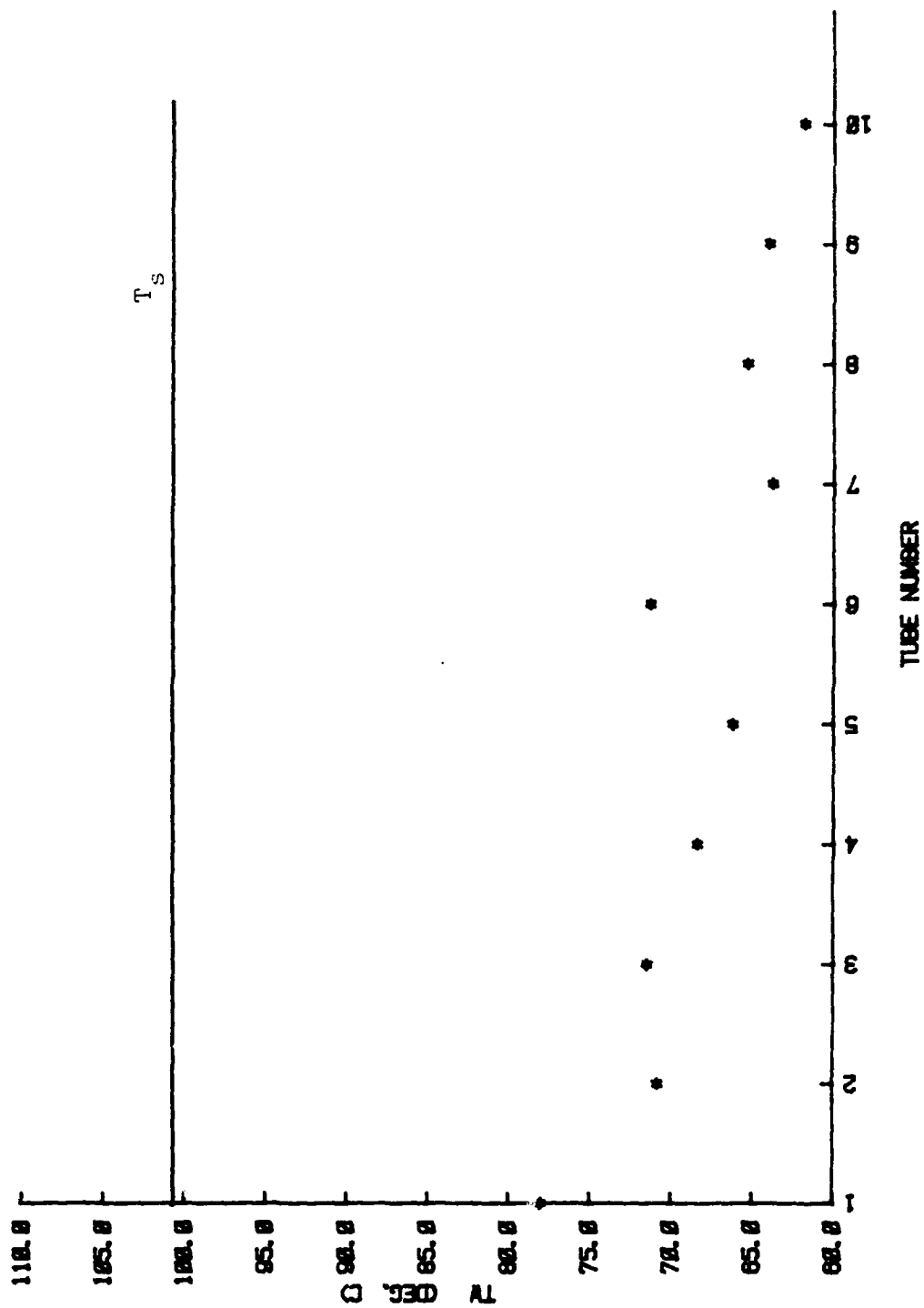
Figure 19: AVG. TV VS TUBE NUMBER   RUN 62
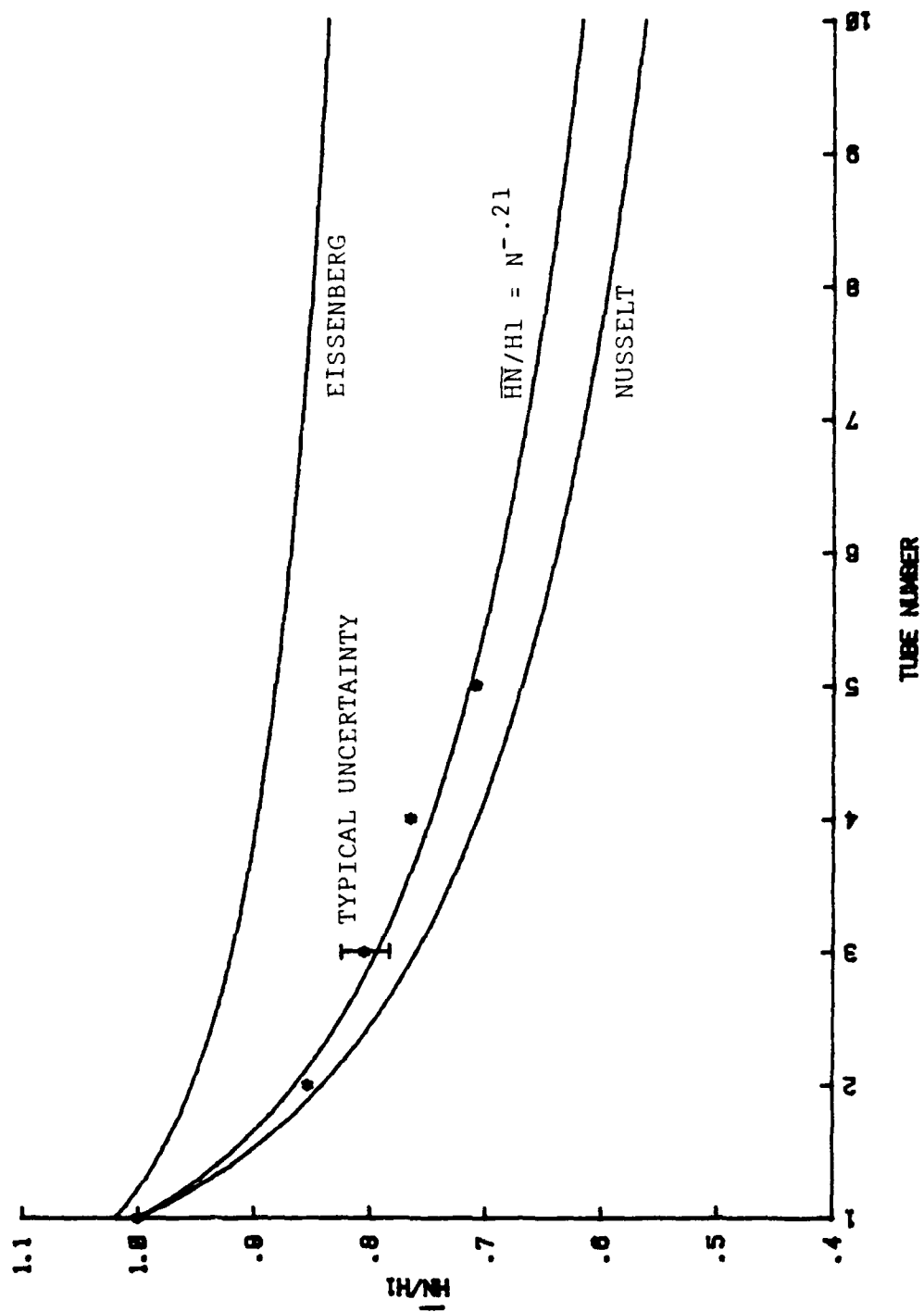
Figure 20: AVERAGE $\overline{HN}/H1$ VS TUBE NUMBER   RUNS 1 - 10
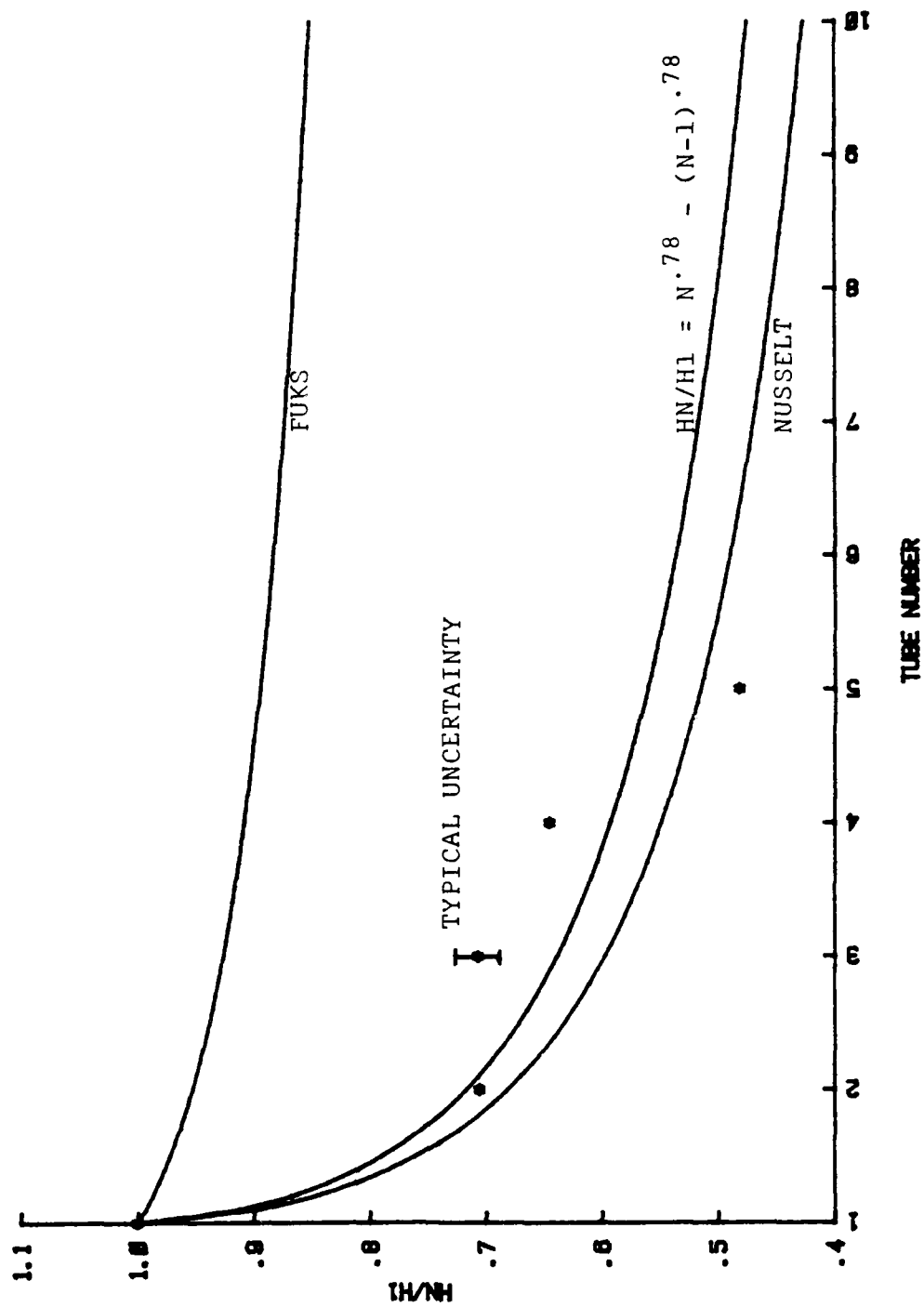
Figure 21: AVERAGE HN/H1 VS TUBE NUMBER   RUNS 1 - 10

129
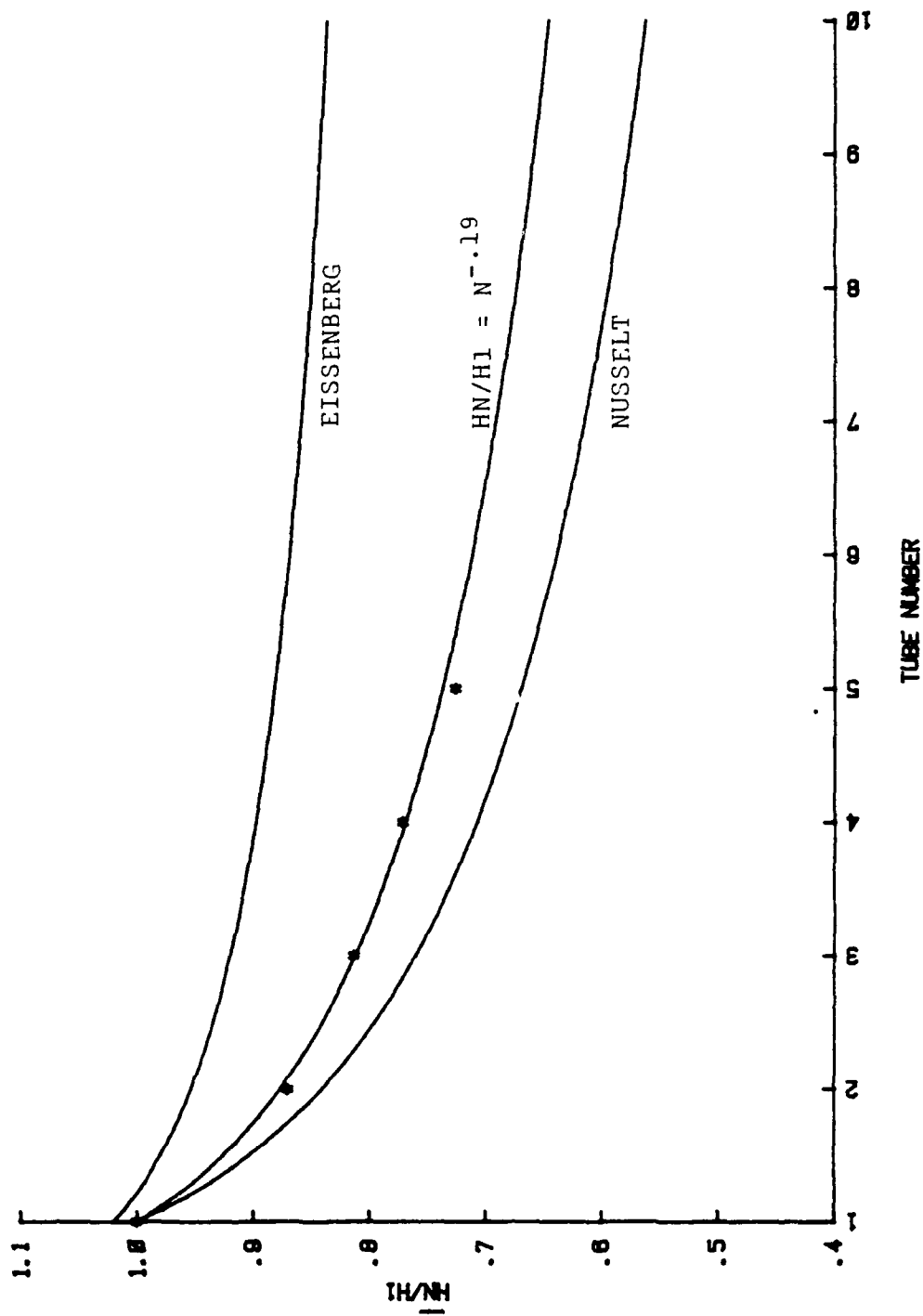
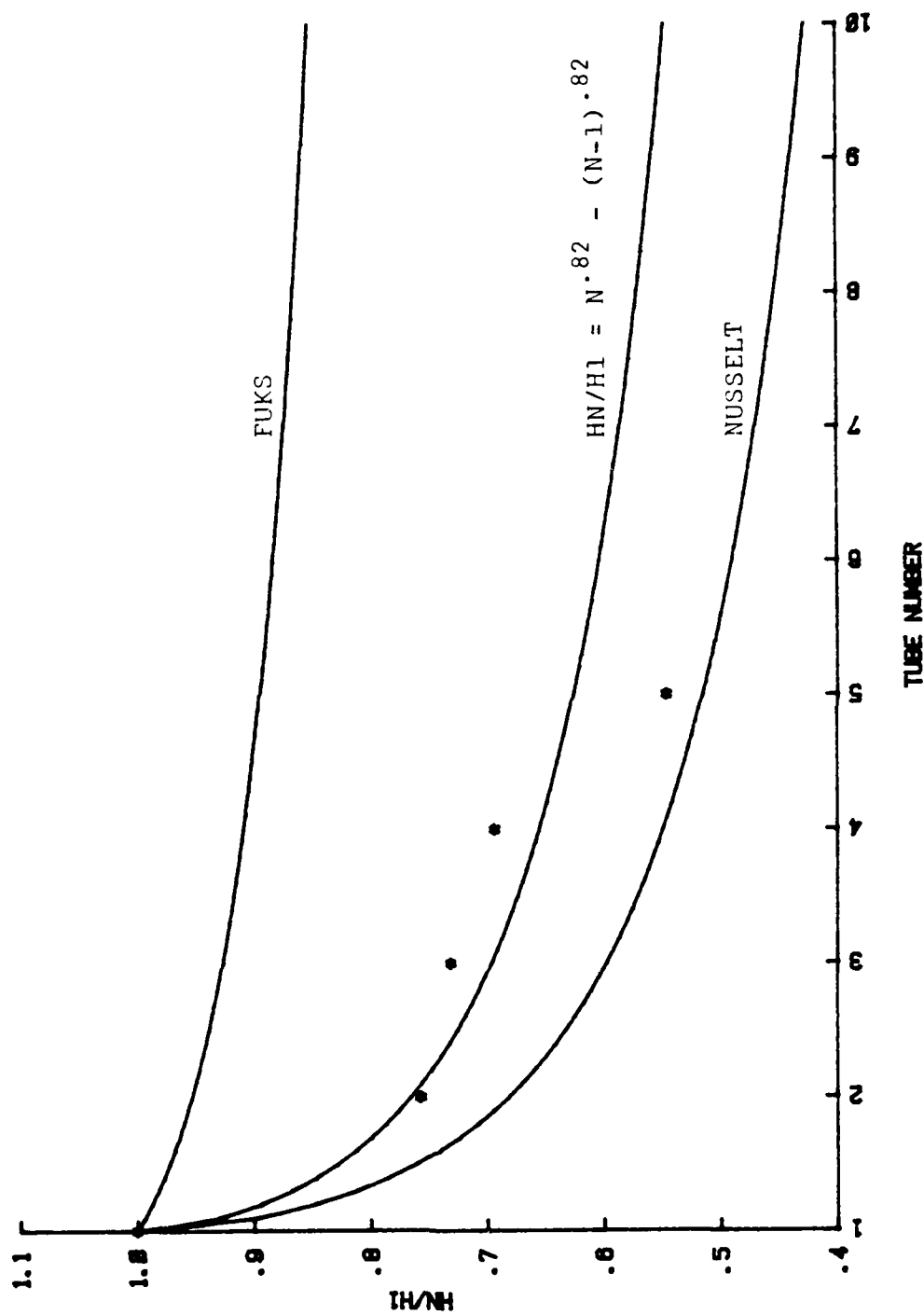Figure 22: AVERAGE $\overline{HN/H1}$ VS TUBE NUMBER   RUNS 11 - 20
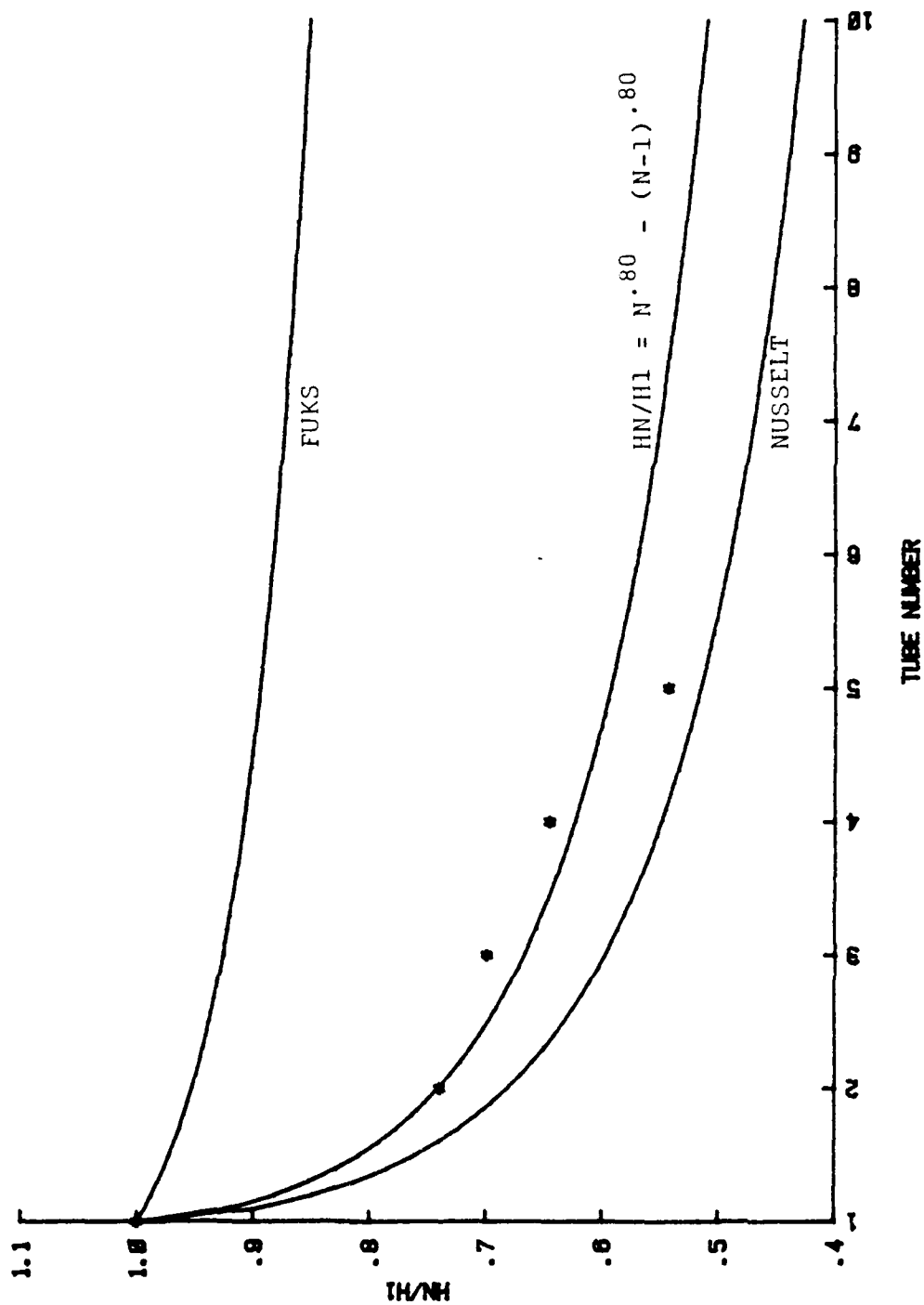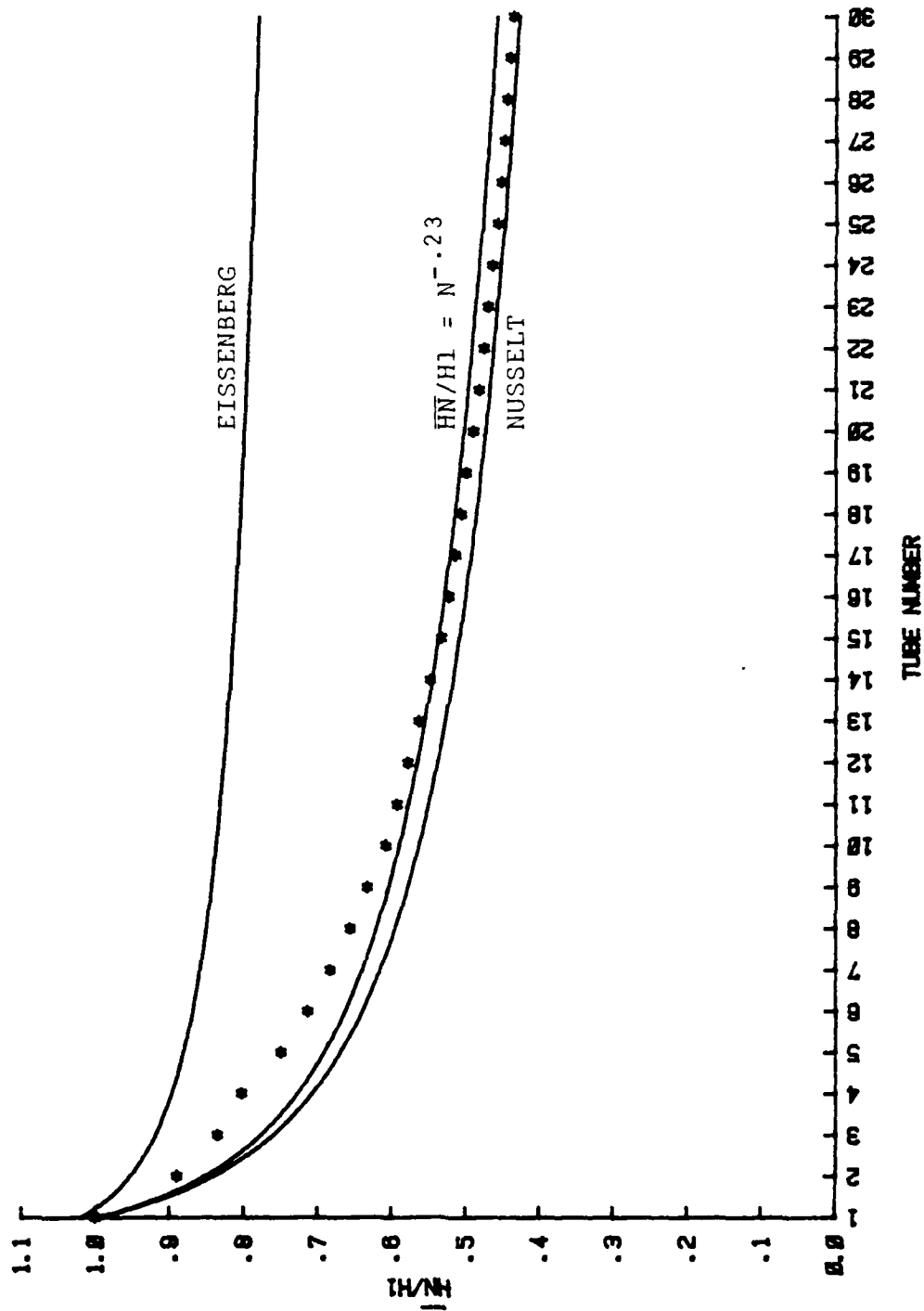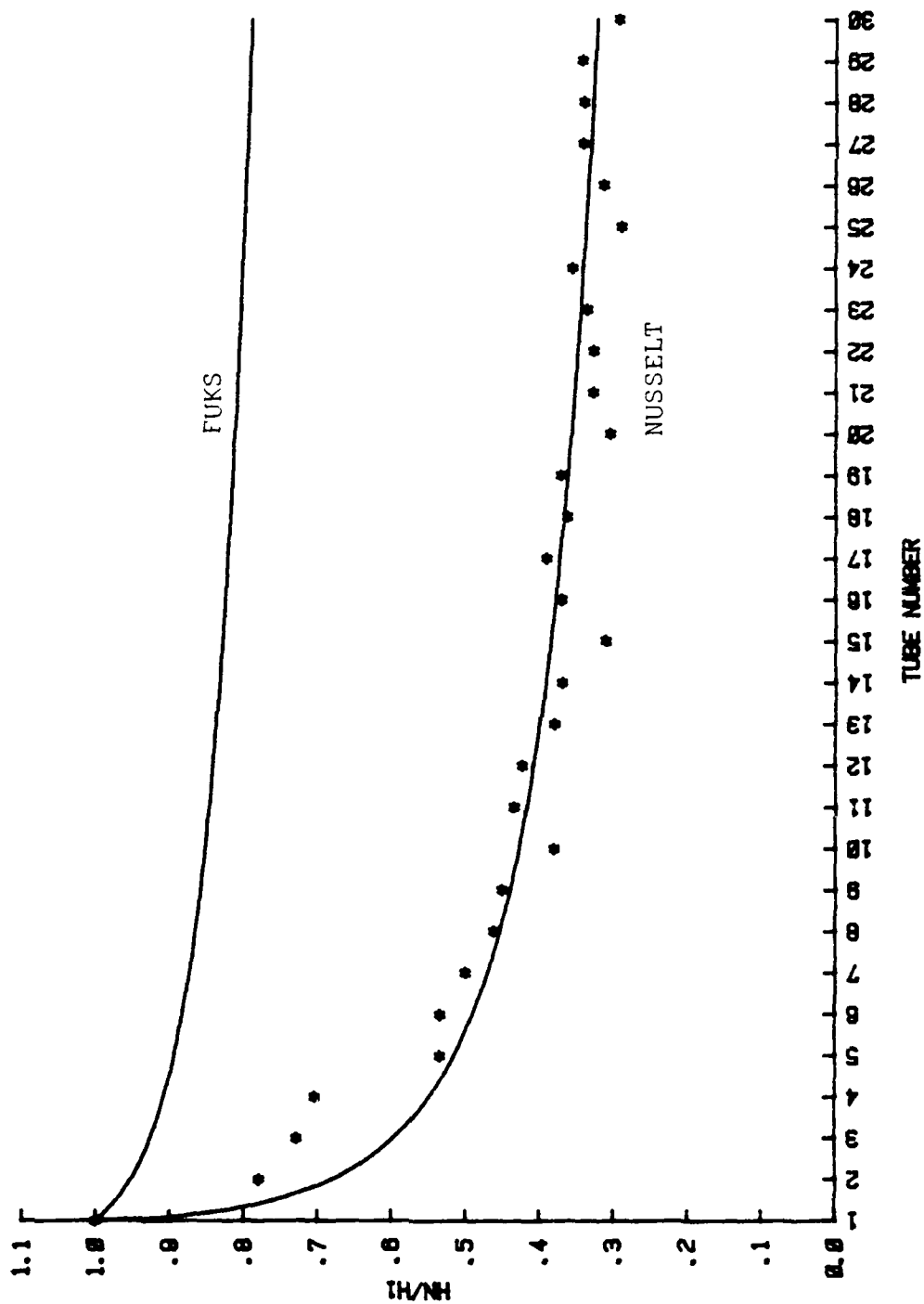
Figure 23: AVERAGE HN/H1 VS TUBE NUMBER   RUNS 11 - 20

131
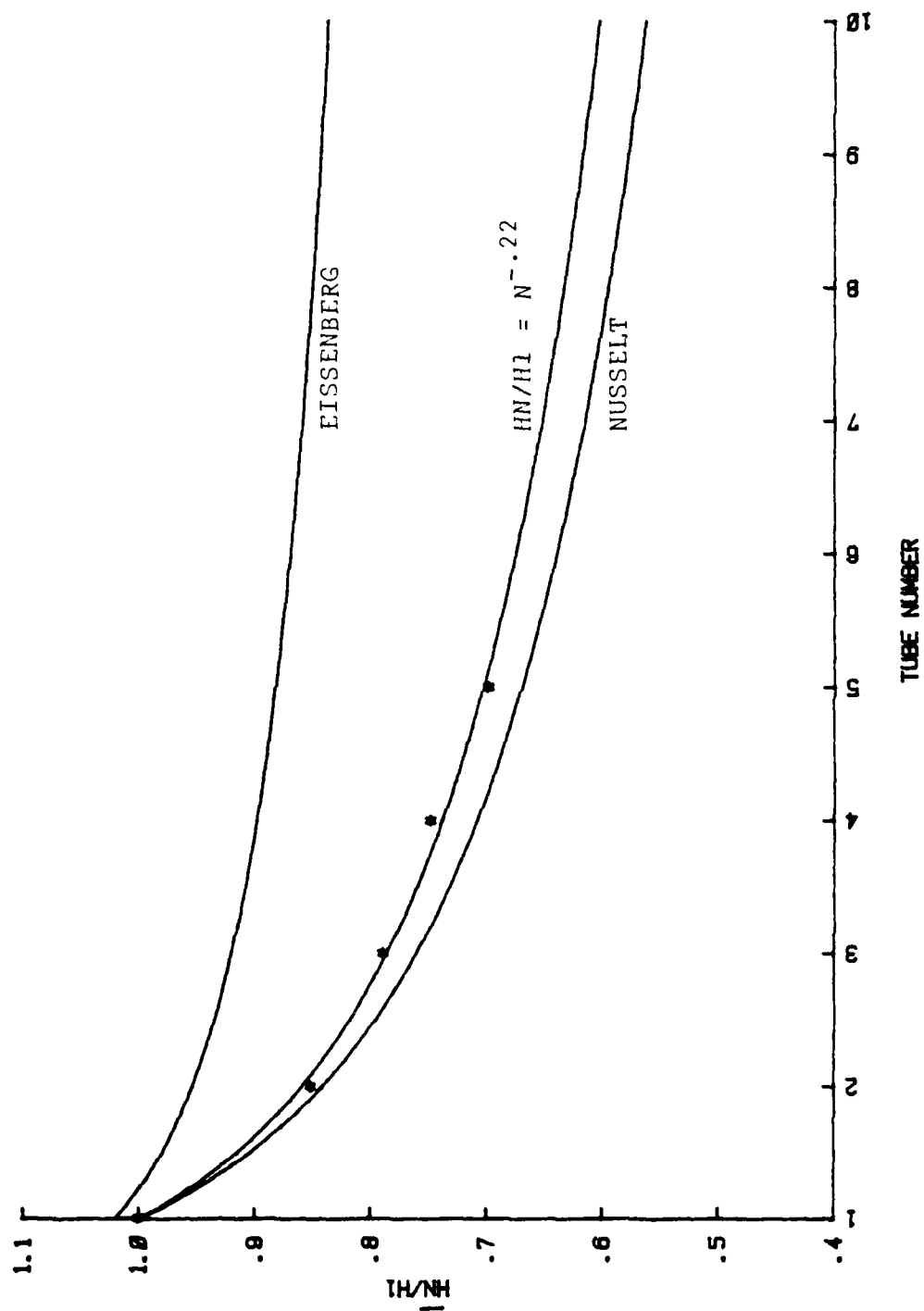
Figure 24: AVERAGE HN/H1 VS TUBE NUMBER   RUNS 21 - 30

132
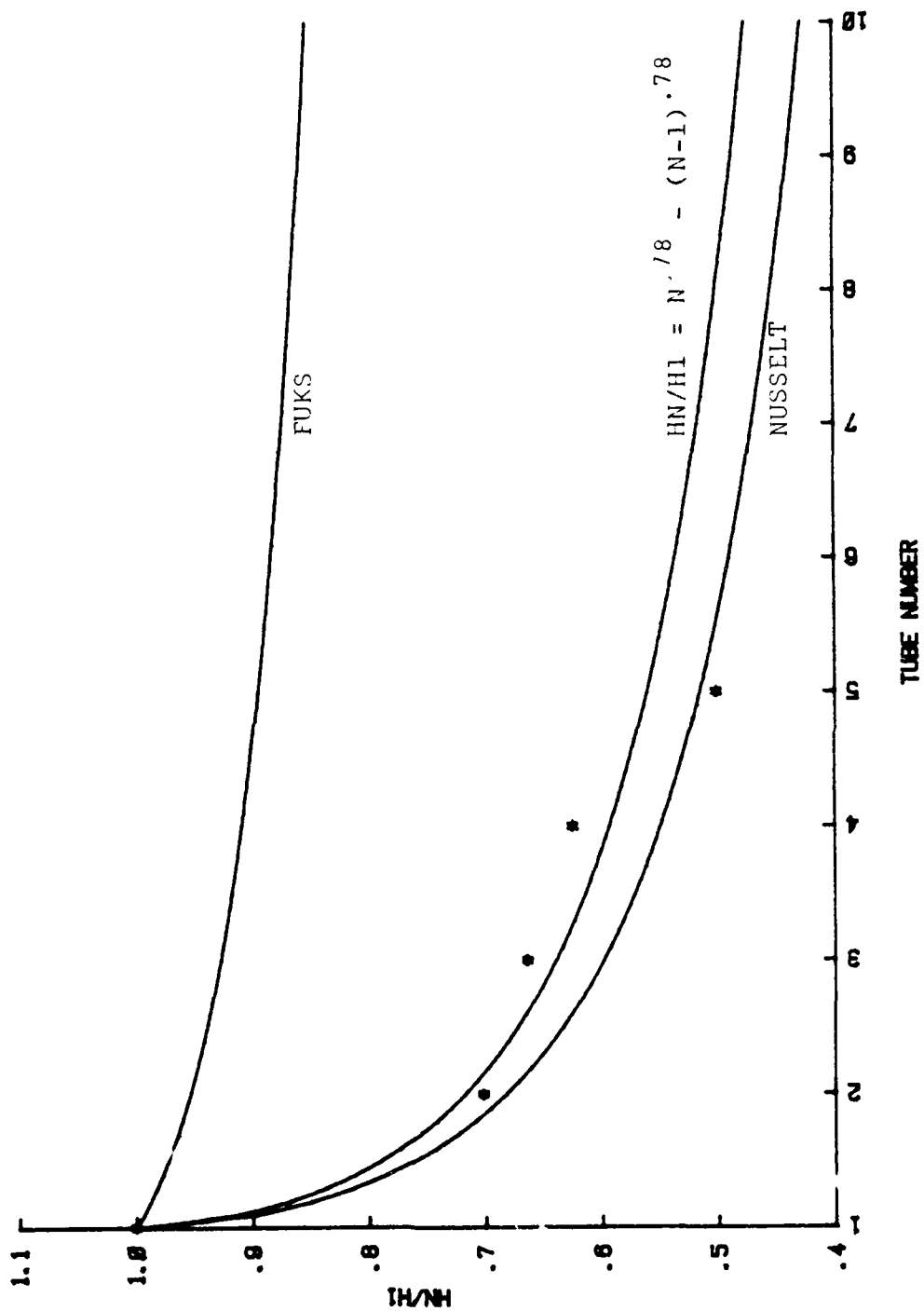
Figure 25 : AVERAGE HN/H1 VS TUBE NUMBER RUNS 21 - 30

$$HN/H1 = N^{.78} - (N-1)^{.78}$$

133
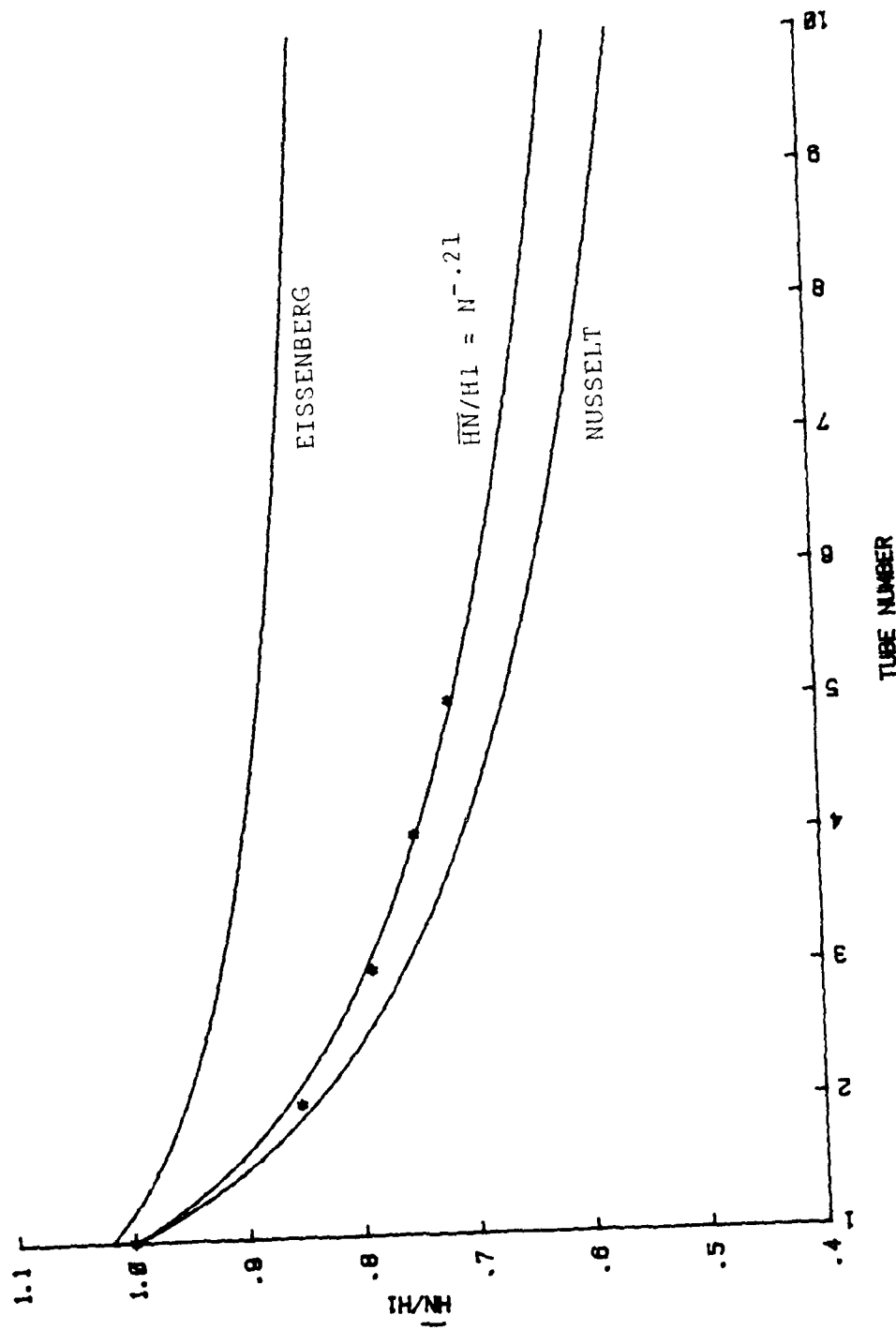
Figure 26: AVERAGE HN/H1 VS TUBE NUMBER RUNS 31 - 40

134
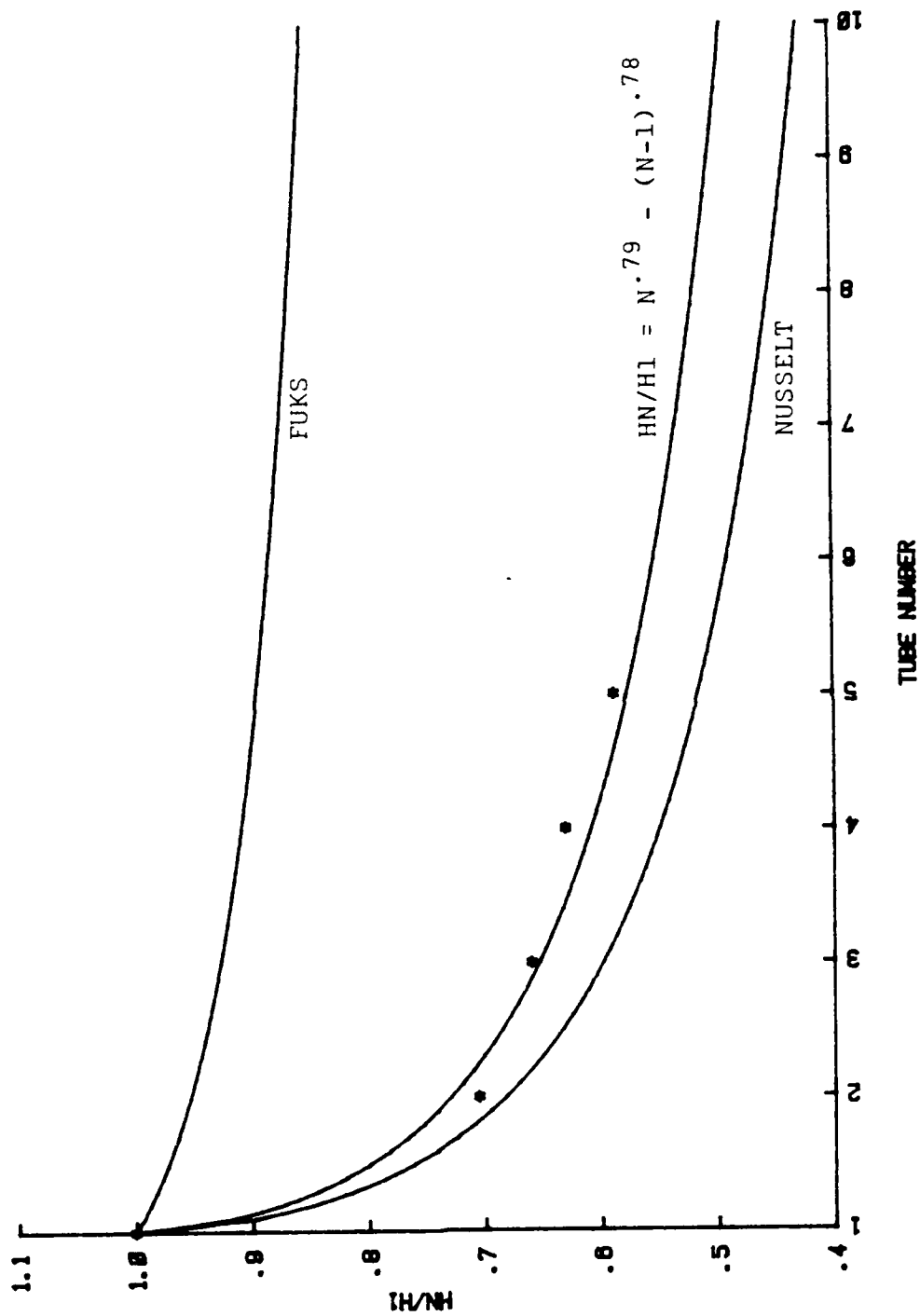
Figure 27: AVERAGE HN/H1 VS TUBE NUMBER   RUNS 31 - 48

135
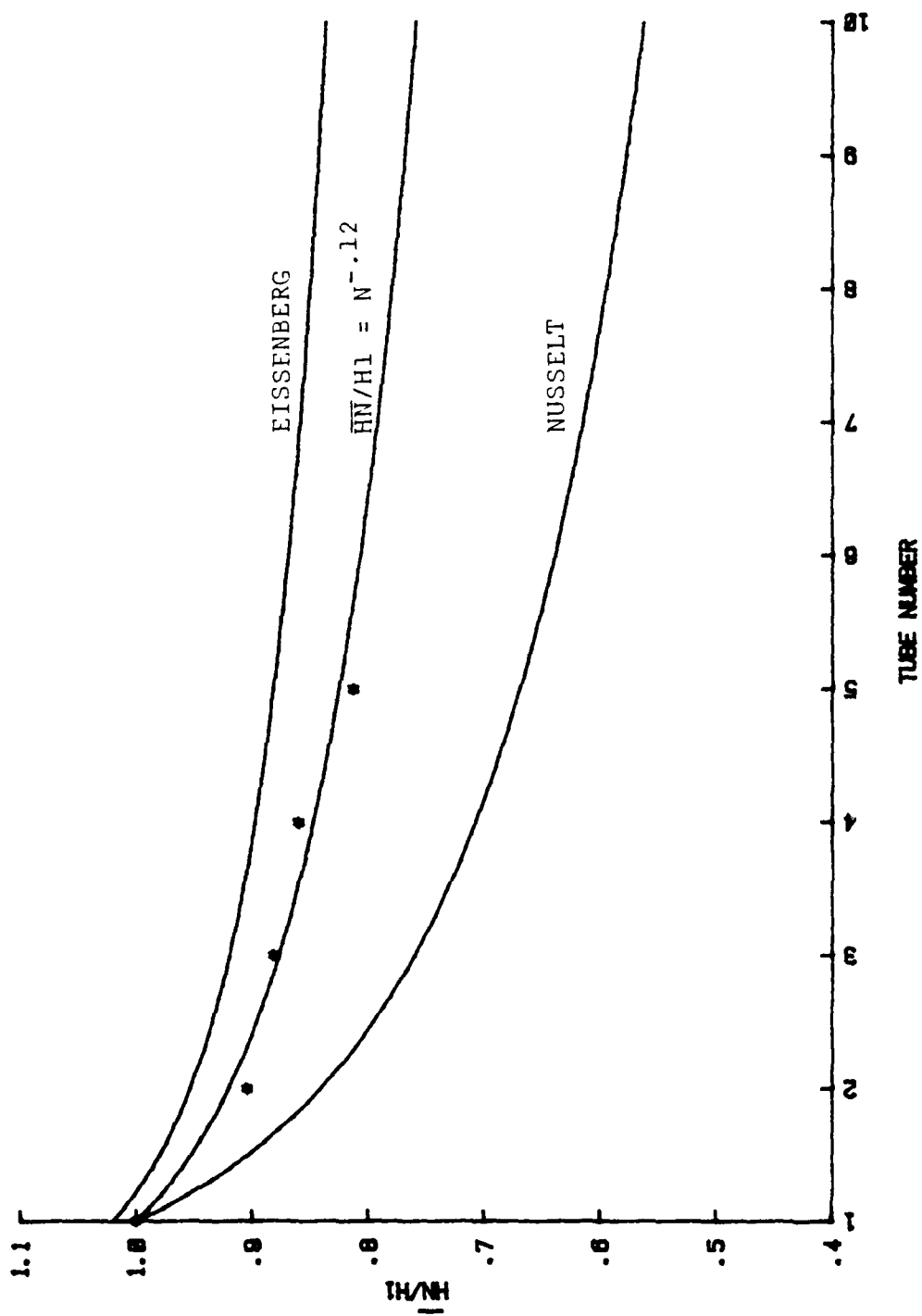
Figure 28: AVERAGE HN/H1 VS TUBE NUMBER RUNS 41 - 45
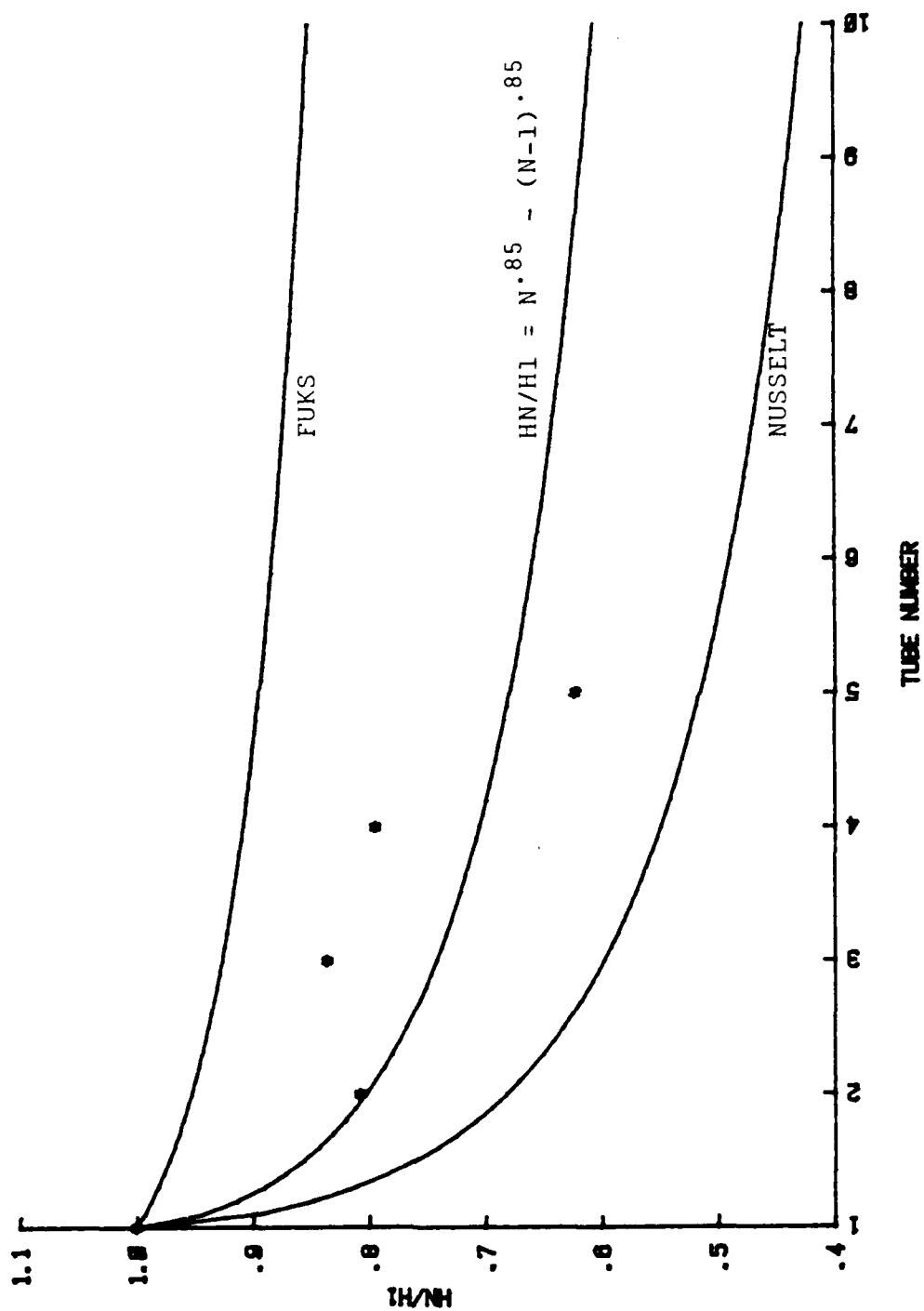
Figure 29: AVERAGE HN/H1 VS TUBE NUMBER   RUNS 41 – 45

137
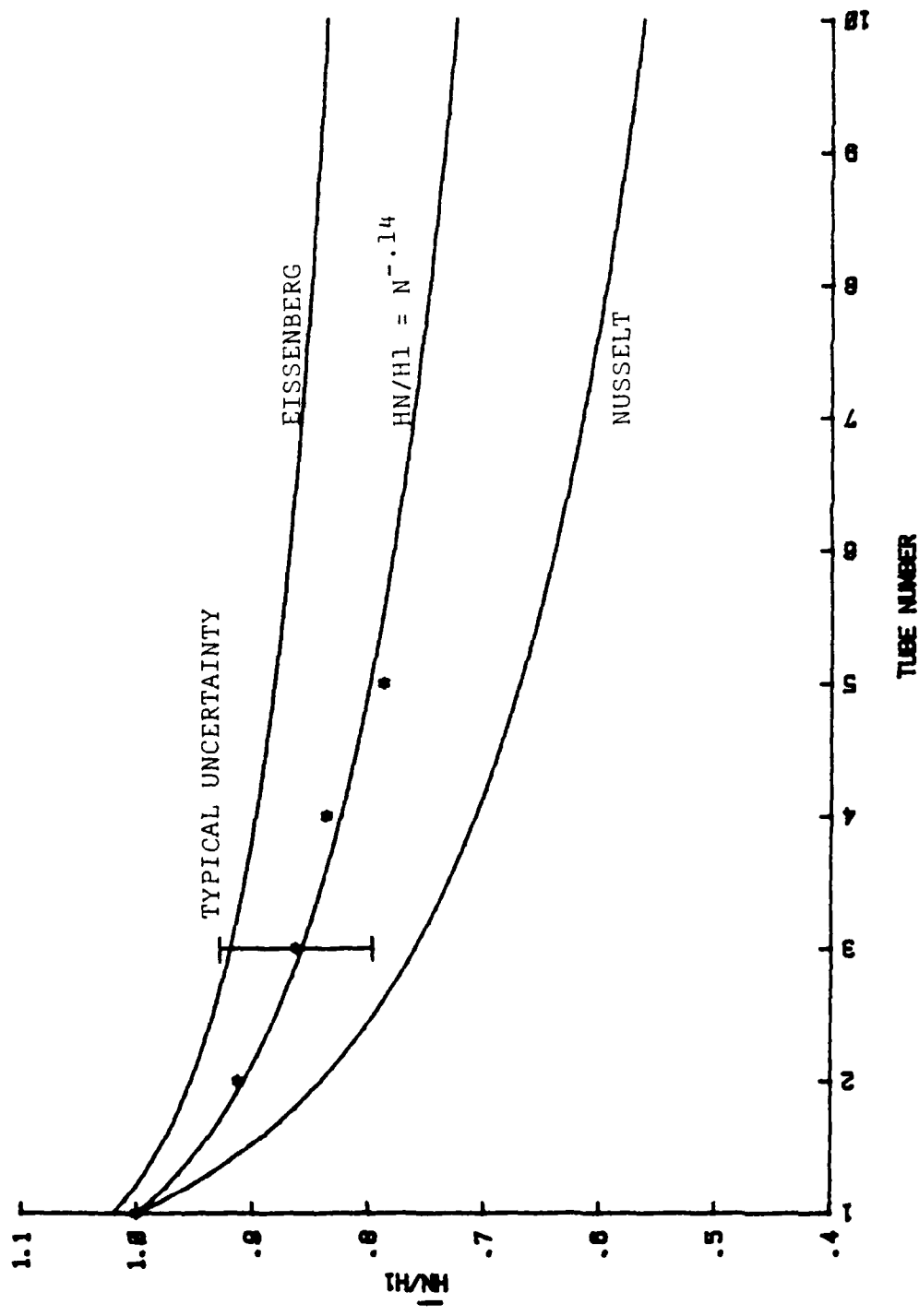
Figure 30: AVERAGE HN/H1 VS TUBE NUMBER   RUNS 46 – 58

138
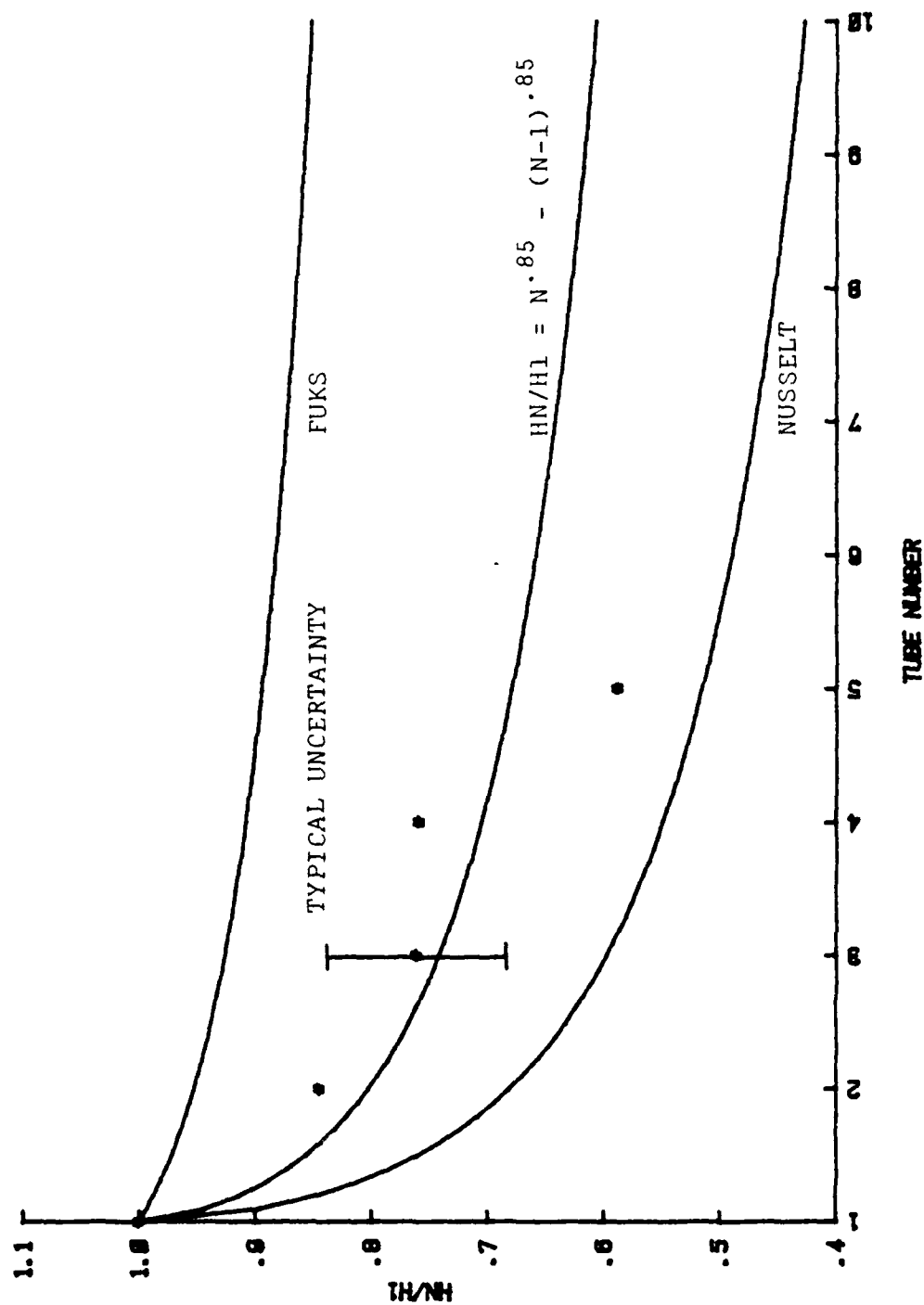
Figure 31: AVERAGE HN/H1 VS TUBE NUMBER   RUNS 46 - 50

139
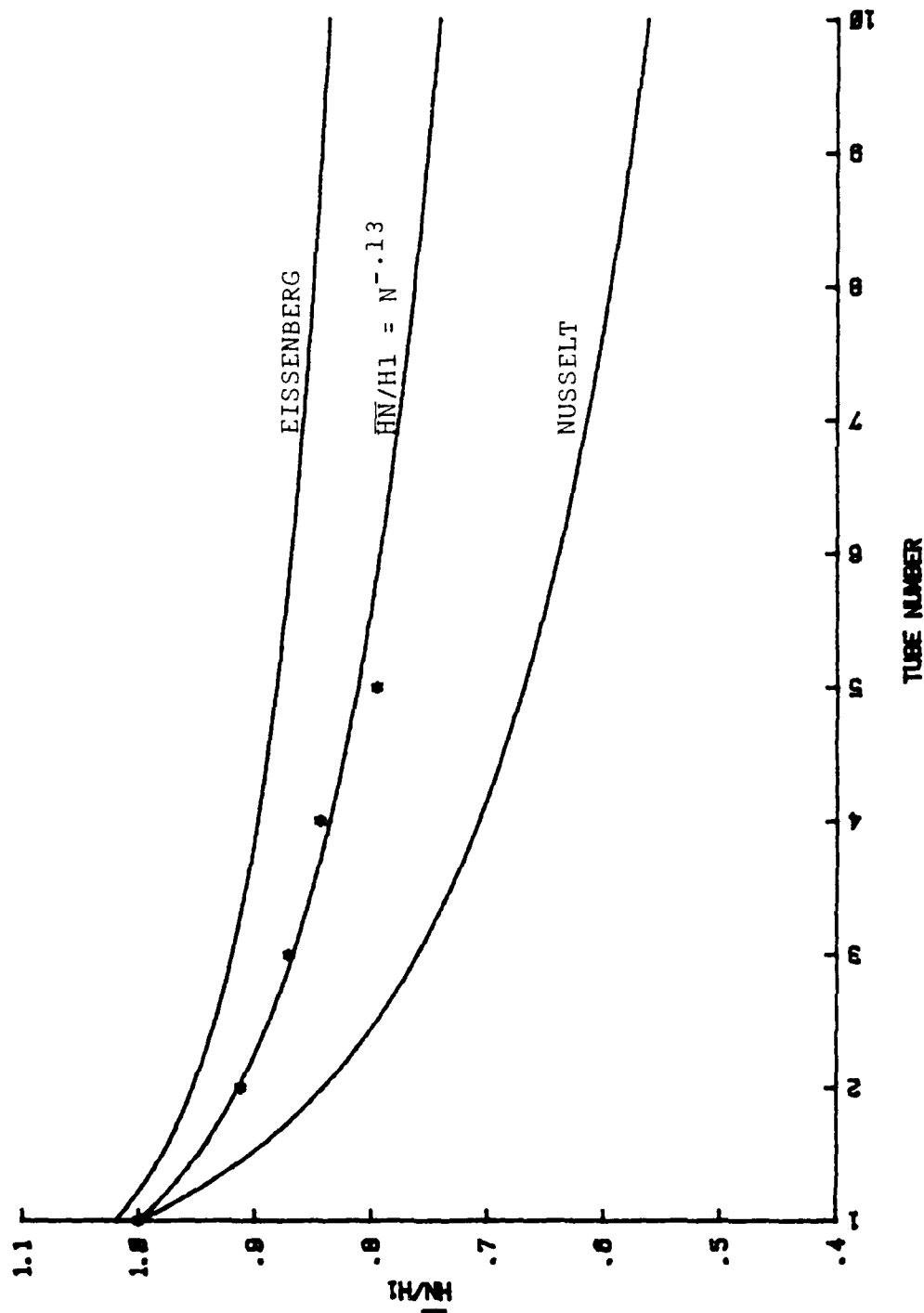
Figure 32: AVERAGE $\overline{HN/H1}$ VS TUBE NUMBER   RUNS 51 - 55

140
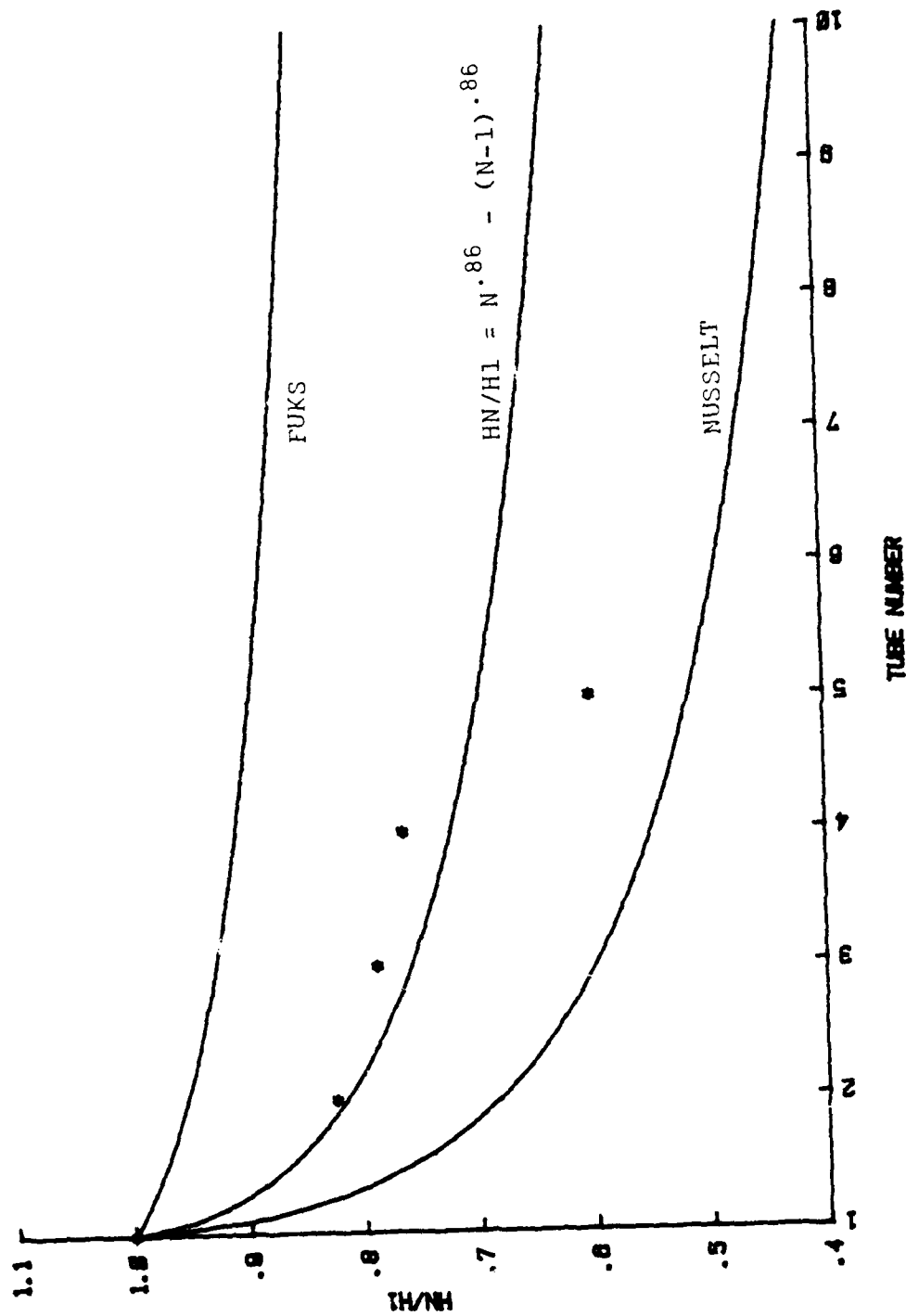
Figure 33: AVERAGE HN/H1 VS TUBE NUMBER   RUNS 51 - 55

141
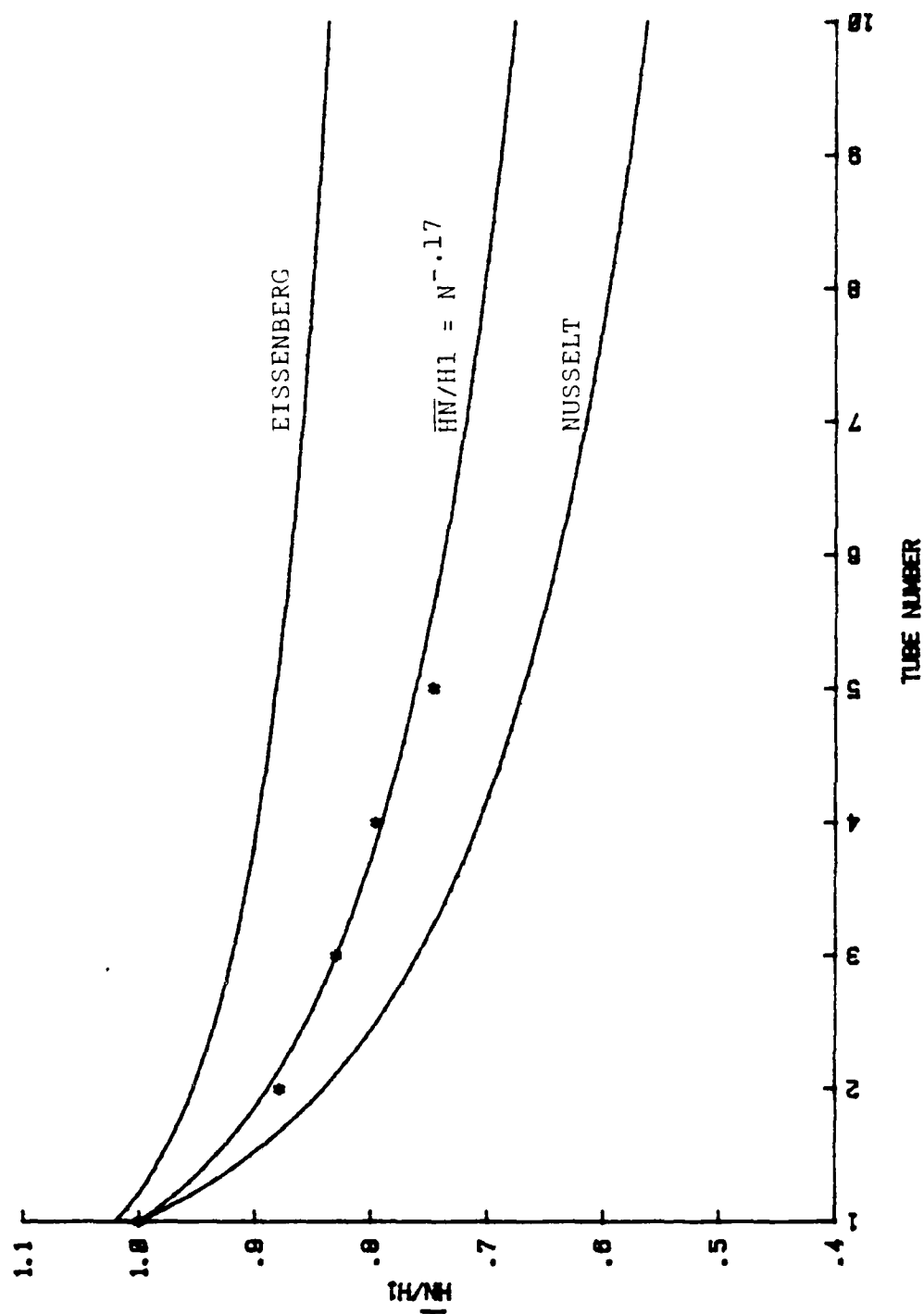
Figure 34: AVERAGE $\overline{HN}/H1$ VS TUBE NUMBER   RUNS 58 - 60

Figure 35 : AVERAGE HN/H1 VS TUBE NUMBER RUNS 56 - 60

143

Figure 36: $\overline{HN}/H1$ VS TUBE NUMBER   RUN 81

144

Figure 37: HN/HI VS TUBE NUMBER   RUN 61

145

EISSENBERG

$\overline{HN}/H1 = N^{-.21}$

NUSSELT
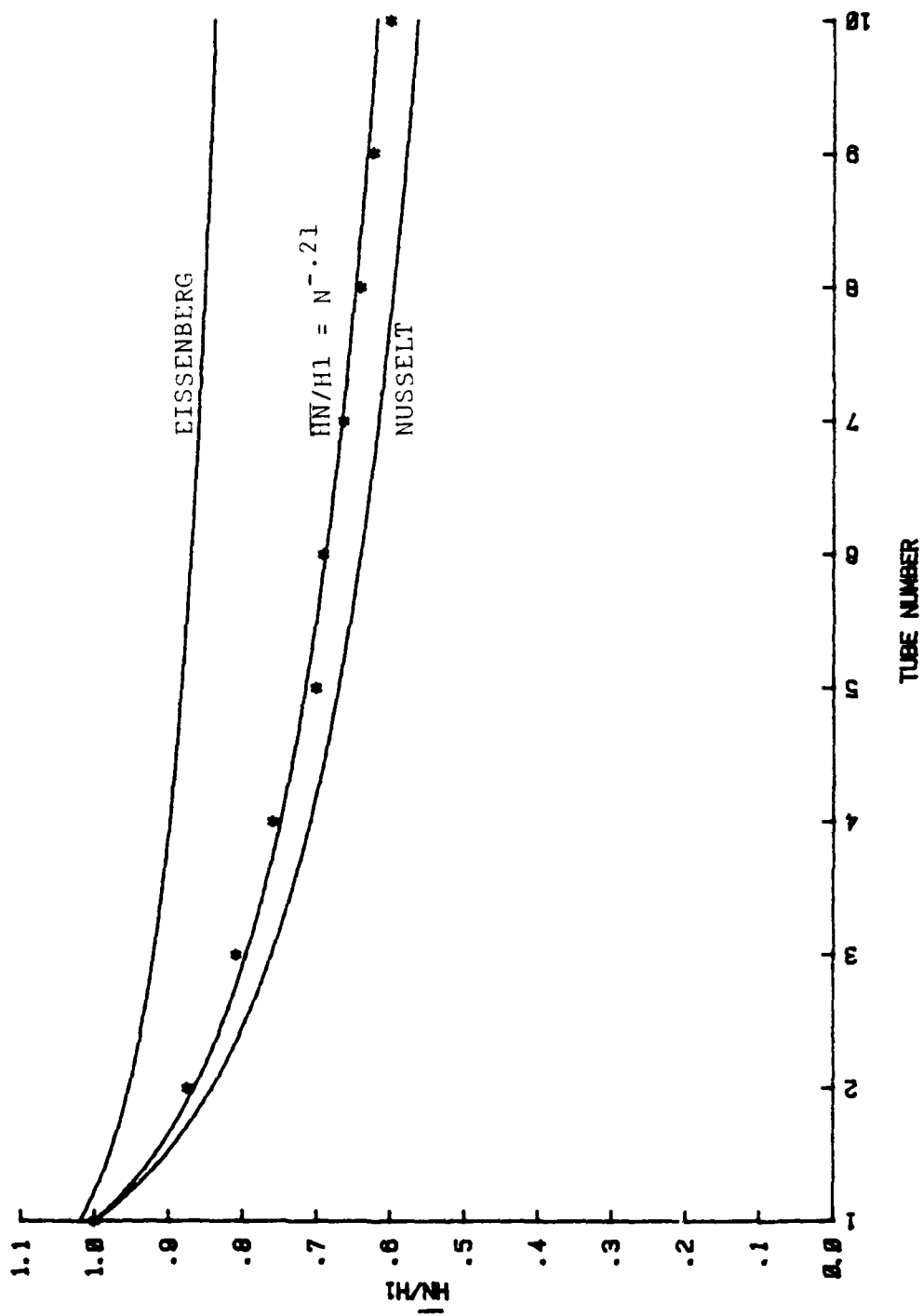
TUBE NUMBER

$\overline{HN/H1}$

Figure 38: $\overline{HN}/H1$ VS TUBE NUMBER   RUN 62

146
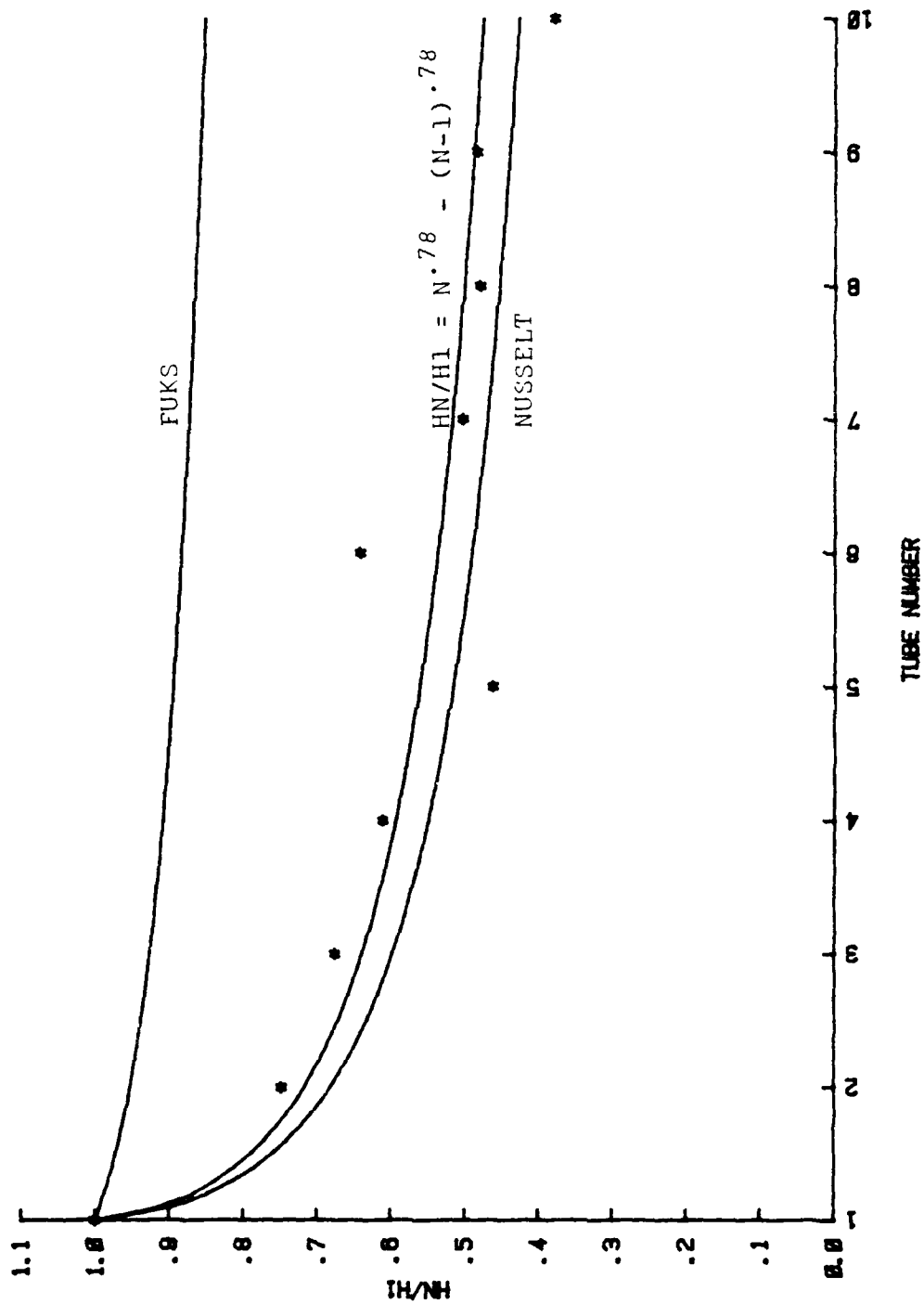
Figure 39: **HN/H1 VS TUBE NUMBER   RUN 62**

147

APPENDIX A: OPERATING PROCEDURES

A.   INITIAL PROCEDURES

1.   Energize the main circuit breaker located in Power
     Panel P-2 on the wall to the right of the test
     apparatus.

2.   Energize the circuit breaker on the left side of the
     old control board by pressing the ON button.

3.   Energize the following switches in the control panel:

     a.   #1 - Porous Tube Water Supply Pump (Feed Pump)

     b.   #2 - Outlets

     c.   #3 - Hot Water Heater

     d.   #4 - Condensate Pump

     e.   #6 - Cooling Tower

     f.   #7 - Cool Water Pump

4.   Ensure all test apparatus valves are closed.

5.   Fill the desuperheater and porous tube condensate
     supply tanks with distilled water. Set the tempera-
     ture controller for the porous tube water supply tank
     at about $50^\circ C$, fully open the recirculation valve,
     P-1, and start the pump to begin heating the water.
     The controller will have to be reset to the proper
     supply temperature once steady state conditions are
     obtained.

6. Fill the cooling water supply tank. This can be done by the use of a hose connected to the house water supply, by backfilling with valves CK1-1 and CW-4 open, or by opening valve WS-1 and the water supply valve on the steam hot water heater.

7. Start the air compressor following the posted instructions.

3. Energize the instrumentation as per Appendix B.

3. OPERATION

1. House Steam

a. Open the main supply valve.

b. Open valve MS-3 until the pressure gage indicates the desired steam supply pressure.

c. Fully open MSD-1 to drain any condensate.

d. Open valves MS-4 and MS-5 until the desired steam supply pressure is obtained and readjust MS-3 as necessary.

2. Condensate and Vacuum Systems

a. Open valve C-4 to supply cooling water to the secondary condenser.

b. Open valve A-1 to energize air ejector.

c. To collect the condensate in the test condenser hotwell, operate the system with valve C-1 closed. After a test run is completed, open valve C-1 to drain the condensate into the secondary condenser hotwell.

d. Whenever the secondary condenser hotwell level approaches half full, the hotwell must be pumped down to maintain vacuum. To pump down the hotwell, open valves C-2 and C-3 and start the condensate pump. Secure the pump down by securing the condensate pump and closing valves C-2 and C-3.

3. Cooling Water System

a. Open valves CW-1, CW-2, and CW-3.

b. Ensure valves CK1-1 and CW-4 are closed.

c. Energize the two cooling water pumps.

d. Open valves CW-5, CW-6, CW-7, CW-8, and CW-9 to obtain the desired cooling water rates.

4. Desuperheater System

a. Start the supply tank pump.

b. Open the recirculation valve D-1 one turn.

c. Set the desuperheater rotameter to a 10-20% flow rate by adjusting valve D-3.

d. Fully open valve D-4.

e. Depending upon the house steam state point, the desuperheater may or may not be required. The optimum test condenser steam inlet temperature is such that the degree of superheat is less than $10^{\circ}C$. The system is not required when running the test apparatus under atmospheric pressure conditions. The temperature is adjusted by regulating the flow rate of water to the desuperheater spray nozzles via the rotameter.

150

5. Porous Tube Water Supply System

   a. Once steady state conditions have been achieved
      for a run, reset the temperature controller to
      the proper inundation temperature.

   b. Adjust the rotameter to the required flow rate
      for each run. The supply tank recirculation valve
      may have to be adjusted to achieve the desired
      flow rate, but should never be fully closed since
      pump damage and non-uniform water temperature
      may occur.

   c. Refill the supply tank as required with distilled
      water to maintain the tank level above the heating
      element.

6. Miscellaneous

   To maintain a clear test condenser window, open valve
   A-2 and then energize and adjust the air heater power
   supply. When securing, always turn off the power
   supply first and allow the air heater to cool before
   securing valve A-Z.

C. SECURING THE TEST APPARATUS

   1. Secure the steam valves MS-5, MS-4, MS-3, and the
      main supply valve.

   2. Secure the air compressor.

   3. Secure the desuperheater by securing the pump and
      valves D-1 and D-3. Drain the supply tank by opening
      valve D-2 (if desired).

4. Secure the porous tube water supply system by securing the pump, temperature controller, and valves P-1 and P-4. Drain the supply tank by opening valve P-3 (if desired).

5. Secure the air ejector by closing valve A-1.

6. Secure the test condenser viewing window air heater as prescribed above.

7. Secure the instrumentation.

8. Allow the test section to cool down for about one-half hour, then secure the cooling water pumps and close valves CS-1, CW-2, CW-3, CW-5, CW-6, CW-7, CW-8, CW-9, and C-4.

9. Drain the test condenser and secondary condenser hotwells.

10. Secure all circuit breakers.

11. Drain the cooling water system piping and rotameters by opening valve CW-10 and cracking open the cooling water rotameter supply valves.

12. Drain the cooling water supply tank by opening the drain valve via the remote operating rod.

13. Ensure all valves are secured.

APPENDIX B: AUTODATA NINE SCANNER OPERATION

1. Plug the power cord into the wall outlet.

2. Turn the main power switch on. The pressure transducer
    power supply has a separate switch, located inside the
    back door of the Autodata Nine Scanner, which must also
    be turned on.

3. Set the time.

    a. Place all alarms and output switches in the off
        position.

    b. Set the data and time on the thumbwheels.

    c. Set the display switch to "time."

    d. Lift the "set time" switch.

4. Assigning Multiple Channels

    a. Set the display switch to "all."

    b. Check that all alarms and switches are "off."

    c. Set the scan switch to "continuous."

    d. Lift the "slow" switch.

    e. Set the first channel thumbwheels to "000" and the
        last channel thumbwheels to "001."

    f. To assign channel "000" and "001," depress and hold
        the "10V" and "HI RES" buttons for at least one scan
        and lift the scan start switch to start scanning.

g. Set the last channel thumbwheels to "039" setting the first channel thumbwheels to "002."

h. Depress the "skip" button and lift the scan switch to skip channels 002 through 039.

i. Set the last channel thumbwheels to "039" before setting the first channel thumbwheels to "040."

j. To assign channels, depress and hold the "T/$^\circ$C" and "HI RES" buttons for at least one computer scan.

k. Set the scan switch to the fast scan position.

5. Interval Scan

a. Set the thumbwheels to the time interval desired between scans.

b. Depress the "stop enter" switch.

c. Set the display switch to "interval."

d. Depress the "set interval" switch.

e. Set the scan switch to "interval."

f. Set the first channel thumbwheels to "000."

g. Set the last channel thumbwheels to "089."

h. Lift the "scan start" switch.

6. Optional Devices as Required

a. Printer on/off.

b. Single channel display.

APPENDIX C: UNCERTAINTY ANALYSIS

The general form of the Kline and McClintock [Ref. 23] "second order" equation is used to calculate the uncertainty. If the resultant, R, is some function of the primary variables X, X_2, ..., X_n, then the uncertainty is given by.

$$\delta R = \left[\left(\frac{\partial R}{\partial X_1} \delta X_1 \right)^2 + \left(\frac{\partial R}{\partial X_2} \delta X_2 \right)^2 + \dots + \left(\frac{\partial R}{\partial X_n} \delta X_n \right)^2 \right]^{1/2} \tag{C-1}$$

where δX_1, δX_2, ..., δX_n are the uncertainties in each of the measured variables X_1, X_2, ..., X_n.

1. Uncertainty in the Steam Side Heat Transfer Coefficient, h from Equation (11):

$$h = \frac{\dot{m} \, C_p \, (T_{co} - T_{ci})}{A \, (T_s - T_w)}$$

Applying Equation (C-1) to the above, the following equation is obtained:

$$\frac{\delta h}{h} = \left[\left(\frac{\delta \dot{m}}{\dot{m}}\right)^2 + \left(\frac{\delta C_p}{C_p}\right)^2 + \left(\frac{\delta T_{co}}{T_{co} - T_{ci}}\right)^2 + \left(\frac{\delta T_{ci}}{T_{co} - T_{ci}}\right)^2$$

$$+ \left(\frac{\delta A}{A}\right)^2 + \left(\frac{\delta T_s}{T_s - \bar{T}_w}\right)^2 + \left(\frac{\delta \bar{T}_w}{T_s - \bar{T}_w}\right)^2\right]^{1/2} \qquad (C-2)$$

The following uncertainties were assigned to the variables:

$\delta m = 0.01$ kg/s

$\delta C_p = 0.004$ kJ/kg $\cdot$ $^\circ$C

$\delta T_{co} = 0.1$ $^\circ$C

$\delta T_{ci} = 0.1$ $^\circ$C

$\delta A = 0.0001$ m^2

$\delta T_s = 0.5$ $^\circ$C

$\delta \bar{T}_w = 1.0$ $^\circ$C

2. Uncertainty in the Normalized Average Heat Transfer Coefficient, $\overline{h_N}/h_1$

The normalized average heat transfer coefficient is obtained for the Nth tube by taking the average of the heat transfer coefficients of the first N tubes and dividing this by the heat transfer coefficient of the first tube:

$$\frac{\overline{h_N}}{h_1} = \frac{(h_1 + h_2 + \ldots + h_N)/N}{h_1}$$

156

Applying Equation (C-1) to the above, the following equation results:

$$\frac{\delta(\overline{h_N}/h_1)}{(\overline{h_N}/h_1)} = \begin{cases} \left[\sum_{i=1}^{N} \left(\frac{\delta h_i}{\sum_{i=1}^{N} h_i} \right)^2 + \left(\frac{\delta h_1}{h_1} \right)^2 \right]^{1/2} & \text{for } N \geq 2 \\ \\ 0 & \text{for } N = 1 \end{cases} \tag{C-3}$$

where

$\quad N$ = the tube number.

The uncertainties for δh_1 and δh_i (i = 1, 2, ...N) are obtained from Equation (C-2). For example:

$$\frac{\delta(\overline{h_5}/h_1)}{(\overline{h_5}/h_1)} = \left[\left(\frac{\delta h_1}{h_1+h_2+h_3+h_4+h_5} \right)^2 + \left(\frac{\delta h_2}{h_1+h_2+h_3+h_4+h_5} \right)^2 \right.$$

$$+ \left(\frac{\delta h_3}{h_1+h_2+h_3+h_4+h_5} \right)^2 + \left(\frac{\delta h_4}{h_1+h_2+h_3+h_4+h_5} \right)^2$$

$$\left. + \left(\frac{\delta h_5}{h_1+h_2+h_3+h_4+h_5} \right)^2 + \left(\frac{\delta h_1}{h_1} \right)^2 \right]^{1/2}$$

3. Uncertainty in the Averaged Normalized Average Heat Transfer Coefficient, $(\overline{\overline{h_N/h_1}})$

This coefficient is simply $\overline{h_N}/h_1$ averaged for X number of runs:

$$\left(\overline{\frac{\overline{h_N}}{h_1}}\right) = \frac{1}{X} \sum_{i=1}^{X} \left(\frac{\overline{h_N}}{h_1}\right)_i$$

Applying Equation (C-1) to the above, the following equation results:

$$\frac{\delta(\overline{\overline{h_N/h_1}})}{(\overline{\overline{h_N/h_1}})} = \begin{cases} \left[\sum_{i=1}^{X} \left(\dfrac{\delta(h_N/h_1)_i}{\sum\limits_{i=1}^{X}(h_N/h_1)_i}\right)^2\right]^{1/2} & \text{for } N \geq 2 \\[4ex] 0 & \text{for } N = 1 \end{cases} \qquad (C-4)$$

The uncertainties for the $\delta(\overline{h_N}/h_1)_i$ terms are obtained from Equation (C-3). For example for the third tube and five runs:

N = 3 and X = 5

$$\frac{\delta(\overline{\overline{h_3/h_1}})}{(\overline{\overline{h_3/h_1}})} = \left[\left(\frac{\delta(\overline{h_3}/h_1)_1}{\sum\limits_{i=1}^{5}(\overline{h_3}/h_1)_i}\right)^2 + \left(\frac{\delta(\overline{h_3}/h_1)_2}{\sum\limits_{i=1}^{5}(\overline{h_3}/h_1)_i}\right)^2 \right.$$

$$\left. + \left(\frac{\delta(\overline{h_3}/h_1)_3}{\sum\limits_{i=1}^{5}(\overline{h_3}/h_1)_i}\right)^2 + \left(\frac{\delta(\overline{h_3}/h_1)_4}{\sum\limits_{i=1}^{5}(\overline{h_3}/h_1)}\right)^2 \right.$$

$$+\left(\frac{\delta(\overline{h_3}/h_1)_5}{\sum\limits_{i=1}^{5}(\overline{h_3}/h_1)_i}\right)^2\Bigg]^{1/2} \hspace{2cm} (C-5)$$

where $\sum\limits_{i=1}^{5}(\overline{h_3}/h_1)_i = \left(\frac{\overline{h_3}}{h_1}\right)_1 + \left(\frac{\overline{h_3}}{h_1}\right)_2 + \left(\frac{\overline{h_3}}{h_1}\right)_3$

$$+ \left(\frac{\overline{h_3}}{h_1}\right)_4 + \left(\frac{\overline{h_3}}{h_1}\right)_5$$

4. Uncertainties for the Normalized Local Heat
   Transfer Coefficient, h_N/h_1

This coefficient is simply the heat transfer coefficient

of a given tube, N, divided by that of the first tube or,

for the fifth tube, N=5 and:

$$\frac{h_N}{h_1} = \frac{h_5}{h_1}$$

An application of Equation (C-1) results in the following

equation:

$$\frac{\delta(h_N/h_1)}{(h_N/h_1)} + \begin{cases} \left[\left(\frac{\delta h_1}{h_1}\right)^2 + \left(\frac{\delta h_N}{h_N}\right)^2\right]^{1/2} & \text{for } N \geq 2 \\ \\ 0 & \text{for } N = 1 \end{cases} \hspace{1cm} (C-6)$$

Where the δh_1 and δh_N values are obtained from Equation (C-2).

For example:

$$\frac{\delta(h_2/h_1)}{(h_2/h_1)} = \left[\left(\frac{\delta h_1}{h_1}\right)^2 + \left(\frac{\delta h_2}{h_2}\right)^2\right]^{1/2}$$

$$\frac{\delta(h_5/h_1)}{(h_5/h_1)} = \left[\left(\frac{\delta h_1}{h_1}\right)^2 + \left(\frac{\delta h_5}{h_5}\right)^2\right]^{1/2}$$

5. Uncertainties for the Averaged Normalized Local Heat Transfer Coefficient, $(\overline{h_N/h_1})$

This coefficient is simply the h_N/h_1 values averaged for X number of runs:

$$\left(\frac{\overline{h_N}}{h_1}\right) = \frac{1}{X} \sum_{i=1}^{X} \left(\frac{h_N}{h_1}\right)_i$$

Applying Equation (C-1) to the above, results in the following equation (which is similar to Equation (C-4):

$$\frac{\delta(\overline{h_N/h_1})}{(\overline{h_N/h_1})} = \left\{ \begin{array}{l} \left[\sum_{i=1}^{X} \left(\frac{\delta(h_N/h_1)_i}{\sum_{i=1}^{X}(h_N/h_1)_i}\right)^2\right]^{1/2} \quad \text{for } N \geq 2 \\[20pt] 0 \hspace{5cm} \text{for } N = 1 \end{array}\right. \tag{C-7}$$

Where the $\delta(h_N/h_1)_i$ values are obtained from Equation (C-6). Note that Equation (C-7) has the exact form as Equation (C-4) but with the $(\overline{h_N}/h_1)_i$ terms replaced by $(h_N/h_1)_i$ terms.

160

6. Uncertainties in Nusselt's Single Tube Heat
   Transfer Coefficient, h_{Nu}

From Equation (1):

$$h_{Nu} = .725 \left[\frac{k^3 \, \rho(\rho - \rho_v) \, h_{fg} \, g}{\mu \, D \, (T_s - \overline{T}_w)} \right]^{1/4}$$

Applying Equation (C-1) to the above and considering ρ_v negligible in relation to ρ, the following equation results:

$$\frac{\delta h_{Nu}}{h_{Nu}} = \left[\left(3/4 \, \frac{\delta K}{K} \right)^2 + \left(1/2 \, \frac{\delta \rho}{\rho} \right)^2 + \left(1/4 \, \frac{\delta h_{fg}}{h_{fg}} \right)^2 + \left(1/4 \, \frac{\delta g}{g} \right)^2 \right.$$

$$+ \left(1/4 \, \frac{\delta \mu}{\mu} \right)^2 + \left(1/4 \, \frac{\delta D}{D} \right)^2 + \left(1/4 \, \frac{\delta T_s}{(T_s - \overline{T}_w)} \right)^2$$

$$\left. + \left(1/4 \, \frac{\delta \overline{T}_w}{(T_s - \overline{T}_w)} \right)^2 \right]^{1/2} \tag{C-8}$$

The following uncertainties were assigned to the variables:

$\delta k \quad = \pm 0.001 \; w/m \cdot {}^{\circ}C$

$\delta \rho \quad = \pm 0.1 \; kg/m^2$

$\delta h_{fg} = \pm 0.1 \; kJ/kg$

$\delta g \quad = \pm 0.001 \; m/s^2$

$\delta \mu \quad = \pm 1 \times 10^{-6} \; kg/m \cdot s$

$\delta D \quad = \pm 0.0001 \; m$

$$\delta T_s = \pm 1.0^\circ C$$

$$\delta T_w = \pm 1.0^\circ C$$

7. Uncertainties in Fujii's Correlation

From Equation (9) one can obtain:

$$h_o = 10.74 \; \frac{k_L}{d_o} \left(\frac{U_\infty \; d_o}{\nu_L} \right)^{0.312}$$

where

$$U_\infty \doteq V_m = \frac{\dot{m}_{COND} \, v}{A_{mf}} \quad \text{from Equation (12)}.$$

Applying Equation (C-1) to the equation for V_m one obtains the following equation:

$$\frac{\delta V_m}{V_m} = \left[\left(\frac{\delta \dot{m}_{COND}}{\dot{m}_{COND}} \right)^2 + \left(\frac{\delta v}{v} \right)^2 + \left(\frac{\delta A_{mf}}{A_{mf}} \right)^2 \right]^{1/2} \qquad (C-9)$$

The following uncertainties were assigned to the variables:

$$\delta m_{COND} = \pm 0.0005 \; kg/s$$

$$\delta v = \pm 0.01 \; m^3/kg$$

$$\delta A_{mf} = \pm 0.0001 \; m^2$$

Applying Equation (C-1) to Equation (9), as modified above, results in the equation:

162

$$\frac{\delta h_o}{h_o} = \left[\left(\frac{\delta k_L}{k_L} \right)^2 + \left(.688 \frac{\delta d_o}{d_o} \right)^2 + \left(.312 \frac{\delta V_m}{V_m} \right)^2 + \left(.312 \frac{\delta \nu_L}{\nu_L} \right)^2 \right]^{1/2}$$

(C-10)

The following uncertainties were assigned to the variables:

$\delta k_L = \pm 0.001$ w/m·$^{\circ}$C

$\delta d_o = \pm 0.0001$ m

$\delta \nu_L = \pm 1 \times 10^{-9}$ m^2/s

δV_m is obtained from Equation (C-9).

8. Uncertainties in the Heat Flux, q

From Equation (10):

$q = \dot{m} C_p (T_{co} - T_{ci})$

Apply Equation (C-1) to the above results in the equation:

$$\frac{\delta q}{q} = \left[\left(\frac{\delta \dot{m}}{\dot{m}} \right)^2 + \left(\frac{\delta C_p}{C_p} \right)^2 + \left(\frac{\delta T_{co}}{T_{co} - T_{ci}} \right)^2 + \left(\frac{\delta T_{ci}}{T_{co} - T_{ci}} \right)^2 \right]^{1/2}$$ (C-11)

The following uncertainties were assigned to the variables:

$\delta \dot{m} = \pm 0.01$ kg/s

$\delta C_p = \pm 0.004$ kJ/kg · $^{\circ}$C

$\delta T_{co} = \pm 0.1$ $^{\circ}$C

$\delta T_{ci} = \pm 0.1$ $^{\circ}$C

9. Uncertainties in the Heat Flux Per Unit Area

$$q/A = \frac{\dot{m} C_p (T_{co} - T_{ci})}{A}$$

Applying Equation (C-1) to the above results in the equation:

$$\frac{\delta q/A}{q/A} = \left[\left(\frac{\delta \dot{m}}{\dot{m}} \right)^2 + \left(\frac{\delta C_p}{C_p} \right)^2 + \left(\frac{\delta T_{co}}{T_{co} - T_{ci}} \right)^2 \right.$$

$$\left. + \left(\frac{\delta T_{ci}}{T_{co} - T_{ci}} \right)^2 + \left(\frac{\delta A}{A} \right)^2 \right]^{1/2}$$

or

$$\frac{\delta q/A}{q/A} = \left[\left(\frac{\delta q}{q} \right)^2 + \left(\frac{\delta A}{A} \right)^2 \right]^{1/2} \qquad (C-12)$$

where

δq is obtained from Equation (C-11)

$\delta A = 0.0001 \ m^2$.

Tables C-I and C-II present uncertainty values for various runs. From the tables, the following uncertainties can be assigned to the calculated results of this study:

For atmospheric pressure runs:

$\delta h \doteq \pm 0.7 \ kw/m^2 \cdot {}^{\circ}C$

$\delta \frac{\overline{h_N}}{h_1} \doteq \pm 0.07$

$\delta \frac{h_N}{h_1} \doteq \pm 0.07$

$\delta \left(\overline{\frac{\overline{h_N}}{h_1}} \right) \doteq \pm 0.02$

$$\delta\left(\overline{\frac{h_N}{h_1}}\right) \doteq \pm 0.02$$

$$\delta h_{Nu} \doteq \pm 0.1 \ kw/m^2 \cdot {}^{\circ}C$$

$$\delta q/A \doteq \pm 20 \ kw/m^2$$

For vacuum runs:

$$\delta h \qquad \doteq \pm 2.3 \ kw/m^2 \cdot {}^{\circ}C$$

$$\delta \ \overline{\frac{h_N}{h_1}} \qquad \doteq \pm 0.17$$

$$\delta \ \frac{h_N}{h_1} \qquad \doteq \pm 0.17$$

$$\delta\left(\overline{\overline{\frac{h_N}{h_1}}}\right) \doteq \pm 0.07$$

$$\delta\left(\overline{\frac{h_N}{h_1}}\right) \doteq \pm 0.08$$

$$\delta h_{Nu} \doteq \pm 0.5 \ kw/m^2 \cdot {}^{\circ}C$$

$$\delta h_{o} \doteq \pm 0.3 \ kw/m^2 \cdot {}^{\circ}C$$

$$\delta V_m \doteq \pm 0.4 \ m/s$$

$$\delta q/A \doteq \pm 10 \ kw/m^2$$

Table C-I

Uncertainties for Runs 1-10 and 46-50

RUN #	TUBE #	$\pm\delta h$ (kw/m$^2 \cdot$ $^\circ$C)	$\pm\delta\left(\dfrac{h_N}{h_1}\right)$	$\pm\delta\left(\dfrac{h_N}{h_1}\right)$	$\pm\delta\left(\overline{\dfrac{h_N}{h_1}}\right)$	$\pm\delta\left(\overline{\dfrac{h_N}{h_1}}\right)$
1	1	1.1	0	0	--	--
	2	0.7	0.08	0.07	--	--
	3	0.7	0.07	0.07	--	--
	4	0.6	0.06	0.06	--	--
	5	0.4	0.06	0.05	--	--
2	1	1.0	0	0	--	--
	2	0.6	0.08	0.07	--	--
	3	0.7	0.07	0.08	--	--
	4	0.6	0.06	0.06	--	--
	5	0.4	0.06	0.05	--	--
3	1	1.1	0	0	--	--
	2	0.7	0.08	0.08	--	--
	3	0.7	0.07	0.07	--	--
	4	0.6	0.07	0.07	--	--
	5	0.5	0.06	0.05	--	--
4	1	1.0	0	0	--	--
	2	0.7	0.08	0.08	--	--
	3	0.7	0.07	0.07	--	--
	4	0.6	0.07	0.07	--	--
	5	0.5	0.06	0.05	--	--
5	1	0.9	0.0	0.0	--	--
	2	0.7	0.08	0.08	--	--
	3	0.7	0.08	0.08	--	--
	4	0.6	0.07	0.07	--	--
	5	0.4	0.06	0.05	--	--

166

RUN #	TUBE #	$\pm\delta h$ (kw/m² · °C)	$\pm\delta\left(\dfrac{\overline{h}_N}{\overline{h}_1}\right)$	$\pm\delta\left(\dfrac{h_N}{h_1}\right)$	$\pm\delta\left(\dfrac{\overline{h}_N}{\overline{h}_1}\right)$	$\pm\delta\left(\dfrac{h_N}{h_1}\right)$
6	1	1.0	0.0	0.0	—	—
	2	0.7	0.08	0.08	—	—
	3	0.7	0.08	0.08	—	—
	4	0.6	0.07	0.07	—	—
	5	0.4	0.06	0.05	—	—
7	1	1.0	0.0	0.0	—	—
	2	0.6	0.08	0.07	—	—
	3	0.7	0.07	0.07	—	—
	4	0.6	0.07	0.07	—	—
	5	0.4	0.06	0.05	—	—
8	1	0.9	0.0	0.0	—	—
	2	0.6	0.08	0.07	—	—
	3	0.7	0.07	0.08	—	—
	4	0.6	0.07	0.07	—	—
	5	0.5	0.06	0.06	—	—
9	1	1.0	0.0	0.0	—	—
	2	0.6	0.08	0.07	—	—
	3	0.7	0.07	0.08	—	—
	4	0.6	0.07	0.07	—	—
	5	0.5	0.06	0.05	—	—
10	1	1.0	0.0	0.0	—	—
	2	0.6	0.08	0.07	—	—
	3	0.7	0.07	0.08	—	—
	4	0.6	0.07	0.07	—	—
	5	0.4	0.06	0.05	—	—

RUN #	TUBE #	$\pm\delta h$ (kw/m² · °C)	$\pm\delta\left(\dfrac{\overline{h}_N}{\overline{h}_1}\right)$	$\pm\delta\left(\dfrac{h_N}{h_1}\right)$	$\pm\delta\overline{\left(\dfrac{h_N}{h_1}\right)}$	$\pm\delta\overline{\left(\dfrac{h_N}{h_1}\right)}$
1-10	1	—	—	—	0.0	0.0
	2	—	—	—	0.02	0.02
	3	—	—	—	0.02	0.02
	4	—	—	—	0.03	0.02
	5	—	—	—	0.02	0.02
46	1	3.0	0.0	0.0	—	—
	2	2.1	0.18	0.17	—	—
	3	2.1	0.17	0.18	—	—
	4	2.0	0.16	0.18	—	—
	5	1.5	0.15	0.13	—	—
47	1	4.2	0.0	0.0	—	—
	2	2.5	0.22	0.20	—	—
	3	2.7	0.19	0.20	—	—
	4	2.4	0.18	0.19	—	—
	5	1.8	0.17	0.14	—	—
48	1	3.5	0.0	0.0	—	—
	2	2.2	0.20	0.19	—	—
	3	2.3	0.18	0.18	—	—
	4	2.2	0.16	0.18	—	—
	5	1.6	0.15	0.14	—	—
49	1	3.2	0.0	0.0	—	—
	2	2.0	0.20	0.19	—	—
	3	2.2	0.18	0.18	—	—
	4	2.2	0.17	0.19	—	—
	5	1.5	0.15	0.14	—	—

RUN #	TUBE #	$\pm\delta h$ $(kw/m^2 \cdot {}^{\circ}C)$	$\pm\delta\dfrac{\overline{h_N}}{\overline{h_1}}$	$\pm\delta\dfrac{h_N}{h_1}$	$\pm\delta\left(\dfrac{\overline{h_N}}{\overline{h_1}}\right)$	$\pm\delta\left(\dfrac{h_N}{h_1}\right)$
50	1	3.3	0.0	0.0	—	—
	2	2.2	0.20	0.20	—	—
	3	2.1	0.18	0.18	—	—
	4	2.1	0.16	0.17	—	—
	5	1.6	0.15	0.14	—	—
46-50	1	—	—	—	0.0	0.0
	2	—	—	—	0.09	0.08
	3	—	—	—	0.07	0.08
	4	—	—	—	0.07	0.08
	5	—	—	—	0.07	0.06

Table C-II

Selected Uncertainties for Top Tubes

RUN #	$\pm\delta h_{Nu}$ (kw/m$^2\cdot^\circ$C)	$\pm\delta h_o$ (kw/m$^2\cdot^\circ$C)	$\pm\delta V_m$ (m/s)	$\pm\delta q/A$ (kw/m^2)
1	0.1	--	--	20
11	0.1	--	--	20
21	0.1	--	--	20
31	0.1	--	--	20
41	0.5	0.5	0.4	9
46	0.5	0.3	0.3	9
51	0.5	0.3	0.4	10
56	0.5	0.3	0.3	10

APPENDIX D: SAMPLE CALCULATIONS

The following illustrates the calculation procedures of this study. Tubes 1 and 2 of runs 1 and 46 were chosen as examples. The data used came from Tables II and III; while, the uncertainties were obtained from Appendix C and Tables C-I and C-II thereto.

A.   ATMOSPHERIC PRESSURE RUN EXAMPLE, RUN 1

1. $q = \dot{m} \, C_p (T_{co} - T_{ci})$, $q/A = \dot{m} \, C_p (T_{co} - T_{ci})/A$

   Tube 1

   $\dot{m} = 10.977$ kg/min = 0.18295 kg/s

   $T_{co} = 33.5^{\circ}C$ $T_{ci} = 27.1^{\circ}C$

   $T_B = (T_{co} + T_{ci})/2 = 30.3^{\circ}C$

   C_p (at $30.3^{\circ}C$) = 4.180 kJ/kg$\cdot^{\circ}C$

   $q = 4.8942784$ kw

   $A = \pi(.3048)(.0159)$ m^2

   $q/A = 321.45983$ kw/m^2

   $\delta q/A = \pm 20$ kw/m^2

   $q/A = 320 \pm 20$ kw/m^2

   Tube 2

   $\dot{m} = 0.18295$ kg/s

   $T_{co} = 33.0^{\circ}C$ $T_{ci} = 27.2^{\circ}C$ $T_B = 30.1^{\circ}C$

   $C_p = 4.180$ kJ/kg$\cdot^{\circ}C$

   $q = 4.4354398$ kw

171

$$A = \pi(.3048)(.0159) \ m^2$$

$$q/A = 291.32297 \ kw/m^2$$

$$\delta q/A = \pm 20 \ kw/m^2$$

$$q/A = 290 \pm 20 \ kw/m^2$$

2. $h = q/A \ (T_s - \overline{T}_w)$

   Tube 1

   $T_s = 101^{\circ}C \qquad \overline{T}_w = 78.2^{\circ}C$

   $q/A = 320 \pm 20 \ kw/m^2$

   $h_1 = 14.035088 \ kw/m^2 \cdot {}^{\circ}C$

   $\delta h_1 = 1.1 \ kw/m^2 \cdot {}^{\circ}C$

   $h_1 = 14.0 \pm 1.1 \ kw/m^2 \cdot {}^{\circ}C$

   Tube 2

   $T_s = 101^{\circ}C \qquad \overline{T}_w = 70.7^{\circ}C$

   $q/A = 290 \pm 20 \ kw/m^2$

   $h_2 = 9.5709571 \ kw/m^2 \cdot {}^{\circ}C$

   $\delta h_2 = 0.7 \ kw/m^2 \cdot {}^{\circ}C$

   $h_2 = 9.6 \pm 0.7 \ kw/m^2 \cdot {}^{\circ}C$

3. $h_N/h_1 = h_2/h_1$

   $h_2/h_1 = 9.6/14.0 = 0.6857$

   $\delta h_2/h_1 = \pm 0.07$

   $h_2/h_1 = 0.68 \pm 0.07$

4. $\overline{h_N}/h_1 = \overline{h_2}/h_1$

   $\overline{h_2} = (h_1 + h_2)/2 = (14.0 \quad 9.6)/2 = 11.8 \ kw/m^2 \cdot {}^{\circ}C$

   $\overline{h_2}/h_1 = 11.8/14.0 \doteq 0.8428$

   $\delta \overline{h_2}/h_1 = \pm 0.08$

   $\overline{h_2}/h_1 = 0.84 \pm 0.08$

5. $\overline{(h_N/h_1)}$ for runs 1-10, tube 2

RUN	h_2/h_1		RUN	h_2/h_1
1	0.68		6	0.77
2	0.62		7	0.67
3	0.71		8	0.69
4	0.76		9	0.68
5	0.73		10	0.69

(Data for runs 2-10 taken from Table V)

$$\overline{(h_2/h_1)} = \frac{1}{10} \sum_{i=1}^{10} (h_2/h_1)_i = \frac{7.05}{10} = 0.705$$

$$\overline{\delta h_2/h_1)} = \pm 0.02$$

$$\overline{(h_2/h_1)} = 0.70 \pm 0.02$$

6. $\overline{(\overline{h_N}/h_1)} = \overline{(\overline{h_2}/h_1)}$

RUN	$\overline{h_2}/h_1$		RUN	$\overline{h_2}/h_1$
1	0.84		6	0.88
2	0.81		7	0.84
3	0.86		8	0.85
4	0.88		9	0.84
5	0189		10	0.85

(Data for runs 2-10 taken from Table V)

$$\overline{(\overline{h_2}/h_1)} = \frac{1}{10} \sum_{i=1}^{10} (\overline{h_2}/h_1)_i = \frac{8.54}{10} = 0.854$$

$$\delta\overline{(\overline{h_2}/h_1)} = \pm 0.02$$

$$\overline{(\overline{h_2}/h_1)} = 0.85 \pm 0.02$$

173

7. h_{Nu} for tube 1

$$h_{Nu} = .725 \left[\frac{k^3 \, \rho(\rho-\rho_v) \, h_{fg} \, g}{\mu \, D \, (T_s - \overline{T}_w)} \right]^{1/4}$$

$$\doteq .725 \left[\frac{k^3 \, \rho^2 \, h_{fg} \, g}{\mu \, D \, (T_s - \overline{T}_w)} \right]^{1/4}$$

$T_s = 101\,^\circ C$ $\overline{T}_w = 78.2\,^\circ C$

$T_f = (T_s + \overline{T}_w)/2 = 89.6\,^\circ C$

$k = 0.674 \; w/m \cdot {}^\circ C$ $\rho = 967.6 \; kg/m^3$

$h_{fg} = 2,254,300 \; J/kg$ $\mu = 3.19 \times 10^{-4} \; kg/m \cdot s$

$g = 9.81 \; m/s^2$ $D = 0.0159 \; m$

$h_{Nu} = 11.094 \; kw/m^2 \cdot {}^\circ C$

$\delta h_{Nu} = \pm 0.1 \; kw/m^2 \cdot {}^\circ C$

$h_{Nu} = 11.1 \pm 0.1 \; kw/m^2 \cdot {}^\circ C$

B. VACUUM RUN EXAMPLE, RUN 46

1. $q = \dot{m} \, C_p(T_{co} - T_{ci})$, $q/A = \dot{m} \, C_p(T_{co} - T_{ci})/A$

   Tube 1

   $\dot{m} = 0.18295 \; kg/s$

   $T_{co} = 22.2\,^\circ C$ $T_{ci} = 19.7\,^\circ C$ $T_B = 21.0\,^\circ C$

   $C_p = 4.182 \; kJ/kg \cdot {}^\circ C$

   $q = 1.9127423 \; kw$

   $A = \pi(.3048)(.0159) \; m^2$

   $q/A = 125.63033 \; kw/m^2$

   $\delta q/A = \pm 10 \; kw/m^2$

   $q/A = 130 \pm 10 \; kw/m^2$

174

Tube 2

$\dot{m} = 0.18295$ kg/s

$T_{co} = 22.4^{\circ}C \qquad T_{ci} = 19.7^{\circ}C \qquad T_B = 21.0^{\circ}C$

$C_p = 4.182$ kJ/kg$\cdot^{\circ}C$

$q = 2.0657616$ kw

$A = \pi(.3048)(.0159)$ m^2

$q/A = 135.68075$ kw/m^2

$\delta q/A = \pm 10$ kw/m^2

$q/A = 140 \pm 10$ kw/m^2

2. $h = q/A \, (T_s - \overline{T}_w)$

Tube 1

$T_s = 52.2^{\circ}C \qquad \overline{T}_w = 44.9^{\circ}C$

$q/A = 130 \pm 10$ kw/m^2

$h_1 = 17.808219$ kw/m$^2\cdot^{\circ}C$

$\delta h_1 = \pm 3.0$ kw/m$^2\cdot^{\circ}C$

$h_1 = 18.0 \pm 3.0$ kw/m$^2\cdot^{\circ}C$

Tube 2

$T_s = 52.2^{\circ}C \qquad \overline{T}_w = 42.2^{\circ}C$

$q/A = 140 \pm 10$ kw/m^2

$h_2 = 14.0$ kw/m$^2\cdot^{\circ}C$

$\delta h_2 = \pm 2.1$ kw/m$^2\cdot^{\circ}C$

$h_2 = 14.0 \pm 2.1$ kw/m$^2\cdot^{\circ}C$

3. $h_N/h_1 = h_2/h_1$

$h_2/h_1 = 14.0/18.0 = 0.77777778$

$\delta h_2/h_1 = \pm 0.17$

$h_2/h_1 = 0.78 \pm 0.17$

4. $\overline{h_N}/h_1 = \overline{h_2}/h_1$

   $\overline{h_2} = (h_1 + h_2)/2 = (18.0 + 14.0)/2 = 16.0 \text{ kw/m}^2 \cdot {}^{\circ}\text{C}$

   $\overline{h_2}/h_1 = 16.0/18.0 = 0.88888889$

   $\delta h_2/h_1 = \pm 0.18$

   $\overline{h_2}/h_1 = 0.89 \pm 0.18$

5. $(\overline{h_N/h_1})$ for runs 46-50, tube 2

RUN	h_2/h_1
46	0.78
47	0.80
48	0.82
49	0.84
50	0.88

   (Data for runs 47-50 taken from Table V)

   $\overline{(h_2/h_1)} = \frac{1}{5} \sum_{i=1}^{5} (h_2/h_1)_i = 4.12/5 = 0.824$

   $\delta(\overline{h_2/h_1}) = \pm 0.08$

   $\overline{(h_2/h_1)} = 0.82 \pm 0.08$

6. $(\overline{\overline{h_N}/h_1})$ for runs 46-50, tube 2

RUN	$\overline{h_2}/h_1$
46	0.89
47	0.90
48	0.91
49	0.92
50	0.94

   (Data for runs 47-50 taken from Table V)

   $\overline{(\overline{h_2}/h_1)} = \frac{1}{5} \sum_{i=1}^{5} (\overline{h_2}/h_1)_i = 4.56/5 = 0.912$

   $\delta(\overline{\overline{h_2}/h_1}) = \pm 0.09$

   $(\overline{\overline{h_w}/h_1}) = 0.91 \pm 0.09$

7. h_{Nu} for tube 1

$$h_{Nu} = .725 \left[\frac{k^3 \rho^2 h_{fg} g}{\mu D (T_s - \overline{T}_w)} \right]$$

$T_s = 52.2^{\circ}C$ $\overline{T}_w = 44.9^{\circ}C$ $T_f = 48.6^{\circ}C$

$k = 0.638$ w/m·$^{\circ}C$ $\rho = 990.7$ kg/m^3

$h_{fg} = 2,377,500$ J/kg $\mu = 5.76 \times 10^{-4}$ kg/m·s

$g = 9.81$ m/s^2 $D = 0.0159$ m

$h_{Nu} = 12.519$ kw/m^2·$^{\circ}C$

$\delta h_{Nu} = \pm 0.5$ kw/m^2·$^{\circ}C$

$h_{Nu} = 12.5 \pm 0.5$ kw/m^2·$^{\circ}C$

8. V_m

$V_m = \dot{m}_{COND} \, v/A_{mf}$

$A_{mf} = N_c \, d \, (P_T - \pi/4 P_T) \, L$

$N_c = 3 \, 1/3$ $d = 0.0159$ m

$P_T = 1.5$ $L = 0.3048$ m

$A_{mf} = 0.01577318$ m^2

$\delta A_{mf} = \pm 0.0001$ m^2

$A_{mf} = 0.0158 \pm 0.0001$ m^2

$\dot{m}_{COND} = [(\dot{V}_{TC} + \dot{V}_{SC}) \times 10^{-6}] \, \rho$

$\dot{V}_{TC} = 4.32$ ml/s $\dot{V}_{SC} = 7.69$ ml/s

$\rho = 990.7$ kg/m^3

$\dot{m}_{COND} = [(4.32 + 7.69) \times 10^{-6} \text{ m}^3/\text{s}] \, 990.7 \text{ kg/m}^3$

        $= 1.1876 \times 10^{-2}$ kg/s

$\delta \dot{m}_{COND} = \pm 0.0005$ kg/s

$\dot{m}_{COND} = 0.0119 \pm 0.0005$ kg/s

v = 10.947 m^3/kg

V_m = 8.24489 m/s

δV_m = ±0.3 m/s

V_m = 8.2 ± 0.3 m/s

9. h_o

$$h_o = 10.74 \ \frac{k_L}{d_o} \ \left(\frac{V_m d_o}{\nu_L}\right)^{0.312}$$

k_L = 0.638 w/m·°C d_o = 0.0159 m

V_m = 8.2 ± 0.3 m/s ν_L = 0.581 x 10^{-16} m^2/s

h_o = 20.135 kw/m^2·°C

δh_o = ±0.3 kw/m^2·°C

h_o = 20.1 ± 0.3 kw/m^2·°C

APPENDIX E: COMPUTER PROGRAM AND DOCUMENTATION

The computer program listed in Table E-1 uses the HP-85 computing system and basic language. The program uses an inter-active approach.

A. DIRECTIONS/QUESTIONS OF THE COMPUTER PROGRAM

The following is a list of directions/questions and responses required of the operation:

1. Line 50 - "Enter run number." The opertor inputs the number designation of the run.

2. Line 80 - "What is the number of tubes?" The operator inputs the number of active tubes simulated in the experiment.

3. Line 130 - "Enter water and steam temperatures." The operator inputs for each tube the two cooling water inlet temperatures, the three cooling water outlet temperatures, and the steam saturation temperature.

4. Line 150 - "Enter tube wall temperatures." The operator inputs for each tube the top, bottom, and averaged center wall temperatures.

5. Line 170 - "Enter cooling water mass flow rate and specific heat." The operator inputs the cooling water mass flow rate and specific heat for each tube.

Items 3-5 will be displayed for each active tube.

B. COMPUTATIONS OF THE PROGRAM

1. Lines 210-240 - The average cooling water inlet and outlet temperatures are calculated.

2. Lines 310-315 - The heat transferred and heat flux are calculated by:

$$q = \dot{m} \, C_p \, (T_{co} - T_{ci}) \text{ and,}$$
$$q/A = \dot{m} \, C_p \, (T_{co} - T_{ci})/A$$

3. Line 330 - The outside heat transfer coefficient is calculated by:

$$h = \frac{q}{A \, (T_s - \bar{T}_w)}$$

4. Lines 340-350 - The average heat transfer coefficient is calculated.

5. Line 360 - The normalized heat transfer coefficient is calculated.

C. DATA OUTPUT

1. Line 70 - Run number.

2. Line 250 - Average cooling water outlet temperature.

3. Line 260 - Average cooling water inlet temperature.

4. Line 270 - Average tube wall temperature.

5. Line 320 - Tube number.

6. Line 370 - Normalized heat transfer coefficient.

7. Line 380 - Heat transferred.

8. Line 381 - Heat flux.

9. Line 382 - The outside heat transfer coefficient.

10. Line 383 - The average heat transfer coefficient.

D. GRAPHICS OUTPUT

The graphics are plotted using a peripheral plotter. The operator must ensure that a 8 1/2" x 11" sheet of paper is in the plotter. The program will stop before plotting the graphics and will not commence the graphics output until the "continue" key is pressed.

TABLE E-1: COMPUTER PROGRAM

```
10        ! COND1 PLOTS HN/H1 VRS TUBE NUMBER

20        OPTION BASE 1

30        DIM Q(30), M(30), I1(30), I2(30), O1(30), O2(30),
          O3(30), I(30), O(30), K(30), T1(30), T2(30), T3(30)

40        DIM H(30), T0(30), T4(30), T5(30), T6(30), T(30),
          C(30), Q1(30)

50        DISP "ENTER RUN NUMBER"

60        INPUT V

70        PRINT "RUN NUMBER IS," V

80        DISP "WHAT IS THE NUMBER OF TUBES?"

90        INPUT J

100       A1 = PI * .3048 * .0159

110       K1 = 0

120       FOR N = 1 TO J

130       DISP "ENTER WATER AND STEAM TEMPERATURES"

140       INPUT I1(N), I2(N), O1(N), O2(N), O3(N), T0(N)

150       DISP "ENTER TUBE WALL TEMPERATURES"

160       INPUT T4(N), T5(N), T6(N)

170       DISP "ENTER COOLING WATER MASS FLOW RATE AND
          SPECIFIC HEAT"

180       INPUT M(N), C(N)

190       NEXT N
```

```
200     FOR N = 1 TO J
210     O(N) = (O1(N) + O2(N) + O3(N))/3
220     I(N) = (I1(N) + I2(N))/2
230     T(N) = (T4(N) + T5(N) + T6(N))/3
250     PRINT "O = ", O(N)
260     PRINT "I = ", I(N)
270     PRINT "T = ", T(N)
280     PRINT "TØ = ", TØ(N)
290     NEXT N
300     FOR N = 1 TO J
310     Q(N) = M(N) * C(N) * (O(N) - I(N))/60
315     Q1(N) = Q(N)/A1
320     PRINT "TUBE NUMBER = ", N
330     K(N) = Q(N)/A1/(TØ(N) - T(N))
340     K1 = K1 + K(N)
350     K2 = K1/N
360     H(N) = K2/K(1)
370     PRINT "N.H.T.C. = ", H(N)
380     PRINT "Q = ", Q(N)
381     PRINT "Q/A = ", Q1(N)
382     PRINT "H = ",  K(N)
383     PRINT "HN(AVG) = ", K2
385     NEXT N
390     DISP "ENSURE PAPER IN PLOTTER"
400     PAUSE
```

```
410     PLOTTER IS 705

420     LIMIT 32, 235, 28, 182

430     LOCATE 10, 130, 15, 96

440     SCALE 1, 30, 0, 1.1

450     FXD 0,1

460     LAXES 1, .1, 1, 0, 2, .1

470     SETGU

480     MOVE 71, 7.5

490     DEG @ LDIR 0

500     LORG 5

510     LABEL "TUBE NUMBER"

520     MOVE 3, 56.5

530     DEG @ LDIR 90

540     LORG 5

550     LABEL "HN/H1"

560     MOVE 1, 55

570     LDIR 90

580     LORG 5

590     LABEL "_ _"

600     MOVE 71, 2.5

610     LDIR 0

620     LORG 5

630     LABEL "FIG.  HN/H1 VS TUBE NUMBER RUN #," V

640     MOVE 58, 4.5

650     LDIR 0
```

```
660     LORG 5

670     LABEL "_ _"

680     SETUV

690     MOVE 1, 1

700     FOR T = 1 TO 30 STEP .1

710     R = T ^ - .25

720     DRAW T, R

730     NEXT T

740     MOVE 1, 1

750     FOR T = 1 TO 30 STEP .1

760     R = .6 + .42 * T ^ - .25

770     DRAW T, R

780     NEXT T

790     FOR N = 1 TO J

800     MOVE N, H(N)

810     LABEL "*"

820     NEXT N

830     END
```

LIST OF REFERENCES

1. Standards for Steam Surface Condensers, 6th ed., Heat Exchange Institute, 1970.

2. Standards of Tubular Exchanger Manifacturers Association, 4th ed., Tubular Exchanger Manifacturers Association, Inc., 1959.

3. Search, H. T., A Feasibility Study of Heat Transfer Improvement in Marine Steam Condensers, MSME, Naval Postgraduate School, Monterey, California, December 1977.

4. Beck, A. C., A Test Facility to Measure Heat Transfer Performance of Advanced Condenser Tubes, MSME, Naval Postgraduate School, Monterey, California, January 1977.

5. Pence, D. T., An Experimental Study of Steam Condensation on a Single Horizontal Tube, MSME, Naval Postgraduate School, Monterey, California, March 1978.

6. Reilly, D. J., An Experimental Investigation of Enhanced Heat Transfer on Horizontal Condenser Tubes, MSME, Naval Postgraduate School, Monterey, California, March 1978.

7. Fenner, J. H., An Experimental Comparison of Enhanced Heat Transfer Condenser Tubing, MSME, Naval Postgraduate School, Monterey, California, September 1978.

3. Ciftci, H., An Experimental Study of Filmwise Condensation on Horizontal Enhanced Condenser Tubing, MSME, Naval Postgraduate School, Monterey, California, December 1979.

9. Marto, P. J., Reilly, D. J., Fenner, J. H., "An Experimental Comparison of Enhanced Heat Transfer Tubing," Advances in Enhanced Heat Transfer, Proceedings of the 18th National Conference, American Society of Mechanical Engineers, New York, New York, 1979.

10. Demirel, I., The Effects of Condensate Inundation on Condensation Heat Transfer in Tube Bundles of Marine Condensers, MSME, Naval Postgraduate School, Monterey, California, December 1980.

11. Eshleman, D. E., An Experimental Investigation of the Effect of Condensate Inundation on Heat Transfer in a Horizontal Tube Bundle, MSME, Naval Postgraudate School, Monterey, California, March 1980.

186

12. Morrison, R. H., _A Test Condenser to Measure Condensate Inundation Effects in a Tube Bundle_, MSME, Naval Post-graduate School, Monterey, California, March 1981.

13. Nobbs, D. W., _The Effect of Downward Vapour Velocity and Inundation on the Condensate Rates on Horizontal Tubes and Tube Banks_, Ph.D Thesis, University of Bristol, Bristol, England, April 1975.

14. Eissenberg, D. M., _An Investigation of the Variables Affecting Steam Condensation on the Outside of a Horizontal Tube Bundle_, Ph.D Thesis, University of Tennessee, Knoxville, Tennessee, December 1972.

15. Jakob, Max, _Heat Transfer_, Vol. 1, J. Wiley & Sons, Inc., 1948.

16. Kutateladze, S. S., _Heat Transfer in Condensation and Boiling_, Translated from a publication of the State Scientific and Technical Publishers of Literature on Machinery, Moscow-Leningrad, 1952 for the United States Atomic Energy Commission.

17. Shklover, G. G. and Buevich, A. V., "The Mechanism of Film Flow with Steam Condensation in Horizontal Bundles of Tubes," _Teploenergetika_, 25(4) 62-65, 1978.

18. Yung, D., Lorenz, J. J., and Ganic, E. N., "Vapor/Liquid Interaction and Entrainment in Falling Film Evaporators," _Transactions of ASME_, Vol. 102, February 1980.

19. Fuks, S. H., "Heat Transfer with Condensation of Steam Flowing in a Horizontal Tube Bundle," _Teploenergetika_, 4(1) 35-39, 1957. English Translation NEL 1041, National Engineering Laboratory, East Kilbride.

20. Chen, M. M., "An Analytical Study of Laminar Film Condensation: Part 2 - Single and Multiple Horizontal Tubes," _Journal of Heat Transfer_, February 1965.

21. Fujii, T., "Vapor Shear and Condensate Inundation," Research Institute of Industrial Science, Kijushu University, Fukuoka, Japan, 1979.

22. Knudsen, J. G. and Katz, D. L., _Fluid Dynamics and Heat Transfer_, pp. 332-335, McGraw-Hill Book Company, 1958.

23. Kline, S. J. and McClintock, F. A., _Describing Uncertainties in Single Sample Experiments_, Mech. Engin., Vol. 74, pp. 3-8, January 1953.

INITIAL DISTRIBUTION LIST

		No. Copies
1.	Defense Technical Information Center Cameron Station Alexandria, Virginia 22314	2
2.	Library, Code 0142 Naval Postgraduate School Monterey, California 93940	2
3.	Department Chairman, Code 69 Department of Mechanical Engineering Naval Postgraduate School Monterey, California 93940	2
4.	Professor P. J. Marto, Code 69Mx Department of Mechanical Engineering Naval Postgraduate School Monterey, California 93940	5
5.	Professor R. H. Nunn, Code 69Nn Department of Mechanical Engineering Naval Postgraduate School Monterey, California 93940	1
6.	Mr. R. W. Kornbau Code 2721 David Taylor Naval Ship Research and Development Center Bethesda, Maryland 20084	2
7.	LT P. J. Noftz, USN (N411) Commander Naval Surface Forces, U.S. Atlantic Fleet Norfolk, Virginia 23511	2
8.	Commander Naval Sea Systems Command Navy Department Washington, DC 20362	1

DATE
ILME
_8